MULTI-STRATEGIES FOR CONTROL OF MOTILITY VIA MORA SIGNALING PATHWAY IN PSEUDOMONAS PUTIDA

NG WEI LING

NATIONAL UNIVERSITY OF SINGAPORE

2012

MULTI-STRATEGIES FOR CONTROL OF MOTILITY VIA MORA SIGNALING PATHWAY IN PSEUDOMONAS PUTIDA

NG WEI LING

(B. Sc.(Hons), NUS)

A THESIS SUBMITTED FOR THE DEGREE OF DOCTOR OF PHILOSOPHY

DEPARTMENT OF BIOLOGICAL SCIENCES
NATIONAL UNIVERSITY OF SINGAPORE
2012

ACKNOWLEDGEMENTS

I would like to express my heartfelt gratitude to my supervisor **A/P Sanjay Swarup** for his valuable guidance and advice in the seven years that I had spent in his lab.

I thank **National University of Singapore** for providing me with Research Scholarship and the **Mechanobiology Institute** for their excellent support and funding.

It is my pleasure to thank **Ms Liew Chye Fong** for her excellent support and unfailing help. My thanks to fellow colleagues and ex-lab mates especially **Dr. Sheela Reuben, Dr. Ayshwarya Ravichandran, Mr Dennis Heng**, **Ms June Fu**, **Ms Wong Chui Ching, Mr. Amit Rai** and **Ms. Tanujaa Suriyanarayanan** for creating a conducive and joyful working environment in which we had countless fruitful scientific discussions and words of encouragement.

My thanks to **Mr Allan Tan**, **Mr Chong Ping Lee**, **Ms Tong Yan** and **Mdm Loy Gek Luan** for all the advice and technical support given to me. I am deeply appreciative for the administrative support of the office staff from the Department of Biological Sciences and special thanks to **Ms Reena Devi a/p Samynadan** for being so helpful in graduate administration matters.

I am grateful to my family members and friends for their encouragement. Special thanks are extended to my mother, **Mdm Toh Kim Huay** for her support. I could not find the words to describe my deepest appreciation and gratitude to **Mr Keven Ang** for his constant support, love and encouragement, without whom I would never have been able to complete this thesis.

CONTENTS

SUMMARY

Motility is a highly regulated process required in many aspects of growth, survival and pathogenesis. In the case of swimming motility, flagellar biogenesis usually begins during the log phase to stationary phase transition where there is a reduction in nutritional levels and cessation of cell division. Previously, our lab described MorA, a well-conserved membrane-localized negative regulator of motility that controls the timing of flagellar development. It was found to affect motility, chemotaxis and biofilm formation in *Pseudomonas putida* PNL-MK25. As *morA* loss leads to hypermotility, random mutagenesis was carried out on the *morA* mutant strain to identify members of its signaling pathway by screening for transposon double mutants that exhibited reversion in motility. Of the genes identified, *cyaA*, *morC* and the substrate-binding region of ABC type transporter system for glycine betaine (*opuAC*) were selected for further study.

cyaA expression in the absence of *morA* leads to increased motility while *cyaA* expression in the presence of *morA* leads to reduction in motility. Hence, MorA exerts a dominant effect over CyaA. Also, *cyaA* acts in an antagonistic manner with *morA* to control motility while biofilm formation is unaffected. In contrast, the disruption of *opuAC* in Δ*morA* was not able to revert the hypermotility phenotype. Δ*opuAC* exhibited a 3-fold increase in motility and a reduction in biofilm formation as compared to the wild type, suggesting that it acts as a negative regulator of motility independently of MorA. Interestingly, Δ*opuAC* was found to increase pyoverdine production in M9 medium by 45%.

Homology analysis indicates that ASNEF and EAL motif is conserved in MorC. Phenotypic characterization of Δ*morC* and Δ*morA*Δ*morC* reveals that MorC is a positive regulator of motility that functions downstream of MorA in a non-dosage dependent manner while not affecting biofilm formation or chemotaxis. GFP-tagged MorC was found to be expressed throughout the cell in the early- and late-log phase but not in the mid-log phase. Hence, MorC function is regulated in a growth-phase dependent manner without being sequestered to a specific cellular location.

A truncated MorC construct, in which the PDE domain was removed, was not able to complement for the loss of *morC*. This suggests that the PDE domain is critical for its function. Site-directed mutagenesis of the E and L residues of the EAL motifs in PDE domain located at the active site led to loss of complementation while mutations away from the active site resulted in hyperactivity that increased motility. This hyperactivity was lost in the absence of MorA, suggesting that long-range conformational changes may be involved in the regulation of MorC. While MorC PDE domain is critical for its function, it may not be dependent on its enzymatic activity.

While MorC is a positive regulator of *fliC* expression, flagellated cell numbers suggest that MorC does not control motililty by increasing flagellar number or affecting flagellar structure. Rather, MorC controls cell speed in the early and late-log phase in an EAL motif-specific manner. This is the first report to suggest specific function to the E and L residues in the EAL motif.

Here, we showed that the *cyaA* and *morC* controls motility without perturbation of biofilm formation while *opuAC* controls motility and biofilm. A different strategy was demonstrated by each of the gene studied: CyaA acts in an antagonistic manner with MorA; OpuAC functions independently of MorA while MorC functions downstream of MorA.

LIST OF ABBREVIATIONS

Bacterial strains

E. coli	*Escherichia coli*
G. xylinus	*Gluconacetobacter xylinus*
H. pylori	*Helicobacter pylori*
P. aeruginosa	*Pseudomonas aeruginosa*
P. fluorescens	*Pseudomonas fluorescens*
P. putida	*Pseudomonas putida*
S. typhimurium	*Salmonella typhimurium*

Units and Measurements

Abs	absorbance
bp	base pair
cm	centimetre
C_t	threshold cycle
ºC	degree Celcius
fps	frames per second
g	centrifugal force
h	hour
kb	kilo base pair
kDa	kilodalton
kV	kilovolt
L	litre
M	moles per litre
mg	milligram
min	minute
ml	millilitre
mM	millimole
ng	nanogram
nm	nanometre
nt	nucleotide
O.D.	optical density
rpm	revolutions per minute
s	second
mbp	Million base pair
mg	microgram
mL	microlitre
mM	micromoles
mm	micrometre
UV	ultraviolet
V	volts
w/v	weight per volume

v/v	volume per volume
%	percent

Chemicals and reagents

Amp	ampicillin
BSA	bovine serum albumin
cAMP	3’5’-cyclic adenosine monophosphate
c-di-GMP	cyclic diguanylate, cyclic-bis(3'-->5') dimeric guanosine monophosphate
cGMP	3’5’- cyclic guanosine monophosphate
Cb	carbenicillin
Cm	chloramphenicol
EDTA	ethylene-diamine-tetra-acetate
Gm	gentamycin
GMP	guanosine monophosphate
GTP	guanosine triphosphate
HCl	hydrochloric acid
IPTG	isopropyl β-D-1-thiogalactopyranoside
Km	kanamycin
LB	Luria-Bertani
M9	M9 salts minimum medium
NaCl	sodium chloride
NaOH	sodium hydroxide
PBS	phosphate-buffered saline
pGpG	5’ linear diguanylic acid
ppGpp	Guanosine tetraphosphate
Rf	rifampicin
RNA	ribonucleic acid
SDS-PAGE	sodium dodecyl sulphate polyacrylamide gel electrophoresis
Tet	tetracycline

Enzymes

DGC	diguanylate cyclase
PDE	phosphodiesterase

Others

ABC	ATP-binding cassette
α	alpha
β	beta

CCW	counterclockwise
cDNA	complementary deoxyribonucleic acid
Ct	cycle threshold
CW	clockwise
EAL	canonical “Glu-Ala-Leu” motif with phosphodiesterase activity
EPS	extracellular polymeric substances
et al.	*et alia*
GFP	green fluorescent protein
GGDEF	canonical “Gly-Gly-Asp-Glu-Phe” motif of a domain with diguanylate cyclase activity
HD-GYP	“His-Asp-Gly-Tyr-Pro” motif of a domain with phosphodiesterase activity
HPLC	high performance liquid chromatography
H20	water
I-site	Inhibitory site
PAC	PAS-associated C-terminal domain
PAGE	polyacrylamide gel electrophoresis
PAS	Per-Arnt-Sim domain
PCR	polymerase chain reaction
PGPR	plant growth-promoting rhizobacterial
RT-PCR	reverse transcriptase polymerase chain reaction
spp.	species
TEM	transmission electron microscopy
TLC	thin layer chromatography
M	mid-log phase
T	log-to-stationary transition phase
WT	wild type

LIST OF FIGURES **PAGES**

LIST OF TABLES **PAGES**

LIST OF PUBLICATIONS/CONFERENCES

PUBLICATIONS

Wong CC, Ng WL, Huang WD, Sun Q, Sivaraman J, Swarup S. Recruitment of phosphodiesterase catalytic residues for the regulation of diguanylate cyclase activity affects biological functions (In review)

Ng, WL, Fu SJ, Swarup S. MorC is a positive regulator of motility that functions downstream of MorA in a growth-phase dependent manner (in preparation)

CONFERENCES

Ng WL, Swarup S. Cyclic-di-GMP signaling pathway in motility and biofilm formation networks in *Pseudomonas putida*. 14th Biological Sciences Graduate Congress, Bangkok. Chulalongkorn University: Bangkok, Thailand, 2009.Poster.

Ng, WL, Swarup S. Cyclic-di-GMP signaling pathway in motility and biofilm formation networks in *Pseudomonas putida*. 6th International Conference on Structural Biology and Functional Genomic, Singapore. National University of Singapore: Singapore, 2010. Poster 115.

Ng WL, Swarup S. Cyclic-di-GMP signaling pathway in motility and biofilm formation networks in *Pseudomonas putida*. 15th Biological Sciences Graduate Congress, Kuala Lumpur. University of Malaya: Kuala Lumpur, Malaysia, 2010.Poster.

Wong CC, Ng WL, Huang WD, Swarup S. Motility of *Pseudomonas* spp. is controlled by the signalling messenger cyclic diguanylate. 6th International Conference on Structural Biology and Functional Genomic, Singapore. National University of Singapore: Singapore, 2010. Poster 113.

Wong CC, Ng WL, Huang WD, Swarup S. Motility of *Pseudomonas* spp. is controlled by the signalling messenger cyclic diguanylate. 15th Biological Sciences Graduate Congress, Kuala Lumpur. University of Malaya: Kuala Lumpur, Malaysia, 2010.Oral presenter (No: CMB-14), awarded second prize.

Chapter 1. Introduction

1. INTRODUCTION

Bacterial cells can exist either as free-swimming planktonic s or in surface-attached communities known as biofilms. Both movement and ability to form biofilm are key processes for the survival of bacteria in diverse environments. The classical growth and developmental changes in planktonic cells are represented by the lag phase, logarithmic (log) phase, log-to-stationary transition phase and the stationary phase. The log-to-stationary transition phase is marked by the cessation of cell division as nutrients get depleted and with the onset of flagellar development (Amsler *et al.*, 1993; Givskov *et al.*, 1995). The complex biogenesis of the flagellar apparatus requires a well-coordinated regulation of the flagellar pathway. When bacteria come in contact with surfaces, their attachment followed by biofilm formation takes place. During this phase, flagella are shed and bacteria become sessile. Therefore, emergence of flagella is generally considered as a developmental hallmark in many types of bacteria.

While flagellar appearance marks a developmental change in free-living planktonic cells, formation of biofilms leads to yet another developmental pathway in surface-attached bacterial communities. Biofilms are essential elements in virulence, colonization, and survival. Planktonic cells undergo multiple developmental changes during their transition from free-swimming organisms to cells that makeup the biofilms (Stoodley *et al.*, 2002). Flagella-mediated motility is required in many instances, such as initial cell-to-substrate interactions and/or subsequent biofilm development (O'Toole and Kolter, 1998). Appropriate levels of flagellin subunits

seem to be a key factor since over expression of flagellin in *E. coli* results in reduced adhesion to hydrophilic substrates (Landini and Zehnder, 2002). In fully developed biofilms, bacteria such as *P. putida* may even lack flagella (Sauer and Camper, 2001).

To interact with the environment and then react rapidly, bacterial signaling network is highly complex. Signaling systems utilized by bacteria includes cell-cell signaling such as quorum sensing, two-component phosphorelays and second messenger signaling. Genomic and signaling studies on new models led to the finding that signaling proteins are typically modular in nature with each conserved domain performing a distinct biochemical function. Thus it became possible to predict protein function through bioinformatics studies that in recent years, with the availability of complete bacterial genome sequences, has helped reveal a new class of proteins containing GGDEF and EAL domains, although they are absent in archea and eukaryotes (Jenal, 2004; Mills *et al.*, 2011). Gram-negative bacteria tend to have more of such proteins than Gram-positive bacteria (Galperin *et al.*, 2001; Pei and Grishin, 2001). These domains are known to play a part in regulation of several processes such as cell development, virulence, motility and cellulose biosynthesis (Aldridge *et al.*, 2003; Ausmees *et al.*, 1999; Huang *et al.*, 2003; Merkel *et al.*, 1998). Proteins containing GGDEF and EAL motifs have been described in many prokaryotic proteins, often in combination with other putative sensory-regulatory domains such as the PAS and PAC domains whose proposed functions are as sensors for light, redox potential or oxygen concentration (Tamayo *et al.*, 2007; Yan and Chen, 2010). Adaptations involving changes in exopolysaccharides and proteinaceous appendages are regulated in diverse bacteria via proteins with GGDEF and EAL domains. These proteins are predicted to regulate cell adhesion

to surfaces by controlling the level of a secondary messenger, c-di-GMP (D'Argenio and Miller, 2004; Jenal, 2004). The abundance of genes encoding GGDEF and EAL containing proteins argues for the existence of a dedicated regulatory network that converts a variety of different signals into c-di-GMP to function as a secondary messenger in signal transduction (Christen *et al*., 2006).

Interestingly, bidomain proteins with both GGDEF and EAL domains constitute nearly a third of proteins with GGDEF and EAL domains. Most bidomain proteins are found to have a single functional domain. As such, it has been proposed that the noncatalytic domain functions in a regulatory capacity (Wolfe and Visick, 2008). In cases where both domains are active, one or the other enzymatic activities is activated by sensory cues or interaction with other proteins. For instance, MorA affects flagellar motor function by reducing rotation speeds and increasing pauses through its diguanylate cyclase (DGC) activity. While DGC is the dominant activity, it also exhibits weak phosphodiesterase (PDE) activity. The PDE domain affects DGC activity via two novel inter-domain interactions. The PDE domain constitutively imparts a 6-fold increase in DGC activity through the glutamate residue of its EAL motif as well as reduces DGC activity through product inhibition in a dose-dependent manner via the leucine of its EAL motif (Wong, 2011).

MorA is a negative motility regulator identified in our laboratory. It affects the number and timing of flagella expression and biofilm formation in *Pseudomonas* species. MorA is conserved among diverse proteobacteria groups and cyanobacteria. All *Pseudomonas* genomes sequenced thus far possess morA homologs including *P.*

aeruginosa PAO1 (PA4601), *P. fluorescens* Pf0-1 (Pfl01_4876) and *P. putida* KT2440 (PP0672).

Video microscopy showed that the *morA* mutant cells were highly motile throughout different growth phases. Most of the wild type (WT) cells were, however, non-motile in all the three growth phases. Hence, *morA* mutants had a developmental restriction removed on the timing of flagellar formation, resulting in the presence of flagella throughout the growth stages without affecting cell division or cell size.

The loss of *morA* has been shown to affect the *fliC* expression in *P. putida*. This suggests that the disruption of *morA* resulted in derepression of flagellin and expression and, consequently, flagella were constitutively produced. MorA is, therefore, a key component of an alternative regulatory system that normally restricts the timing of expression of the flagellar biosynthesis pathway to late phases of growth in *P. putida* by derepressing flagellin expression in the log-to-stationary phase. A consequence of this appears to be the impairment of biofilm formation. However, when tested for function in *Pseudomonas* species, its role in flagellar development and biofilm formation appears to vary between species. In *P. putida*, expression analyses revealed that transcript levels of the flagellar master regulators *fleQ* and *fliA* remained unchanged between WT and *morA* mutant strains (Choy, 2005). The mechanism by which *morA* regulates flagellin expression in the *P. putida* remains, hitherto, unknown.

As *morA* loss leads to hypermotility, we screened for hypermotility reversion to wild type levels in a library of mutants with *morA* mutation genetic background in order to identify downstream signaling pathway members in the motility pathway in *P. putida*.

A total of 3500 transposon insertion mutants were generated and screened via plate motility assay followed by video microscopy. It was reasoned that any disruption in the flagellar pathway would cause serious defects in swimming motility via the malformation or malfunction of the flagella, resulting in non-motile cells. 76 motility reversion mutants had reversion of the hypermotility phenotype of *morA* mutants to those of wild type while not resulting in non-motility. Thus far, a total of 22 genes have been identified via single primer PCR, of which five genes are of particular interest (Ng, 2006).

Previously, the MorA signaling pathway members were tentatively identified and characterized. In this Thesis, we created targeted knockout mutants in various combinations to investigate the interactions of MorA with MorC, CyaA and the substrate-binding region of ABC-type glycine betaine transport system (OpuAC). I studied their roles in regulating motility, biofilm formation and other related phenotypes. Hence, I set the following objectives for my study:

1. To ascertain the phenotypes observed previously with *morA* mutant and to explore *morA* function in *P. fluorescens* (Pf0-1) (Chapter 4).

   I created markerless knockout strains of *morA* in *P. putida* PNL-MK 25 and Pf0-1 to study if the phenotype observed is conserved across species. Markerless knockout strains of various genes of interest namely: *morC*, *cyaA* and *opuAC* were also created for further studies.

2. To understand the role of CyaA and OpuAC in MorA signaling pathway controlling motility (Chapter 5).

I carried out phenotypic assays with markerless knockout (single and double) mutants to verify if CyaA and OpuAC was involved in MorA regulation of motility. Furthermore, their putative relationship in biofilm formation was also examined.

3. To understand the contribution of MorC and its PDE domain towards the function of MorC in MorA signaling pathway (Chapter 6).

   I carried out phenotypic assays to corroborate with data collected with the motility reversion mutant, O13. I then further established that its function waμμμs dependent on the PDE domain via genetic studies. As MorC contains ASNEF and EAL motifs, I explored the possibility that the function of MorC is dependent on the PDE domain. Site-directed mutants were generated and the biological outcomes were studied. I also carried out cellular localization and gene expression studies as part of the characterization.

4. To investigate the mechanism of MorC function on the motility pathway (Chapter 6).

   In order to understand the specific effects that MorC exerts on the motility pathway, I carried out assays pertaining to flagellin expression and motor function.

This Thesis is organized into Chapters on Introduction, Literature review, Materials and methods, and three Results and Discussion Chapters.

Chapter 2. Literature Review

2.1. Pseudomonads

Pseudomonads are aerobic Gram-negative non-sporing rod-shaped bacteria that are about 3 μm x 0.5μm in size. They are oxidase positive, motile with polar flagella, and do not produce gas. The *Pseudomonas* genus covers a diverse group of bacteria that is ecologically significant. They occur frequently in soil and water and members of the genus can be found in a range of environmental niches. While these are mainly plant pathogens, some species are recognized human and animal pathogens.

The almost universal distribution of the *Pseudomonas* species suggests a great deal of genomic diversity and genetic adaptability. As such, the taxonomy of *Pseudomonas* is difficult to study with classical procedures. These protocols were first developed for the description and identification of organisms implicated in sanitary bacteriology (Palleroni, 2008). The difficulty in identification resulted in many bacterial species being grouped into this genus. After the use of ribosomal RNA composition and sequences as the central criteria in taxonomy studies, it was found that they could be separated into five homology groups. Since then, the number of species in the genera has contracted by ten-fold.

Now, only members of the ribosomal RNA group I are included in the genus, while the four other ribosomal RNA groups have been reclassified in the genera *Burkholderia* (group II), *Delftia* (group III, previously known as *Camamonas*), *Brevundimonas* (group IV) and *Stenotrophomonas* (group V). In addition, phylogentic

analysis of the *Pseudomonas* genus using *gyrB* and *rpoD* nucleotide sequences identified two intra-generic subclusters. Cluster I is further categorized into two complexes while cluster II into three complexes (Yamamoto *et al*., 2000).

Pseudomonads can be further divided into four groups: oxidisers, alkali producers, pathogens and fluorescent species. The fluorescent species are known to produce a fluorescent pigment (Collins *et al.*, 2004). For example, *P. aeruginosa* produces both pyocyanin (blue) and pyoverdine (yellow) that together impart the well-known green pigmentation while *P. fluorescens* and *P. putida* produces only fluorescein.

2.1.1. *Pseudomonas putida*

P. putida is commonly found in soil and water habitats and grows optimally at 25-30ºC. It has multiple polar flagella that are usually 2 to 3 wavelengths in length that allows it to react quickly after sensing environmental changes such as the presence of chemoattractants (Harwood *et al.*, 1989).

The first annotated genome sequence of *P. putida* was first completed in 1995 at The Institute for Genomic Research in Germany. The circular genome was found to contain 6.2 million DNA base pairs of which approximately 60% is made up of guanine and cytosine. The genome comprises of at least eighty genes encoding for oxidative reductases and majority of the genes were involved in the detection of environmental cues to allow it to respond rapidly (Nelson *et al.*, 2002).

The TOL and OCT plasmids found in *P. putida* are able to degrade pollutants such as alkylbenzoate (Muller, 1992; Vandenburgh and Wright, 1983). *Pseudomonas putida* has been designated by the US National Institutes of Health as a "safety strain". It is also an ideal model organism for research on bioremediation as it contains the most number of genes involved in degradation of aromatic or aliphatic hydrocarbons (Nelson *et al.*, 2002).

P. putida possesses a very complex metabolism that allows it to withstand many environmental stresses and degrade a variety of pollutants. For example, *P. putida* CA-3 is able to degrade styrene by either vinyl side chain oxidation or the attack on the aromatic nucleus of the molecule (O'Connor *et al*, 1996) while the fluorescent pigment, siderophores, acts as an iron chelating compound that allows the bacteria to enhance levels of iron and promote the active transport chain (Boopathi and Rao, 1999). The ferric pyoverdine complexes are also used in metabolic processes where oxygen is the electron acceptor (Lopez and Henkels, 1999).

To respond to chemical and physical stresses, *P. putida* can alter its degree of fatty acid saturation, the cyclopropane fatty acids formation, and the *cis-trans* isomerization. During the transition from growth to stationary phase, higher fatty acid saturation leads a cell membrane that is more fluid. This in turn leads to improved substrate uptake that allows for better survivability (Härtig *et al.*, 2005).

2.1.2. *Pseudomonas putida* PNL-MK25

Pseudomonas putida PNL-MK25 is an antibiotic-resistant derivative of the plant growth-promoting rhizobacterial (PGPR) strain ATCC 39169 (Adaikkalam and Swarup, 2002). *P. putida* ATCC 39169 has been described as being effective in promoting the growth of root crops and inhibiting diseases such as root rot (Suslow, 1986). This makes it highly suited for use in environmental biotechnology.

P. putida PNL-MK25 has been previously well-characterized in our laboratory. In a previous study, the expression of *gus*-tagged genes was examined in 12 Tn*5*-*gus* mutants of *P. putida* PNL-MK25 under various conditions chosen to mimic the soil environment (Syn *et al.*, 2004). Two genes, *nql* and *cyoD*, were consistently amongst the most highly expressed under the variety of low-nutrient conditions tested. The promoters of *nql* and *cyoD* are, thus, potentially useful in driving the expression of foreign genes in nutrient-scarce conditions in soil.

This strain also has moderate levels of copper tolerance due to the presence of the *cueAR* operon, which encodes a putative P1-type ATPase (Adaikkalam and Swarup, 2002). Moreover, *P. putida* PNL-MK25 is also desirable as a target strain for further studies due to its ability to tolerate high levels of the solvent, xylene (Syn, 2001). In another *P. putida* strain, this high level of tolerance has been shown to be due to a combination of three efflux pumps, TtgABC, TtgDEF, and TtgGHI, with TtgGHI playing the key role (Rojas *et al.*, 2001; Rojas *et al.*, 2003).

Phylogenetic analysis shows that most of the gene sequences of this strain are more closely related to *P. fluorescens* Pf0-1 strain rather than any other *P. putida* strains (Adaikkalam and Swarup, 2002; Syn *et al.*, 2004).

2.2. Signaling network in bacteria

In bacterial systems, the operon hypothesis pointed to a simple regulatory mechanism, namely the activation of a transcription factor through the direct sensing of a diffusible environmental cue. Through joint effort in bacterial behavior and physiological studies, Adler, Koshland and many other researchers had uncovered new and distinctive signaling systems (Aravind *et al.,* 2010).

The mainstream view in the early 1990s was that eukaryotic and prokaryotic signaling systems are different from each other. In areas where there are similarities such as the usage of cyclic nucleotides as signaling molecules, there was no evidence to suggest that the machinery involved was conserved between the bacteria and the eukaryotes. The viewpoint changed largely due to genomic studies as well as signaling studies on new models. This advancement in knowledge led to the finding that signaling proteins are typically modular in nature and each conserved domain performed a distinct biochemical function. Thus, it is possible to predict the protein function based on the domains found in it via bioinformatics studies.

As bacteria are constantly interacting with their environment by exchanging information with other cells, sensing and responding to environmental cues, the signaling network is a complex and essential part of life. Signaling systems includes

cell-cell signaling such as quorum sensing, two-component phosphorelays and second messenger signaling.

The signaling cascade involves signal generation, perception, transmission and response. Signals can be generated by small chemicals or through protein-receptor interactions. For most of the signaling systems studied thus far, the complete signaling process is not elucidated fully in that some steps or components are not known.

Sequence analysis of the signaling proteins led to the discovery of several new domains belonging to different functional categories. These included: (i) The sensor domains which recognizes and respond to diverse signals; (ii) novel signaling receptors; (iii) intramolecular signal transmitter domains; (iv) novel enzymatic domains and (v) bacterial peptide tagging systems.

2.2.1. Cyclic-di-GMP signaling

The most prevalent cyclic nucleotides are 3'-5'-cyclic adenosine monophosphate (cAMP), 3'-5'-cyclic guanosine monophosphate (cGMP), bis-(3'-5')-cyclic dimeric guanosine monophosphate (c-di-GMP) and guanosine tetraphosphate (ppGpp). Of all the second messengers, c-di-GMP is more ubiquitous in bacterial system. It was first discovered in *Gluconacetobacter xylinus* as an allosteric cellulose synthase (Ross *et al*, 1987). Thus far, c-di-GMP has been shown to regulate many key bacterial functions such as motility, biofilm formation, and pathogenesis (Romling and Amikam, 2006).

C-di-GMP turnover is controlled by the opposing action of DGCs and PDEs (Fig. 2-1). DGCs contains GGDEF domain and can synthesize c-di-GMP from two molecules of GTP. All cyclase domains seem to be derived from different families of nucleic acid polymerases.

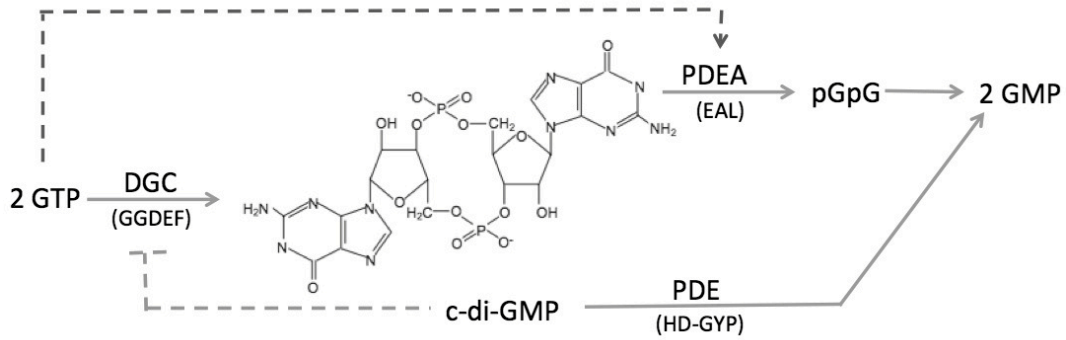

Fig. 2-1. Schematic of c-di-GMP synthesis and degradation. The GGDEF motif containing DGCs catalyzes c-di-GMP synthesis from 2 molecules of GTP. The synthesis of c-di-GMP can be subjected to negative allosteric feedback regulation (indicated by dashed line). Degradation of c-di-GMP into the linear form 5'-pGpG is catalyzed by the EAL domain and positively regulated by GTP (indicated with dashed line and arrow). c-di-GMP is hydrolyzed by PDEAs that contains the EAL motif into linear pGpG before being hydrolyzed by other PDEs into two moelcules of GMP. HD-GYP domain PDEs hydrolyze c-di-GMP completely into two GMPs. (Modified from Tamayo *et al.,* 2007)

Current research suggests that cNMP cyclase and GGDEF domains are related to the classical palm-domain polymerases whereas the *E.coli* CyaA-like cyclases are related to the polymerase β superfamily (Tao *et al.,* 2010). PDEs catalyze the hydrolysis of c-di-GMP into pGpG or GMP. (Tal *et al*, 1998). The phosphodiesterases belong to at least four major families:

1) The HD superfamily: HD-GYP c-di-GMP phosphodiesterase and cNMP phosphodiesterase
2) The calcineurin-like superfamily
3) The metallo-β-lactamase superfamily and
4) The EAL superfamily (Aravind and Koonin, 1998; Galperin *et al*., 1999)

Proteins with DGC or PDE domains can be found widely in most bacterial phyla but are absent from archea and eukarya (Jenal, 2004). Such proteins display typical multimodular arrangement where the catalytic domains are fused to various signal receiver and/or localization domains. Thus it is likely that c-di-GMP is used to link environmental cues to lead to appropriate alterations in bacterial physiology and behavior.

An array of extrinsic and cellular signals can be collected and incorporated to regulate different cellular phenotypes through the use of c-di-GMP signaling modules (Fig. 2-2). One of the most common sensor domains is the PAS domain. The PAS motif is an acronym of the *Drosophila* period clock protein (PER), vertebrate aryl hydrocarbon receptor nuclear translocator (ARNT) and *Drosophila* single-minded protein (SIM). It has been found in many proteins that can sense redox potential, cellular energy levels and light. In the case of *E. coli*

AER, the PAS motif contains a binding pocket for flavin adenine dinucleotide (FAD). It has been postulated that the FAD functions as a redox-sensing moiety. In RbdA, low-oxygen concentration is sensed by PAS domain that in turn controls its PDE activity in regulation of biofilm dispersal (An *et al.*, 2010).

Signals from other systems can also be incorporated to regulate c-di-GMP levels. For example, quorum-sensing signals activate phosphatase action on TpbB, which is in turn deactivated and lead to reduction in biofilm formation (Ueda and Wood, 2009). Other examples include the assimilation of diffusible signal factor, environmental cues and histone-like nucleoid structuring protein to control for biofilm dispersal and virulence, twitching motility and curli formation respectively.

Signals sent by c-di-GMP are transferred to different output functions through the binding of c-di-GMP to effector components. There are currently four types of c-di-GMP effector classes known are: the PilZ family proteins, FleQ transcription factor, PelD, and I-site effectors (Hengge, 2009). Riboswitches that carry the conserved RNA GEMM (genes for the environment, membranes and motility) domain also binds to c-di-GMP as a ligand (Sudarsan *et al.,* 2008). Recently, *Xc*CLP, a member of the CRP/FNR superfamily was identified to be a c-di-GMP receptor in the diffusible signal factor-mediated pathways (Chin *et al.,* 2010).

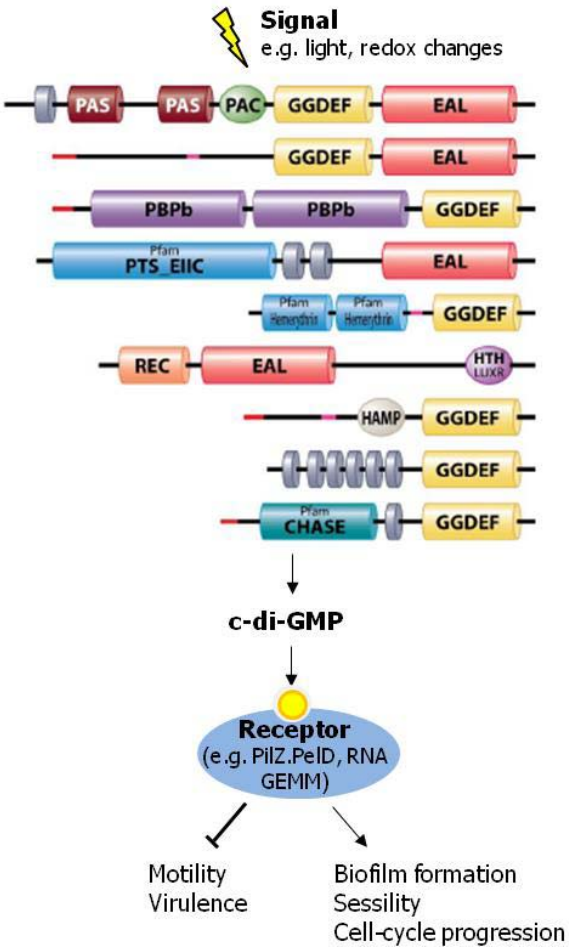

Fig. 2-2. Components of a c-di-GMP signaling module. Sensory domains found on the proteins detect different environmental cues. The activities of DGCs or PDEs on the same protein are then turned on to modulate the c-di-GMP levels. Effector proteins bind to c-di-GMP and subsequently control functions such as motility and biofilm formation. (Adapted from Karatan and Watnick, 2009)

2.2.2. Occurrence of c-di-GMP signaling enzymes

Current databases reported 11,248 proteins that contain GGDEF and EAL domains. Of these, 9943 proteins possess the GGDEF domain and 5574 contains the EAL domain (Seshasayee *et al.,* 2010). 3769 proteins in this list are hybrid GGDEF–EAL bidomain proteins (Fig. 2-3). These proteins are found across 867 prokaryotic genomes and the number of c-di-GMP signaling proteins within each species varies. For example, species within the *Clostridium* genus have between 0 and 43 potential proteins while in *Mycobacterium* genus, the number ranges from 0-22 (Bordeleau *et al.,* 2011; Gupta *et al.,* 2010).

Though suggested to be ubiquitous, there are also bacteria that can successfully form biofilms without c-di-GMP signaling (Holland *et al*., 2008). Majority of bacterial species with genome sizes below 2Mbp and 15% of bacterial species with genome sizes over 2Mbp do not show bioinformatics indications of c-di-GMP production (Seshasayee *et al.,* 2010). Hence, the complexity of the signaling systems is not linearly correlated with genome size, pointing to a highly flexible make-up.

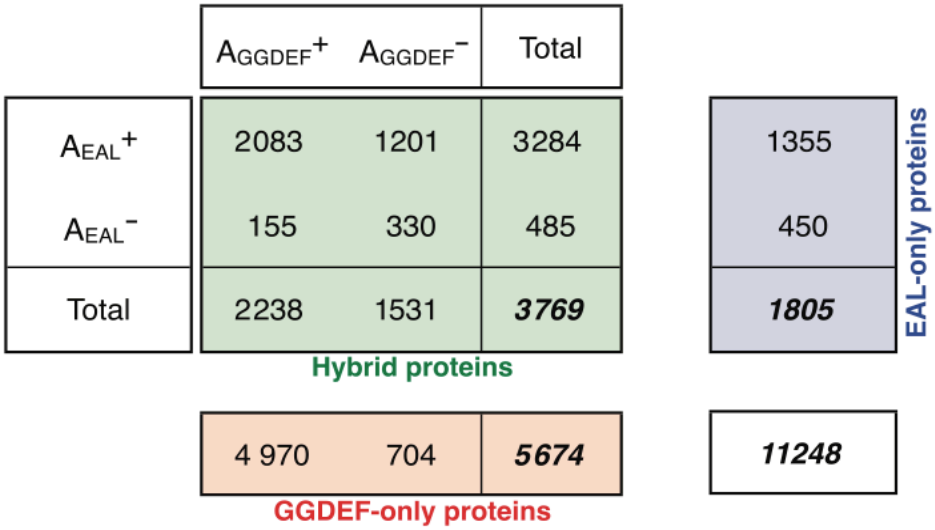

Fig. 2-3. Occurrence of GGDEF and EAL domains across 867 bacterial genomes. GGDEF-EAL, GGDEF-only and EAL-only domain containing proteins are reflected in green, red and blue respectively. Different combinations of intact (A_{GGDEF+} and A_{EAL+}) and degenerate (A_{GGDEF-} and A_{EAL-}) sites in hybrid proteins are denoted with green boxes. (Source: Seshasayee *et al*., 2010)

2.2.3. Redundancy of c-di-GMP signaling enzymes

The large number of c-di-GMP signaling proteins found in a single species suggests that there is redundancy. This is, however, only observed in cases where the intracellular c-di-GMP level is modulated by several proteins, which then regulate phenotypes via specific regulators (Boehm *et al.,* 2010). In majority of the cases, specific enzymes can alter phenotypes through its function (Huang *et al.,* 2003 ; Kuchma *et al.,* 2007). Thus, it is of interest to find out how the activities of these proteins are separated in the cell.

The sequestration of c-di-GMP signaling enzymes were suggested to explain how signaling specificity exists among these large sets of signaling enzymes (Hengge, 2009). Proteolysis of specific signaling proteins was reported to occur to achieve temporal sequestration (Perry *et al.,* 2004). Furthermore, it was shown that the expression levels of c-di-GMP genes vary in different conditions, resulting in different enzymes being active (Jonas *et al.,* 2008; Weber *et al.,* 2006). Distinct cellular localization of the enzymes was also described to affect the protein function (Paul *et al.,* 2004; Ryan *et al.,* 2006). Functional sequestration is also described as a way to control cross talk. This occurs when the signaling process happens through particular effectors that are activated by specific protein-protein interactions (Ryan *et al.,* 2006).

Partner domains found on the proteins mediate the sequestration of the proteins via these varied ways. These partner domains may sense specific environmental cues or

contains localization signals (Table 2-1). This may well be the reason why these proteins have such diverse domain architectures.

Table 2-1. Spatial localization signals and partner domain occurrence for GGDEF and EAL proteins.

	GGDEF	EAL	Hybrid
Total proteins	5674	1805	3769
Localization signals			
With localization signal[1] *n* (%)	3193 (56)	643 (36)	2142 (56)
Sec signal peptide, *n*	3090	605	2030
Tat signal peptide, *n*	1438	417	1076
Lipoprotein signal, *n*	112	14	100
Partner domains			
With partner domains	2550 (45)	473 (26)	2636 (70)
With PAS domain	801	21	1740
With GAF domain	445	41	357
With REC domain	552	123	237
With HAMP domain	327	6	394
With HDOD domain	28	128	0
With unannotated sequence[2]	1195	491	507

[1]*The sets of proteins corresponding to each of the four localization signals are not mutually exclusive. 96% of proteins containing at least one of the four signals have transmembrane helices.*

[2]*Proteins with unannotated sequence stretches (> 100 amino acids) are not included in the total number of proteins with partner domains.*

(Source: Seshasayee *et al*., 2010)

2.2.4. GGDEF-EAL bidomain proteins

The existence of GGDEF-EAL bidomain proteins with potentially opposing enzymatic activities is a cipher, as it makes no apparent sense for these proteins to be widely encoded by microbial genomes. Thus far, research shows that functioning of these proteins fall roughly into three types. In many cases, only one of the domains is active while the other domain is inactive as it is encoded with degenerate sequences that possibly may have been functional previously. Some examples of such bidomain proteins include GcpC and GcpF involved in the cellulose synthesis and YciR, which regulates the transcription of CgsD, a curli and cellulose regulator. In the first two instances, *in vivo* assays showed that they are functionally DGCs and not PDEs (García *et al.,* 2004) while YciR is functionally PDE (Weber *et al.,* 2006).

BphG1 and SrcC are bidomain proteins that consist of functional DGCs and PDEs. Specific triggers such as light or presence of other proteins is required to activate one of the enzymatic activities at any given time. In the case of BphG1, the protein is cleaved into two species when expressed in *E. coli,* the larger species exhibited DGC activity while the smaller species have PDE activity that is activated by light (Tarutina *et al.,* 2006). ScrC, on the other hand, acts as a PDE when expressed with ScrA and ScrB. If expressed alone, c-di-GMP levels were found to increase showing that it could also act as a DGC (Ferreira *et al.,* 2008).

Lastly, inter-domain interaction can also play a role. One common example involves nucleotide (GTP) binding to the DGC domain, which would then activate the PDE. RbdA, CC3396 and FimX are some such examples (An *et al.,* 2010 ; Christen *et al*.,

2005; Kazmierczak *et al*., 2006). Inter-domain interaction can also play a role. An example is MtbDGC, a cysteine mutation in the PDE domain leads to a loss of activity in both DGC and PDE (Gupta *et al.,* 2010).

2.3. Bacterial motility

Motility is an important biological feature and requires a large amount of cellular energy. Its roles are exhaustive and include increased nutrient acquisition, evasion of toxins, dispersal in environment and translocation to preferred hosts. Movement can occur by swimming in aqueous environment or on surfaces by swarming or twitching. These are mediated by the flagella or Type IV pili. Swarming motility can be differentiated from swimming motility, as swarming is required for the bacterial cells to move across a hydrated, viscous semisolid surface while swimming allows movement through a low-viscosity environment.

2.3.1. Flagellar-mediated motility

Most bacterial movement is dependent on the flagellum (pl. flagella). While the location of flagella on the cell varies with different bacteria, there are four basic types of arrangements: (i) peritrichous, where the flagella cover the entire cell surface; (ii) monotrichous, where there is a single polar flagellum; (iii) lophotrichous, where there are several flagella at one pole; and (iv) amphitrichous, where there are tufts of flagella at both poles of the cell. *Pseudomonas* species possess a variety of such arrangements. For example, *P. aeruginosa* has a single polar flagellum while *P. putida* and *P. fluorescens* has several polar flagella.

Bacterial cells swim actively by rotating flagellar bundle. Motility can occur in two ways: clockwise and counter-clockwise rotation. The counter clock-wise movement of the flagellar motors and bundling of the flagellar filament results in a smooth swimming "run" that moves the cell forward. In order to change direction, the cell would then "tumble" as the motor moves in a clock-wise direction accompanied with the dissociation of the flagellar bundles (Jarrell and McBride, 2008; Paul *et al.,* 2011).

The motor switches its direction every few seconds to change the swimming direction of the cells for bacteria to seek better environments. Reversal of the motor rotation causes a structural change of the flagellar filament from the left-handed to the right-handed helical form. This makes the flagellar bundle fall apart, as the propelling force is imbalanced that in turn, leads to changes of the swimming direction.

The switch that triggers this change in the helical form of the filament has been found in the atomic structure of flagellin obtained by X-ray crystallographic analysis. When the twisting force produced by quick reversal of the motor rotation is transmitted to the protofilaments, part of flagellin undergoes a slight change in its conformation, thereby making a few of the 11 protofilament strands transform from the L-type into the R-type. As a result, normally left-handed flagellar filament turns into right-handed helical forms (Samatey *et al.,* 2001).

2.3.2. Flagellar structure

Flagellum is a rotary motor of 30nm diameter. While bacterial cells such as E. *coli* is about 1-2μm in length, the FliC filament can be as long as 15 μm. It is one of the most complex of all prokaryotic organelles, consisting of over 20 proteins with approximately another 30 proteins required for its regulation and assembly. The flagellum comprises of three major substructures: the filament, the hook and the basal body (Bardy *et al.*, 2003). Additional structures include the motor and the type III flagellar protein export apparatus (Macnab, 2004).

Firstly, FliF that makes up the rotor ring assemble in the cytoplasmic membrane. This is followed by the attachment of other proteins to the ring in sequence from the base to the tip to form the motor structure. The motor consists of a rotor/switch (C ring) complex containing three proteins involved in generation of torque and the switching of direction as well as the stator (Fig. 2-4). The reversible motor is powered by the transmembrane proton motive force, which in turn powers flagellar rotation (Manson *et al.*, 1998). It is this rotation of the flagellar filaments that drives bacterial movement.

After the motor is formed, the flagellar filament is assembled by the polymerization of 20,000 to 30,000 copies of flagellin into a helical tube structure. These molecules are transported through a long narrow central channel of the flagellum from the cytoplasm to the distal end of the flagellum where they self-assemble with aid of a cap complex. The cap complex is critical for the efficient self-assembly of flagelin as it prepare just one binding site for the flagellin and guides the binding process. The

filament is made up of 11 strands of protofilament with two different conformations known as L and R types. The mixture of protofilaments with different length produces the helical tube structure. (Samatey *et al.,* 2001)

The proximal end of the filament is connected to the flagellar basal body via a hollow flexible hook that is connected to the rod. The basal body comprises of two MS rings, P ring and L ring. The type III flagellar protein export apparatus consists in part of integral membrane components located in the center of the MS ring, with soluble or peripheral components such as the ATPase that drive the export process. (reviewed by Macnab, 1992).

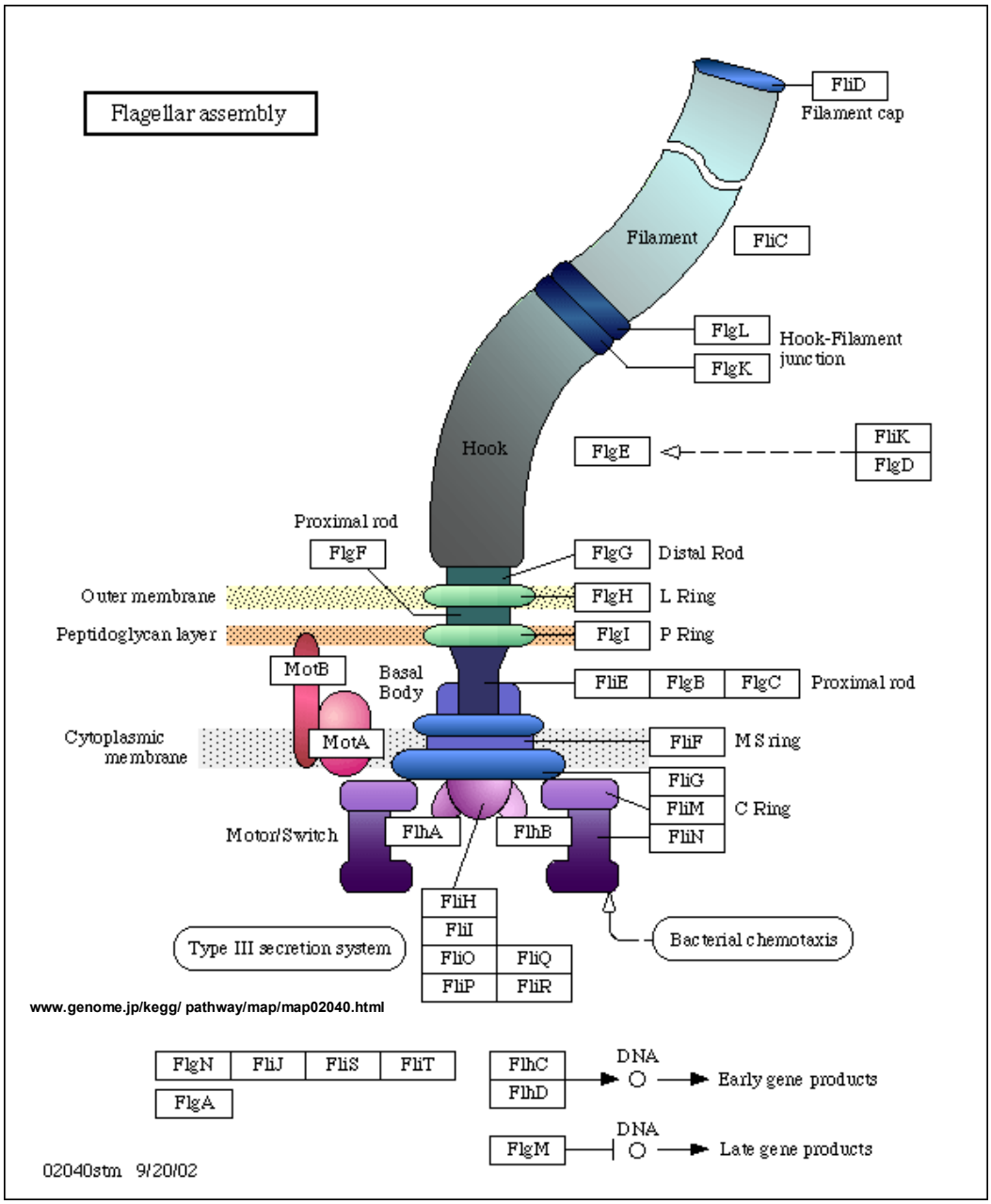

Fig. 2-4. The bacterial flagellum. Basal body hook and filament are shown various colors. Motor components consist of the rotor/switch complex or C ring (violets) and the stator or Mot complexes (reds). The export apparatus consists of membrane components at the center of the basal body MS ring and soluble or peripheral components including the ATPase that drives export. Flagella assembly requires coordinate expression of over 50 genes in a hierarchical manner. (Adapted from www.genome.jp/kegg/ pathway/map/map02040.html.)

2.3.3. Regulation of flagellar formation

Assembly of the flagella apparatus and the regulation of the flagella pathway are highly complex processes. Timing and expression of the flagellar pathway has been well studied in many bacteria (Amsler *et al.*, 1993; Givskov *et al.*, 1995; Prouty *et al.*, 2001). In *E. coli* and *S. typhimurium*, coordinated expression of some 50 genes, organized in a hierarchical manner is required for the assembly and the operation of a flagellum (Aldridge and Hughes, 2002; Dasgupta *et al.*, 2003; reviewed by Macnab, 2003). Genes that are involved in the assembly, function and regulation of flagella can be classified into three classes: (i) *flhDC* master regulator, (ii) those encoding the basal structures and the alternative σ factor FliA (σ^{28}), and (iii) those encoding the filament and chemotaxis machinery.

At the top of the flagellar hierarchy (class I), is the master regulator of the flagellar regulon, *flhDC*. The *flhD* gene encodes a transcription factor, which functions as a positive regulator of the flagellar regulon. In *E. coli,* the *flhD* gene encodes a protein that functions as a global regulator that when overexpressed, can inhibit cell division and therefore indirectly affects the level of gene expression (Prüß and Matsumura, 1997; Prüß *et al*., 1997). The majority of class II genes encode components of the flagellar export system and the basal body. A class II gene, *fliA*, encodes a σ factor, σ^{28} that is specific for flagella genes (Mytelka and Chamberlin, 1996). The class III gene products include flagellin (FliC) which forms the filament, the hook-associated, motor (Mot) and chemotaxis (Che) proteins. The stator forms a channel through which the protons that power the rotation of the flagellum flow (Bardy *et al.*, 2003). The regulatory control for flagellar biogenesis in *P. aeruginosa* was described in detail previously (Dasgupta *et al.*, 2003). The authors based the proposed hierarchy on

the evidence of microarrays of selected mutant strains. Key predictions were validated by promoter activity studies using β-galactosidase reporter assay. In comparison to the three-tiered regulation in multiflagellated *E. coli*, a four-tiered hierarchy (Classes I – IV) is present in monoflagellated *P. aeruginosa*.

At the top of the hierarchy are the transcriptional regulators, FleQ and the alternative σ factor FliA (σ^{28}). FleQ, which is the functional equivalent of *E. coli* FlhDC, and FliA serve to regulate at least 11 operons that set into motion the expression of the rest of the flagella genes. Class II genes encode for the basal structures such as the M, S, and P rings, motor, switch, and the FleSR two-component regulatory system. These genes require FleQ and RpoN (σ^{54}) for their transcriptional activation. The *fleSR* system is believed to control both flagellar synthesis and adhesion to mucin. The *fleR* mutant lacked flagella and was nonmotile and adheres poorly to mucin.

Class III genes encode for the L ring, rod and hook structures, and are positively regulated by the activated response regulator FleR in concert with RpoN. Class IV genes in *P. aeruginosa* are the functional equivalents of Class III genes in *E. coli*, in that they encode for the filament, and the chemotaxis system. The transcription of Class IV genes is dependent on the availability of free FliA following the export of the FliA specific anti-σ factor FlgM through the basal body rod-hook structure (assembled from Class II and III gene products). FlgM has been shown to modulate the activity of FliA and expression of the FliA-dependent flagellin gene *fliC* (Frisk *et al*., 2002).

The importance of transcriptional regulation to the process of flagellar assembly has been known for many years. Also, translational regulation has been recognized to play a significant role (Aldridge and Hughes, 2002). For example, in *Salmonella*, translational regulation influences the secretion of FlgM. Post-translational regulatory mechanisms also control the length of the hook and the ability of the type III secretion system to discriminate between middle and late secretion substrates.

2.3.4. Chemotaxis

Most motile bacteria are able to move towards higher concentration of attractants, usually consisting of signaling molecules or nutrients. Similarly, they are also able to avoid harmful chemicals or repellents. As bacteria are small in size, it is inefficient to make direct spatial detection of chemical gradients. As a result, a chemotactic strategy to make temporal comparisons of effector concentration while moving in a gradient is used instead. This in turn, mean that bacterial cells would swim first and then decide if the chosen direction is in its favor or not. Although swimming direction after each tumble is selected in a random fashion, the presence of a chemical gradient causes cells to bias their random walk by suppress tumbling that result in longer swims towards a favorable direction.

Chemotaxis pathway is well conserved and best studied in the *E. coli* (Fig. 2-5). The response is mediated by a signaling system that depends on protein phosphorylation and is a member of the bacterial two component sensors. The central signaling proteins are the histidine kinase CheA and the response regulator CheY. CheA together with CheW, associates with chemosensory receptors. The ternary complex

formation results in CheA autophosphorylation that in turn, allows the receptors to modulate CheA activity upon chemoeffector binding. CheY is subsequently phosphorylated and then diffuses into the cytoplasm to transmit the signal to the flagellar motors. Binding of CheY enhances the clock-wise rotation of the flagella causing the cells to tumble. As the cell changes direction and swims up a chemo-gradient, the concentration increase results in the inactivation of CheY that in turn, suppress cell tumbling to allow swimming. Adaption to continuous stimulation is mediated by the methyltransferase CheR and methylesterase CheB. These proteins form the core of chemotaxis pathway while other bacteria have more complex systems with multiple sets of chemotaxis genes, receptors and varying mechanism of CheY dephosphorylation.

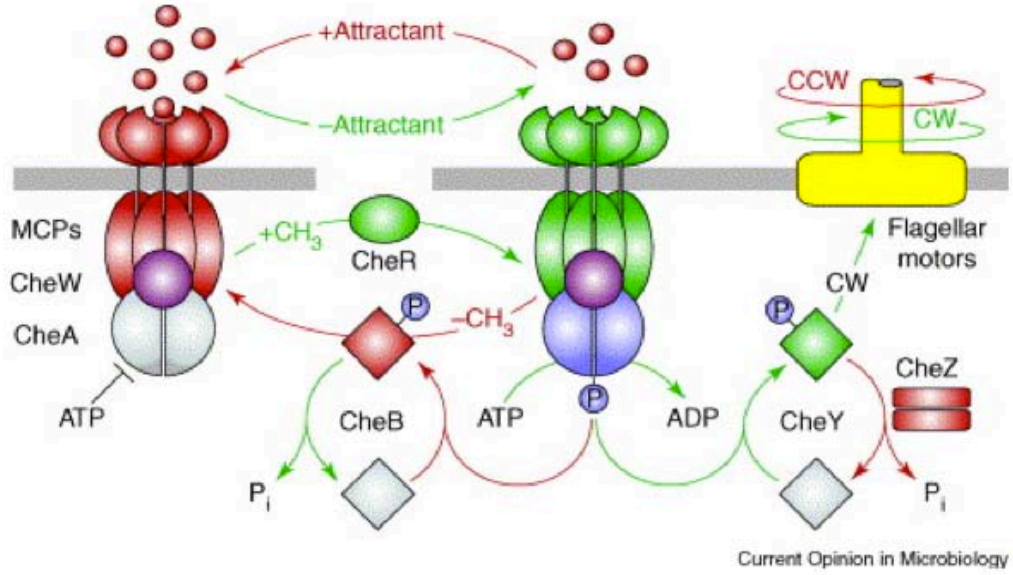

Fig. 2-5. Two-state model of receptor signaling and the chemotaxis phosphorelay pathway. With the exception of the highly schematic rotary flagellar motors, the chemoreceptors (MCPs) and cytosolic signaling proteins (CheA, CheB, CheR, CheW, CheY, CheZ) are depicted in their native subunit organizations. The receptors dimers are arranged further into trimers, which may include the active unit for receptor signaling. Colored modules are representative of active states while the grey modules represent inactive forms. Green modules and reaction arrows represent signaling states that enhance clockwise (CW) flagellar rotation; red modules and reaction arrows represent signaling states that augment counter-clockwise (CCW) flagellar rotation, which is also the default condition in cells. Binding of an attractant ligand or removal of methyl groups shifts chemoreceptor signaling complexes from the kinase-on (green) to the kinase-off (red) signaling state. Attractant release and methyl group addition shift receptor signaling complexes from the inactive CheA (gray) to the active CheA (blue) state. (Adapted from *Parkinson et al.,* 2005)

2.4. Biofilm formation in *Pseudomonas spp.*

Planktonic cells undergo multiple developmental changes during their transition from free-swimming organisms to cells that make up the surface-attached bacterial communities known as biofilms (reviewed by Stoodley *et al*., 2002). Biofilms are formed on both abiotic and biotic surfaces. They are usually persistent, and can resist antibiotic treatment, biocide treatment, and other host immune responses. In general, biofilm development occurs in five stages, namely, attachment, irreversible attachment, early biofilm development, biofilm maturation, and dispersal (Karatan and Watnick, 2009). The level of flagellin expression appears to be a key factor in the initial attachment as overexpression of flagellin in *E. coli* resulted in reduced adhesion (Landini and Zehnder, 2002). In fully developed biofilms, bacteria such as *P. putida* may even lack flagella (Sauer and Camper, 2001).

The first stage of attachment allows monolayer of cells to be formed and initiates subsequent development of the biofilm. The next stage of biofilm formation involves extracellular polymeric substances (EPS) to form "irreversible attachment" of cells and to provide structural support for further development (Branda et al., 2005). The cells in the biofilm then aggregate and form a hydrated polymer network (the biofilm matrix) with EPS, where many different processes occur. Quorum sensing is a key process that coordinates EPS production and cell differentiation in the biofilm during the maturation process that leads to the formation of a mushroom-like macroscopic structure in mature biofilm (Jayaraman and Wood, 2008). Following biofilm maturation, dispersal takes place when the conditions for the biofilms no longer remain ideal.

2.5. MorA as a membrane bound negative motility regulator

MorA is a negative motility regulator that affects the timing of flagella expression and biofilm formation in *Pseudomonas* species. It is conserved among diverse proteobacteria groups and cyanobacteria. All *Pseudomonas* genomes sequenced thus far possess *morA* homologs including *P. aeruginosa* PAO1 (PA4601), *P. fluorescens* PfO-1 (Pflu02005114) and *P. putida* KT2440 (PP0672).

The primary structure of predicted MorA proteins from various *Pseudomonas* species is well conserved with sequence similarity values ranging from 57% to 93%. Members of the *Pseudomonas* MorA family: (i) are present as single copy in the genome, (ii) most possess transmembrane domains, (iii) possess a central sensory domain of PAS-PAC motifs, and (iv) contains C-terminal GGDEF and EAL domains (Fig. 2-6). The N-terminal transmembrane region is more variable (30% to 80% similarity) compared to over 80% similarity in the PAS-PAC and the GGDEF and EAL domains.

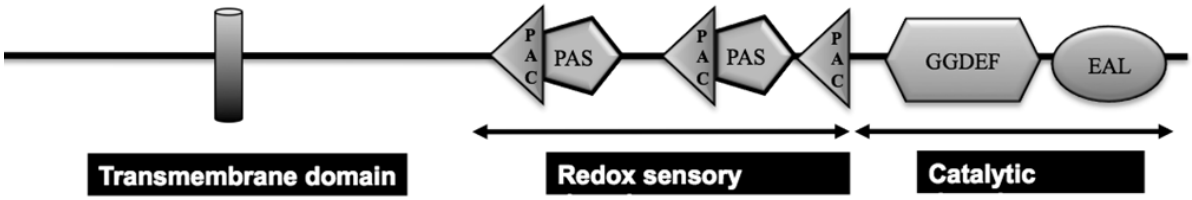

Fig. 2-6. Domain architecture of MorA family members in *Pseudomonas* species. The three conserved regions of the predicted MorA proteins are (i) transmembrane domain(s) (vertical bar) in majority of the proteins, (ii) sensory PAS and PAC domains, and (iii) catalytic GGDEF and EAL domains

Video microscopy showed that the *morA* mutant cells were highly motile throughout the different growth phases. Most of the wild type (WT) cells were, however, non-motile in all the three log growth phases. Hence, *morA* mutants have a developmental restriction removed on the timing of flagellar formation, resulting in the presence of flagella throughout the growth stages without affecting cell division or cell size (Fig. 2-7).

DNA microarray analyses of gene expression in *P. aeruginosa* PAOI and its *morA* mutant using Affymetrix™ chips revealed that the mutation of *morA* altered the expression of 561 genes 2-fold or more, 234 of which were up-regulated and 327 down-regulated (Choy *et al*, 2004). Out of the 234 genes that were up regulated in the *morA* mutant, 111 were genes of known function. Out of the 327 genes that were down regulated in the *morA* mutant, 190 were genes of known function. MorA also affects transcript levels of several (ECF-type) σ factors and their downstream genes, which was validated by quantitative real-time PCR analyses. Additionally, MorA regulates the biosynthetic pathway of the key phosphate donor, acetyl phosphate (AcP) by affecting the transcription of the metabolic gene *pta*. AcP has been further implicated as a regulator of many important pathways, including the flagella pathway (Choy, 2005).

Genes implicated in antibiotic resistance and susceptibility, energy metabolism and secreted factors (toxins, enzymes, alginate) were highly expressed in the *morA* mutant. On the other hand, genes encoding type II secretion system proteins were found to be downregulated in the *morA* mutant. Several classes like transport of small molecules, putative enzymes and transcriptional regulators had similar number of

genes that were either upregulated or downregulated. The expression of genes involved in motility and attachment remained mostly unchanged including genes involved in flagellar or type IV pili biogenesis.

The loss of MorA has been shown to affect the expression *fliC* in *P. putida.* This suggests that the disruption of *morA* resulted in derepression of flagellin expression and, consequently, flagella were constitutively produced. MorA is therefore a key component of an alternative regulatory system that normally restricts the timing of expression of the flagellar biosynthesis pathway to late phases of growth in *P. putida* by derepressing flagellin expression in the log-to-stationary phase. A consequence of this appears to be the impairment of biofilm formation (Fig. 2-8).

In *P. putida*, expression analyses revealed that transcript levels of the flagellar master regulators *fleQ* and *fliA* remained unchanged between WT and *morA* mutant strains (Choy, 2005). Also, global gene expression profiling in *P. aeruginosa* has also demonstrated that over 80 genes were affected by the loss of *morA* although genes involved in motility were not significantly altered in their expression levels. The mechanism by which *morA* regulates flagellin expression in the *P. putida* remains, hitherto, unknown.

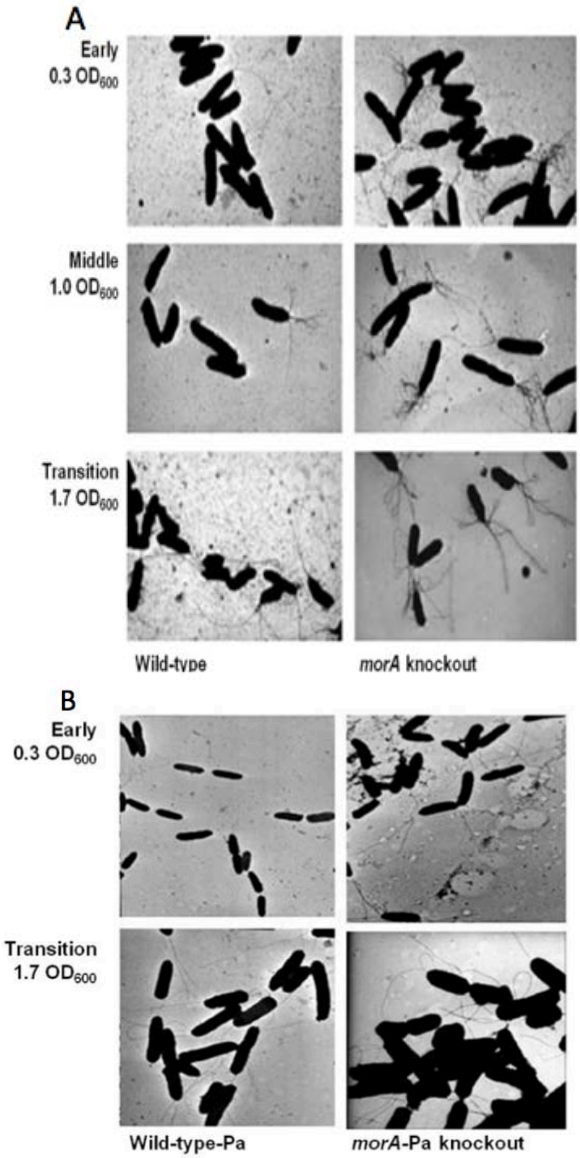

Fig. 2-7. Flagella phenotype of *morA* knockout and WT strains in (A) *P. putida* and (B) *P. aeruginosa*. (A) TEM shows that hyperflagellation phenotype is observed in *P. putida morA* knockout mutant throughout all growth phases. (B) In *P. aeruginosa,* however, hyperflagellation is absent. (Adapted from Choy e*t al.,* 2004)

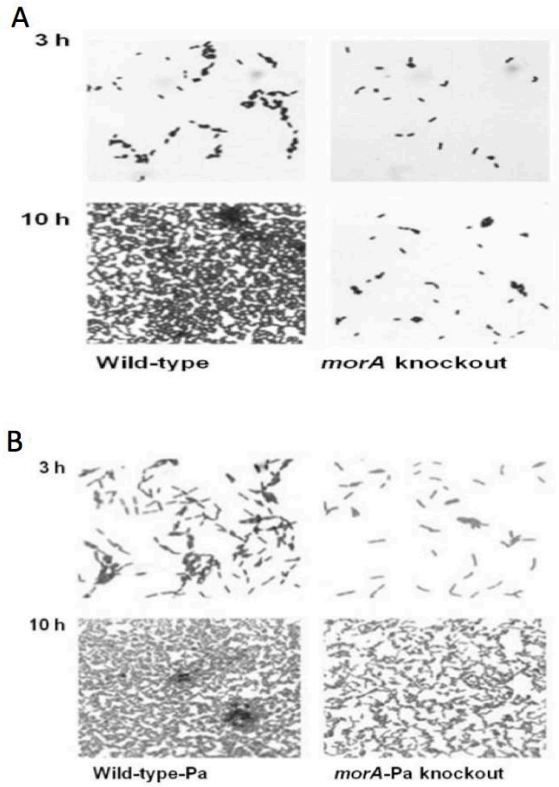

Fig. 2-8. Biofilm formation of *morA* knockout and WT strains in (A) *P. putida* and (B) *P. aeruginosa*. (A) Biofilm formation of *morA* mutant is reduced in both early and late time point when compared to WT. (B) In *P. aeruginosa,* biofilm formation of *morA* mutant is reduced less when compared to WT. However, the difference is not as evident in the late time point (Adapted from Choy *et al.,* 2004).

2.6. Reversion mutants of *morA* phenotype

As *morA* loss leads to hypermotility, we screened for hypermotility reversion to wild type levels in a library of mutants with *morA* mutation genetic background in order to identify downstream signaling pathway members in the motility pathway in *P. putida*. It was reasoned that any disruption in the flagellar pathway would cause serious defects in the motility of the cell via the malformation or malfunction of the flagella causing non-motile cells. Thus non-motile mutants had been excluded from the study during the primary and secondary selection process involving motility plate assay and video microscope analysis respectively. This was by no means an exhaustive search as there may be critical genes in the intermediate pathway that can cause the mutant to be non-motile as well.

Seventy-six motility reversion mutants were able reverse the hypermotility phenotype of *morA* mutants to those of wild type while not resulting in non-motility. Thus far, a total of 22 genes were identified via single primer PCR, of which five genes was of particular interest (Table 2-2) (Ng, 2006).

Motility assay showed that motility of the various mutants varies, though, all the mutants exhibited less motility than *morA* mutant, MorDCK03 (Fig. 2-9). Several mutants namely K14, K15, D11 and D31 showed motility to be even less than that of the WT. As biofilm formation assay was not part of the selection process, it was also performed on the mutants (Fig. 2-10). Results showed that the biofilm formation is varied in the mutants but that most of the mutants presented increased biofilm formation. Lastly, the growth curve (Fig. 2-11) plotted with the various mutant strains showed that the mutations did not affect cell growth.

Table 2-2. Transposon motility reversion mutants in *morA* knockout background identified via single primer PCR. This table shows the mutant name, length of sequence obtained from DNA sequencing and subsequently used for database searching with BLAST tool, similarity as well as the cellular location of the gene product. 22 genes were identified in total of which 5 were conserved hypothetical proteins. Five of the genes were of interest and was highlighted in bold in the table (Ng, 2006). Similarity denotes the amount of High-Scoring Segment Pairs between the query sequence and database sequence. Mutant names are assigned names of the motility revertant mutants. Gene names and cellular localization are based on data derived from NCBI database.

Mutant Names	Similarity (%)	Gene Name	Cellular localization
O13	91	**Putative diguanylate cyclase/phosphodiesterase (GGDEF & EAL domains) with PAS/PAC and GAF sensor(s) morC**	cytosolic
D4	91	**Adenylate cyclase CyaA**	cytosolic
D14	91	**Ankyrin**	cytosolic
K15	97	**Rod shape-determining protein RodA**	transmembrane
Q12	96	**Substrate-binding region of ABC-type glycine betaine transport system**	integral membrane protein/ lipid anchor
H6	92	**Substrate-binding region of ABC-type glycine betaine transport system**	integral membrane protein/ lipid anchor
D11	92	DNA Pol III alpha subunit	cytosolic
L16	97	Isochorismatase hydrolase	cytosolic
J21	92	NAD-dependent epimerase/dehydratase	cytosolic
K14	98	Penicillin-binding protein, transpeptidase	transmembrane
K5	100	extracellular solute-binding protein, family 3	cytosolic
F5	93	Abortive Infection Protein	transmembrane
F2	95	Abortive Infection Protein	transmembrane
Q3	88	Abortive Infection Protein	transmembrane
G18	100	Ribulose-phosphate 3-epimerase	cytosolic
E6	96	Ribulose-phosphate 3-epimerase	cytosolic
E10	93	HIO933-like Protein	cytosolic
M6	91	Catalase-like	cytosolic
H6	100	Binding-protein-dependent transport systems inner membrane component	integral membrane protein/ lipid anchor
D30	85	ribosomal 5S rRNA E-loop binding protein Ctc/L25/TL5 [Pseudomonas fluorescens Pf-5]	cytosolic
D28	98	Exonuclease VII, large subunit	cytosolic

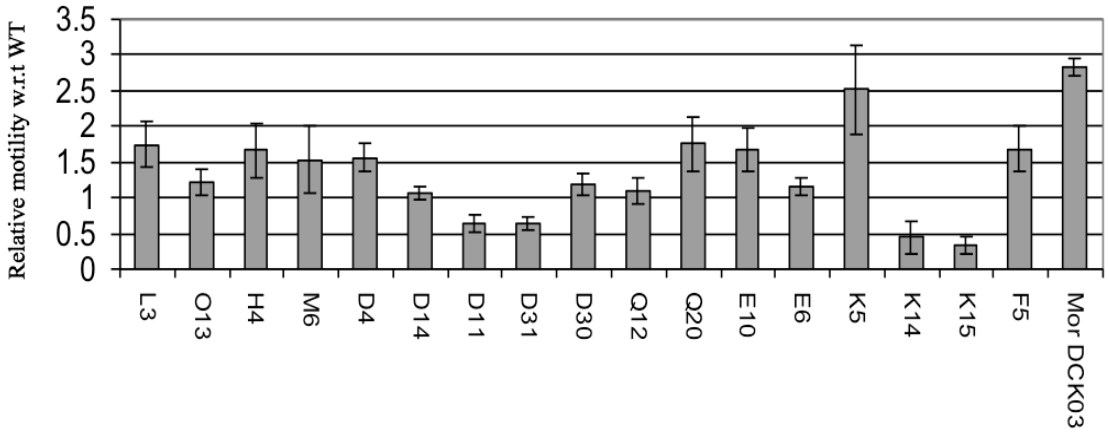

Fig. 2-9. Motility reversion mutants exhibit reduced motility when compared to *morA* mutant. Relative motility is derived by the colony diameter of the mutant over the colony diameter of WT thus the relative motility of WT is equivalent to the value of 1. Mor DCK03 acting as a control showed about 2.8-fold increase in swimming motility through 0.4% (w/v) soft agar compared to WT. This was consistent with the results obtained previously (Choy and Swarup, 2004). Values were based on the average of three independent experiments with five replicates each. Standard errors were represented as vertical bars. Mutant descriptions are listed in Table 2-2 (Ng, 2006).

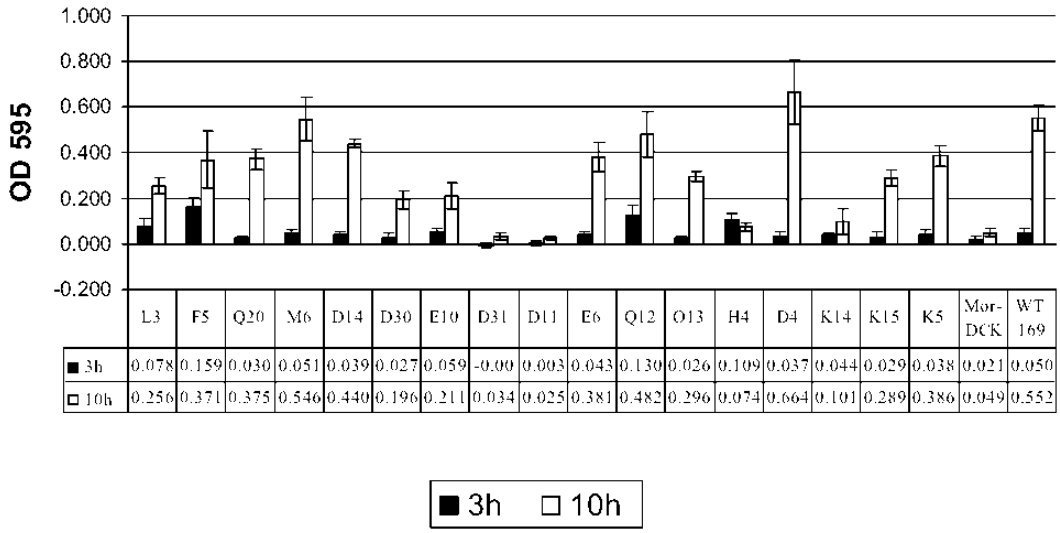

	L3	F5	Q20	M6	D14	D30	E10	D31	D11	E6	Q12	O13	H4	D4	K14	K15	K5	Mor-DCK	WT 169
3h	0.078	0.159	0.030	0.051	0.039	0.027	0.059	-0.00	0.003	0.043	0.130	0.026	0.109	0.037	0.044	0.029	0.038	0.021	0.050
10h	0.256	0.371	0.375	0.546	0.440	0.196	0.211	0.034	0.025	0.381	0.482	0.296	0.074	0.664	0.101	0.289	0.386	0.049	0.552

Fig. 2-10. Motility reversion mutants exhibit varying amount of biofilm formation. Most of the motility reversion mutants exhibited biofilm phenotype intermediate to that of the WT and Mor DCK03 strains. Values were based on the average of three independent experiments with six replicates each. Standard errors were represented as vertical bars (Ng, 2006).

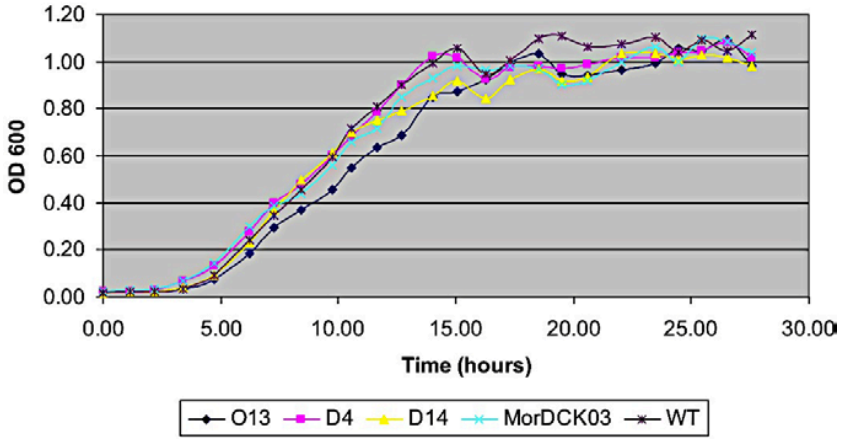

Fig. 2-11. Growth curves of *P. putida* WT and various mutants in LB medium showed no differences in the growth. Absorbance at 600nm (OD_{600}) of bacterial cultures growth in LB medium at 30ºC was measured at intervals of one to two hours. Values are based on the average of two independent experiments with three replicates each (Ng, 2006).

Chapter 3. Materials and methods

3.1. Bacterial strains, plasmids and growth conditions

Bacterial strains and plasmids used in this study are listed in Table 3-1 and 3-2 respectively. *P. putida* and *P. fluorescens* strains were routinely grown at 30ºC while *E.coli* strains were grown at 37ºC in Luria-Bertani (LB) with suitable antibiotics (Table 3-1). The following antibiotics were added at the final concentration noted below to the growth media where necessary, Cm, chloramphenicol 15 μg/mL; Rf, rifampicin 20 μg/mL; Gm, gentamycin 15 μg/mL (*E. coli*) or 30 μg/mL (PNL-MK25); Amp, ampicillin 100 μg/mL; Tet, tetracycline 15 μg/mL (*E. coli*) or 30 μg/mL (PNL-MK25). For solid media, 1.5% final concentration of agar was added. Bacterial growth was measured spectrophotometrically at OD_{600}.

Table 3-1. Bacterial strains used in this study. Flippase recombination target (FRT) sites are utilized to remove the Gm marker from the cell in the generation of markerless knockout mutant strains.

Strains	Relevant characteristics	Source/reference
P. putida PNL-MK25	Antibiotic-resistant derivative of the plant growth-promoting rhizobacterial (PGPR) *P. putida* strain ATCC 39169; Designated as WT. $Cm^r Rf^r$	Adaikkalam and Swarup, 2002
C3H	PNL-MK25 mutant (*morA*::mTn5-*gfp*);$Cm^r Rf^r$ Km^r Gm^r	Choy, 2005
MorDCK03	PNL-MK25 mutant (*morA*::*accCI*);$Cm^r Rf^r$ Gm^r	Choy, 2005
Δ*morA*	PNL-MK25 mutant (*morA*::FRT insertion);$Cm^r Rf^r$	This study
Δ*morC*	PNL-MK25 mutant (*morC*::FRT insertion); $Cm^r Rf^r$	This study
Δ*morA*Δ*morC*	PNL-MK25 mutant (*morA*::FRT insertion) (*morC*::FRT insertion);$Cm^r Rf^r$	This study
Δ*cyaA*	PNL-MK25 mutant (*cyaA*::FRT insertion);$Cm^r Rf^r$	This study
Δ*morA*Δ*cyaA*	PNL-MK25 mutant (*morA*::FRT insertion)(*cyaA*::FRT insertion);$Cm^r Rf^r$	This study
Δ*opuAC*	PNL-MK25 mutant (*opuAC*::FRT insertion);$Cm^r Rf^r$	This study
Δ*morA*Δ *opuAC*	PNL-MK25 mutant (*morA*::FRT insertion)(*opuAC*::FRT insertion);$Cm^r Rf^r$	This study
P. fluorescens WT_{Pf}	Wild-type; Amp^r	Silby *et al.,* 2009
Δ$morA_{Pf}$	Pf0-1 mutant ($morA_{Pf}$::FRT insertion); Amp^r	This study
E. coli DH5□	*(lacZYA-argF)U169 hsdR17(r - m +) recA1 endA1 relA1 deoR*	Lab collection
JM109	*thi-1 hsdR17(rK- mK+) supE44 relA (lac-proAB) [F'traD36 proAB lacIqZ M15]*	Lab collection
BL21	Protein expression strain	Novagen

Table 3-2. Plasmids used in this study.

Plasmid	Relevant characteristics	Source
pEX18ApGW	Suicide vector for markerless knockout mutant generation; Amp^rGm^r	Choi and Schweizer, 2005
pEX18ApGW-*morA*	Double crossover knockout construct for *morA* gene	This study
pEX18ApGW-$morA_{pf}$	Double crossover knockout construct for $morA_{pf}$ gene	This study
pEX18ApGW-*morC*	Double crossover knockout construct for *morC* gene	This study
pEX18ApGW- *opuAC*	Double crossover knockout construct for *opuAC* gene	This study
pEX18ApGW-*cyaA*	Double crossover knockout construct for *cyaA* gene	This study
pGB1	Broad host range vector; Amp^rTet^r	Bloemberg *et al.,*1997
pGB3	pGB1 vector carrying GFP; Amp^rTet^r	Bloemberg *et al.,*1997
pGB1morA	Full-length *morA* gene with its native promoter cloned into pGB1	Choy and Swarup, 2005
pGB1 $morA_{pf}$	Full-length $morA_{Pf}$ gene with its native promoter cloned into pGB1	This study
pGB1cyaA	Full-length *cyaA* gene with its native promoter cloned into pGB1	This study
pGB3morA	Full-length *morA* gene with its native promoter cloned into pGB3	Fu SJ, unpublished data
pGB3morC	Full-length *morC* gene with its native promoter cloned into pGB3	This study
pJET	PCR cloning vector; Amp^r	Fermentas
pCRTOPO4	PCR cloning vector; Amp^r	Invitrogen

Plasmid	Relevant characteristics	Source
pTNS2	Helper plasmid; Amp^r	Choi and Schweizer, 2005
pFLP3	Plasmid encoding FLPase	Choi and Schweizer, 2005
pUC18-miniTn7T-GM	Broad host range mini-Tn7 for integration of single-copy genes into chromosome; Amp^r Gm^r	Choi and Schweizer, 2006
mTn7T-morC	Full-length *morC* gene with its native promoter cloned into pUC18-miniTn7T-GM; Amp^r Gm^r	This study
mTn7T-morC ΔEAL	Mutant *morC,* truncated EAL domain with its native promoter cloned into pUC18-miniTn7T-GM; Amp^r Gm^r	This study
mTn7T-morC-E673K	Mutant *morC,* $_{673}EAL_{675}$ $\rightarrow_{673}KAL_{675}$ with its native promoter cloned into pUC18-miniTn7T-GM; Amp^r Gm^r	This study
mTn7T-morC-L675G	Mutant *morC,* $_{673}EAL_{675}$ $\rightarrow_{673}EAG_{675}$ with its native promoter cloned into pUC18-miniTn7T-GM; Amp^r Gm^r	This study
mTn7T-morC-E754K	Mutant *morC,* $_{754}EAL_{756}$ $\rightarrow_{754}KAL_{756}$ with its native promoter cloned into pUC18-miniTn7T-GM; Amp^r Gm^r	This study
mTn7T-morC-L756G	Mutant *morC,* $_{754}EAL_{756}$ $\rightarrow_{754}EAG_{756}$ with its native promoter cloned into pUC18-miniTn7T-GM; Amp^r Gm^r	This study

3.2. Generation of markerless knockout *Pseudomonas spp.* mutants

The markerless knockout strains were generated using the workflow described in Fig. 3-1. Firstly, 5'gene fragment, 3' gene fragment and an *frt*-flanked *aaCC1* gene cassette were generated using PCR. Fusion PCR was then performed to fuse these fragments together. Conventional molecular biology techniques were then used to introduce the fusion cassette into pEX18ApGW.

The plasmid containing the fusion cassette was then introduced into *P. putida* cells. The resultant clones were then subjected to sucrose selection to identify double-crossover mutants. The clones that were both gentamycin and sucrose resistant were designated putative mutants. To further obtain gentamycin-sensitive clones, pFLP3 were then introduced into these putative clones to facilitate FRT recombination. Since pFLP3 encodes *sacB* (Choi and Schweizer, 2005), Gentamycin sensitive clones were finally subjected to sucrose selection to cure the cells.

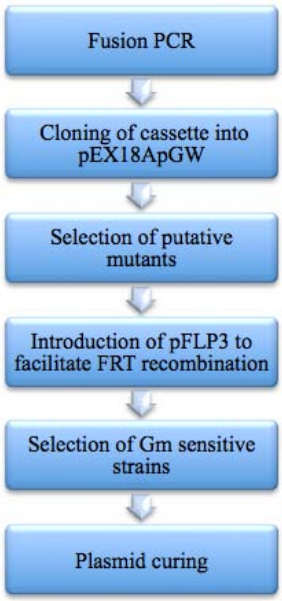

Fig. 3-1. Workflow used for the generation of markerless knockout strains.

3.2.1 Electroporation of *Pseudomonas* culture

Electroporation was carried out as previously described (Choi *et al.,* 2005). Briefly; 6 mL of an overnight culture grown in LB medium was harvested by centrifugation at 16,000g for 2min at room temperature. The cell pellet was then washed twice with 4mL of room temperature 300mM sucrose. The resultant pellet was then resuspended in 200 µL of 300mM sucrose. 500ng of plasmid DNA was mixed with 200 µL electrocompetent cells and transferred to a 2mm gap width electroporation cuvette. After applying a pulse (settings: 25 µF; 200 Ohm; 2.5 kV on a Bio-Rad GenePulserXcell™), 1 mL of LB medium was added immediately and the cells were transferred to a 15mL tube and incubated at 250rpm for 4h at 30ºC. The cells were then plated on plates containing half strength LB with the appropriate antibiotics and incubated at 30ºC for two days or until colonies appeared.

3.2.2 PCR-amplification of the gentamycin resistance gene cassette

A 50µL PCR reaction containing 5ng pPS856 template DNA, 1x BD Clontech Advantage PCR2 buffer, 1x Advantage 2 polymerase mix, 0.2µM of Gm-F and Gm-R primers and 200µM dNTPs. Cycle conditions were 95ºC for 3 min, followed by 30 cycles of 95ºC for 30s, 55ºC for 30s, and 72ºC for 1min 30s and a final extension at 72ºC for 7min. The resulting 1,053bp PCR product was purified by PCR purification clean-up kit and its concentration determined spectrophotometrically via Nanodrop ™.

3.2.3 PCR-amplification of 5' and 3' gene fragments

Two 50µL PCR reactions were prepared. The reaction mixtures contained 20ng genomic DNA, 1x BD Clontech Advantage PCR2 buffer, 1x Advantage 2 polymerase mix, 0.8µM of primers, 5% DMSO and 200µM dNTPs. One mixture contained primers for amplification of the 5' gene fragment while the second mixture contained primers for amplifying the 3' gene fragment. Primers used in generation of gene fragments are described in Table 3-3. Cycle conditions were 95ºC for 3min, followed by 30 cycles of 95ºC for 30s, 60ºC for 30s, and 72ºC for 1min and a final extension at 72ºC for 7min. The resulting PCR product was purified by PCR purification kit and its concentration determined spectrophotometrically via Nanodrop ™.

3.2.4 Fusion PCR of 5' gene fragment, 3' gene fragment and gentamycin cassette

A 50 µL PCR reaction contained 50ng each of the 5' and 3' purified template DNAs, and 50ng of FRT-Gm-FRT template DNA, 1x BD Clontech Advantage PCR2 buffer, 1x Advantage 2 polymerase mix, 5% DMSO and 200µM dNTPs. After an initial denaturation at 95ºC for 3min, 10 cycles of 95ºC for 30s, 50ºC for 30s, and 72ºC for 1 min were run without added primers. The tenth cycle was paused at 30s of the 72ºC extension, primers were added to 0.2µM each, and the cycle was then finished by another 30s extension at 72ºC. The PCR was completed by 20 cycles of 95ºC for 30s, 56ºC for 30s, and 72ºC for 5min, and a final extension at 72ºC for 10min. The resulting PCR product of expected size was purified by gel extraction and its concentration was determined via NanoDrop ™.

3.2.5. Cloning of fusion PCR product into pEX18ApGW

Classical restriction and ligation was carried out for the cloning of markerless knockout cassette via ApaI and SpeI sites that are situated at the *attR1* and *attR2* sites shown in Fig. 3-1.

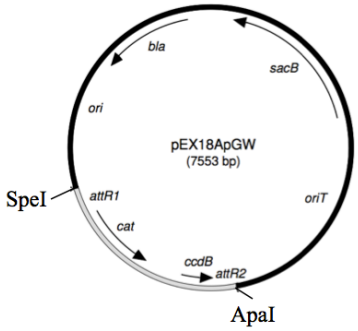

Fig. 3-2. Map of pEX18ApGW suicide vector. Abbreviations: *attR1* and *attR2*, bacteriophage recombination sites; *bla*, β-lactamase-encoding gene; *cat*, chloramphenicol acetyl transferase-encoding gene; *ccdB*, gene encoding gyrase-modifying enzyme (CcdB poisons host DNA gyrase by forming a covalent complex with the DNA gyrase A subunit and thus serves as a counter-selectable marker in *gyrA*+ cloning hosts); *ori*, ColE1-derived replication ori- gin; *oriT*, origin of conjugal transfer; *sacB*, *Bacillus subtilis* levan-sucrase-encoding gene; SpeI and ApaI, restriction enzyme digestion sites. The sequence of this plasmid was deposited in GenBank and assign accession number AY928469 (Modified from Choi and Schweizer, 2005)

Table 3-3. Primers used in markerless knockout generation.

Gene	Primer	Sequence
accC1	GMF-BamHI	5'- TGGAT CCGGACGATCGAATTGG -3'
	GMR-HindIII	5'- TTAAGCT TCATGCATGATCGAATTAGC -3'
morA	Pp-MorA 5'-SpeI	5'- TAACTAGT TGATTTTCAGCAGCGTGGA -3'
	Pp-MorA5'-BamHI	5'- TGGATCC TGGCGGAGTGACATTGG -3'
	Pp-MorA3'-HindIII	5'- TTAAGCTT GACTGAACATCTGCGGCG -3'
	Pp-MorA 3'-ApaI	5'- TAGGGC CCGTAGTAACGCTTGCC -3'
morC	SpeI-PNL-MorC	5'- TAACTAGT TGTCTTCGGTGGCTTCCAG -3'
	BamHI-PNL-MorC	5'- TGGATCC GACGTGTTCTACCAGCCC -3'
	HindIII-PNL-MorC	5'- TTAAGCTT TCGCATCGTGCAGTTGATAG -3'
	ApaI-PNL-MorC	5'- TAGGGCCC CGAGAAATGTTCACTGCAG -3'
$morA_{Pf}$	PfMorA-UpF-GWL	5'-TACAAAAAAGCAGGCTAATGATTGGGACACAGGC-3'
	PfMorA-UpR-GM	5'-TAGAGCGCTTTTGAAGCTAATTCGTTCAGGCTGACCTGTGC -3'
	PfMorA-DnF-GM	5'-ACTTCAAGATCCCCAATTCGTCGGCACCGGTTACTCATCG -3'
	PfMorA-DnR-GWR	5'-TACAAGAAAGCTGGGTGGTCAGTCGAACATGAACAGCG -3'
opuAC	SpeI-PNL-opuAC5'	5'- TAACTAGTATGGGCTCTCGTGGTCGAC-3'
	opuAC5'-UpR-GM	5'-GAGCGCTTTTGAAGCTAATTCGTTTGCCGGCCTGGTCTACAC-3'
	opuAC3'-DnF-GM	5'- GGAACTTCAAGATCCCCAATTCGCGCAGCACTTCGTTGAGC-3'
	ApaI-PNL-opuAC3'	5'- TAGGGCCCATACACCGGCGTGTCGCT-3'

3.2.6. Selection of markerless knockout clones

Thirty colonies were patched on LB+Gm30 plates and then streaked on LB+Gm30 with 10% sucrose for single colonies. Colonies that had grown on the selection plate were then considered putative deletion mutants.

The insertion of gentamycin cassette was verified via colony PCR in the steps described as follows: Cells were scrapped from the cell patch and transferred to 30µL of sterile water in a microcentrifuge tube. The cell suspension was then boiled for 5min. Cell debris was removed by centrifugation at 16,000g for 2min. 2µL of supernatant was used as template DNA in a 10µL PCR reaction containing 1x BD Clontech Advantage PCR2 buffer, 1x Advantage 2 polymerase mix, 0.2µM of primers and 200µM dNTPs. Cycle conditions were 95ºC for 3min, followed by 30 cycles of 95ºC for 30s, 60ºC for 30s, and 72ºC for 2min, and a final extension at 72ºC for 7min. PCR products were analyzed by agarose gel electrophoresis.

Electrocompetent cells of the newly constructed mutant strain were prepared as described in the preceding paragraph and transformed with 20ng of pFLP3 plasmid DNA as described above. After phenotypic expression at 30ºC for 4h, the cell suspension was plated on LB +Tet30 plates. Transformants were purified for single colonies on LB+Tet30 plates. Ten single colonies were tested for antibiotic-susceptibility on LB +Gm30 plates. Gentamycin sensitive isolates were struck for single colonies on a 10%sucrose+LB plates and incubated at 30ºC till single colonies appeared. Ten sucrose-resistant colonies were retested on a 10% sucrose+LB, Gm30 and Tet30. Deletion of the gentamycin cassette was assessed by colony PCR utilizing the conditions and primers described previously.

3.3. Genomic DNA isolation

Genomic DNA was isolated using a protocol previously described in our laboratory (Syn and Swarup, 2000). Three mL of overnight culture was pelleted at 14,000rpm and washed with 1% NaCl. The pellet was then resuspended in 750µL of TES (10 mM Tris-HCl, 10 mM EDTA, pH 8.0, 2% SDS) and incubated at 75ºC for 5min. The cell lystate was then mixed with 750µL of 3:1 Tris-buffered phenol:chloroform. Centrifugation at 14,000rpm for 5min was carried out to separate the phases. This was followed by chloroform extraction. DNA was then precipitated using 0.1 vol of 3M sodium acetate (pH 5.2) and 2.5 vol of absolute ethanol. The resulting pellet was washed with 1mL of 70% ethanol and then dried with a speedvac for 5min. The DNA pellet was dissolved in 150 µL of TE (10 mM Tris-HCl, 2 mM EDTA, pH 8.0) containing 50 µg/mL of RNase.

3.4. Gene expression studies

3.4.1. Complementation and overexpression strains generation

Standard molecular biology techniques were used for creating all constructs. Restriction and modifying enzymes were purchased from New England Biolabs (Beverly, MA) and Fermentas (Gen Burnie, MD). DNA oligonucleotides used were obtained from Sigma Proligonucleotides.

Transposon insertion mutants of *P. putida* PNL-MK25 were generated using pUC18-miniTn7T-GM. Electroporation were used to introduction the construct into various *P. putida* strains using helper plasmid pTNS2. For complementation studies, Δ*morC*

mutants were complemented with *morC* in a single copy with mTn7T introduced into the chromosome at the *att*Tn7 site.

3.4.2. RNA isolation and cDNA preparation

Total RNA was extracted using TRIzol® Reagent (Invitrogen Corp., Carlsbad, CA, USA). Cell pellets from 3 growth phases were collected and resuspended in 1mL of TRIzol. They were then heated at 50ºC for 10min prior to RNA extraction to lyse the cells. After cooling at room temperature for 5min, 200µL of chloroform was added followed by 15s of vortexing. The mixture was then centrifuged at 12,000x g for 15min at 4ºC to separate the three phases. The top phase was then extracted and mixed with 500µL of isopropanol. After which, it was incubated for 10min at room temp and then centrifuged at 12,000 xg for 10min at 4ºC. The RNA pellet was then washed with 1mL of 70% ethanol and then dissolved in DEPC water by incubating for 10min at 60ºC. Genomic DNA is removed by the addition of DNaseI. Subsequently, cDNA was prepared with Maxima® First Strand cDNA Synthesis Kit (Fermentas, Gen Burnie, MD).

3.4.3. Quantitative Real-Time PCR

morC primers for quantitative Real-time PCR were designed with Primer Express software (Applied Biosystems) using DNA sequence obtained during gene walking while the other primers were previously reported (Choy, 2004). The assay was performed using Maxima® SYBR Green qPCR Master Mix (Fermentas, Gen Burnie, MD) as per manufacturer's instructions. The reaction mix (50µL) contained 25µL of

Maxima® SYBR Green qPCR Master Mix, 0.3μM of forward and reverse primers, 2.5μL of cDNA (20ng/μL) and water. The genes and their corresponding primers used for the expression studies are listed in Table 3-4.

3.5. Site-directed mutagenesis and deletion of EAL domain in MorC

Site-directed mutations of MorC were generated using conventional fusion PCR protocol. The plasmid construct, mTn7T-morC was used as the template for the mutagenesis. Firstly, two partial gene fragments were generated to introduce the respective mutations. The two fragments were then fused together using PCR amplification with MorC primers. Amplicons carrying the mutations were cloned into mTn7T-morC using restriction enzyme digestion and ligation.

Table 3-4. Primers used in qRT-PCR.

Gene	Primer	Primer Sequence
16S	16S_SG_F	5’- TGTAGCGGTGAAATGCGTAGA -3’
	16S_SG_R	5’- CGCACCTCAGTGTCAGTATCAGT-3’
23S	23SRNA-FW	5'- CCGAGATTCCCTTAGTAGTG -3'
	23SRNA-RE	5'- TAAGAGACTT TCGCGTACAG -3'
fliC	fliC_SG_F	5'- TGCGTGAACTGGCTGTTAAAG -3'
	fliC_SG_R	5'- GAGCGAATTCAGCGTTGGT -3'
morA	morA_SG_F	5’- GCAGTTGCTCGCGGAAAT -3’
	morA_SG_R	5’- AGGAGTGCACATCGAGCAGTT -3’
morC	morC_MID FW	5’- CGACAGCTGGCCCCAGTACGG -3’
	morC_MID RE	5’- AGAGCAACAGCTGGCAGGGCG -3’

Table 3-5. Primers used for various site-directed and deletion constructs of *morC.*

Primer	Sequence
XbaI-morC WS	5’-AATCTAGACTATCAAAACTGTGGGAGCGAG-3’
HindIII-morC WOS1	5’-TTAAGCTTGAGGCAGAGCGGGCCGCG-3’
KpnI-MorC	5’-TTGGTACCTCGAGGCTGATCAGATATTGG-3’
BMG-morCFW	5'- AAGACGTGTTCTACCAGCCC-3'
AVR-morCRE	5'- TTGCCTAGGC CGGCAGCGG-3'
KAL673FW	5'- CTGCTGGGCATGAAAGCGCTGTTGCGCTGG-3'
KAL673RE	5'- CCAGCGCAACAGCGCTTTCATGCCCAGCAG-3'
EAG675FW	5’-CTGCTGGGCATGGAAGCGGGCTTGCGCTGGAA-3'
EAG675RE	5’-CCAGCGCAAGCCCGCTTCCATGCCCAGCAG-3'
KasI-morC FW	5’-GCGACAAACTGTTGATCAGCC-3’
BamHI-MorC EAL del RE	5’-ATGGATCCTCAACTGGCTTCAGCGTTCAGCG-3’
KAL754 FW	5’-CATCCTCAGGGAAAAAGCGCTGCCGGCCAGTCTGCTCG-3’
KAL754 RE	5’-CGAGCAGACTGGCCGGCAGCGCTTTTTCCCTGAGGATG-3’
EAG 756 FW	5’-CATCCTCAGGGAAGAAGCGGGCCCGGCCAGTCTGCTCG-3’
EAG 756 RE	5’-CGAGCAGACTGGCCGGGCCCGCTTCTTCCCTGAGGATG-3’

3.6. Swimming motility studies

3.6.1. Swimming motility plate assay

Semisolid LB agar plates were made with 0.4% w/v BD Bacto™ Agar. The plates were left to dry for 4h and then inoculated with 1.5µL of overnight bacterial culture diluted to OD_{600}=0.25. The plates were then incubated for 30h at 30ºC. Movement of the bacteria away from the inoculation point was determined relative to that of WT, as previously described (Robleto *et al.*, 2003).

3.6.2. Single cell swimming speed analysis

Overnight cultures were diluted 1:50 in fresh LB before being incubated and grown to the respectively growth phase. Two viewing chambers of 0.8cm x 0.8cm x 100µm were created by sticking a layer of double-sided tape between the microscope slide and coverslip. At each growth phase, cell culture was diluted to optimal density to facilitate tracking and 50µL of cell suspension was loaded into the chamber for image recording. The samples were viewed at 600× magnification on a Nikon ECLIPSE E-600 phase contrast light microscope (Nikon, Japan) and the movement of the cells was recorded using a QICAM 12-bit CCD camera (QImaging, Canada). Cell movements were captured as movies in AVI format for 20s at 10frames per second.

3.6.3. Cell speed image analysis

Bacterial speeds were tracked using Image-Pro Plus 6.3 (Media Cybernetics, USA). Cells are considered motile only if they moved faster than 2.0 µm/s and had travelled

for a length of 3.0μm or more. Speeds of 100 motile cells from three separate videos were taken per strain and average speeds were analyzed.

3.7. Biofilm formation tube assay

The biofilm formation assay was adapted from that of O'Toole and Kolter (1998). It was performed in polystyrene round-bottom tubes using LB medium. Two mL of culture diluted to OD_{600}=0.25 was inoculated into each tube. After inoculation, cultures were incubated for various time intervals at 30ºC with shaking at 250 rpm. At various time intervals, non-adherent cells were removed by rinsing with 5mL of distilled water. Biofilms were stained with 0.1% (w/v) crystal violet solution for 1h followed by rinsing with distilled water. Bound crystal violet was solubilized in 2 mL 1% SDS and quantitated by obtaining OD_{595} value spectrophotometrically.

3.8. Chemotaxis assay

The assay used was adapted from Shi *et al.* (1998). Overnight cultures were pelleted at 3000 xg for 5min, washed and then resuspended in half-strength M9 medium to OD_{600}=1.0. One mL of culture was then mixed with 24mL of 0.4% (w/v) soft agar prepared in half-strength M9 medium. This mixture was then poured into a petri dish holding a 1% agarose plug in the center that contains 100mM aspartic acid to act as a chemoattractant.

3.9. Intracellular localization study

Bacterial cells were diluted 1:25,000 in fresh LB before being incubated and grown to respective growth phases. At each growth phase, 20μL bacterial culture was collected and viewed by confocal laser scanning microscopy (CLSM) and image acquisitions were performed with a Zeiss LSM510 CLSM (Carl Zeiss, Jena, Germany) meta microscope. Images were obtained using a 63/1.4 objective.

3.10. Transmission electron microscopy (TEM)

Bacterial cells were harvested at various growth intervals and then pelleted at 2000 xg for 20min. The cell pellet was then washed 0.9% saline solution and then fixed in 2% formaldehyde. A drop of cell suspension and a drop of 3% (w/v) uranyl acetate (pH 4.5) were added onto a Formvar-coated copper grid (150 mesh). The mixture was left for 2min before the grid was dried under a heating lamp. The grids were viewed at 1100x magnification in a FEI T12 transmission electron microscope operating at 120 kV (Oregon, USA).

3.11. *In silico* three-dimensional modeling of MorC PDE domain

The structural model for the MorC PDE domain was constructed using the Swiss-Model Server (Arnold, 2006; Kiefer *et al.,* 2009) with the coordinates of the tdEAL structure (PDB ID: 3n3t). The coordinates of c-di-GMP and Mg2+ for MorC PDE domain were taken from its corresponding PDB IDs. Domain boundaries for modelling were determined by the Simple Modular Architecture Research Tool (Schultz *et al.,* 1998; Letunic *et al.,* 2009). Using BLAST, sequence similarity

between EAL MorC and tdEAL was found to be 41% (Appendix I).

3.12. Protein expression studies

3.12.1. Creating constructs for MorC recombinant protein expression

Full and partial *morC* gene fragments, were amplified from mTn7T-MorC for cloning into the C-terminus His6-tagged protein expression vectors (Fig. 3-2). The list of primers is presented in Table 3-5. PCR amplification was performed using *pfu* polymerase (Fermentas, USA), and products were cloned into the C-terminus His6-tagged pET22b expression vector (Novagen, Germany). The resultant constructs were then verified by using sequencing vector primers T7-terminator and SP6, with the BigDye® Terminator v3.1 Cycle Sequencing Kit (Life Technologies, USA) according to the manufacturer's instructions. Constructs were then introduced into *E. coli* BL21 cells for protein expression.

Table 3-6. Primer used for the creation of recombinant MorC protein expression constructs.

Primers	Sequence
NdeI-MorCFW	5'- AACATATGAAGAGCCAGCCCGATGC -3'
HindIII-morCFL RE	5'- TTAAGCTTCCATGGCCAGGGTCAGG-3'
NdeI-DGC/PDE FW	5'- AACATATGACTAAACTCGCGCAGCAAC-3'
HindIII-DGC/PDE RE	5'- TTAAGCTTCTCATCACCCGGAATCGG-3'
HindIII-DGC RE	5'- TTAAGCTTGTAACTGGCTTCAGCGTTC-3'
NdeI-EAL FW	5'- AACATATGTTCACTGAAGCGCTGAACG-3'
NdeI-PAS/GAF FW	5'- AACATATGGAGGTAGTGACGCAGTTG-3'
HindIII- PAS/GAF RE	5'- TTAAGCTTCGAAGACATCACCCAGACT-3'

3.12.2. Testing of catalytic protein expression clones for yield and solubility

E. coli BL21 cells transformed with the protein expression plasmids were grown using overnight cultures at 37ºC with shaking at 200rpm, until OD_{600} reached 0.8. Induction was then carried out by the addition of 0.1mM IPTG into the culture followed by incubation overnight at 20ºC with shaking at 200rpm. Bacterial cells were then harvested and recombinant protein expression was verified through SDS-PAGE analyses using a 10% SDS-PAGE gel and Coomassie blue stain (Sambrook *et al.,* 1989). Bacterial cells containing expressed proteins were then lysed by sonication in lysis buffer containing 300mM NaCl, 50mM NaH_2PO_4, 20mM Imidazole and 1% Triton-X, pH8.0. The soluble and insoluble protein fractions were separated by centrifugation at 12,000 rpm for 30min. These fractions were then examined for solubility by SDS-PAGE analyses.

To obtain recombinant MorC proteins for enzymatic assays and c-di-GMP binding assays, several constructs were designed and cloned into pET22b vector for expression (Fig. 3-2). After sequence verification, these constructs were introduced into BL21 for expression. SDS-PAGE of ASNEF+ EAL and EAL protein fractions (Fig. 3-2) showed that the soluble fractions contained little or no recombinant proteins. As such, these constructs were sent as requests to the Protein Expression Facility in Department of Biological Sciences, National University of Singapore for recombinant protein construct creation with GST tag as well as for trials to fuse the 6His-tag to the N-terminal. Thus far, these constructs have not yielded positive results.

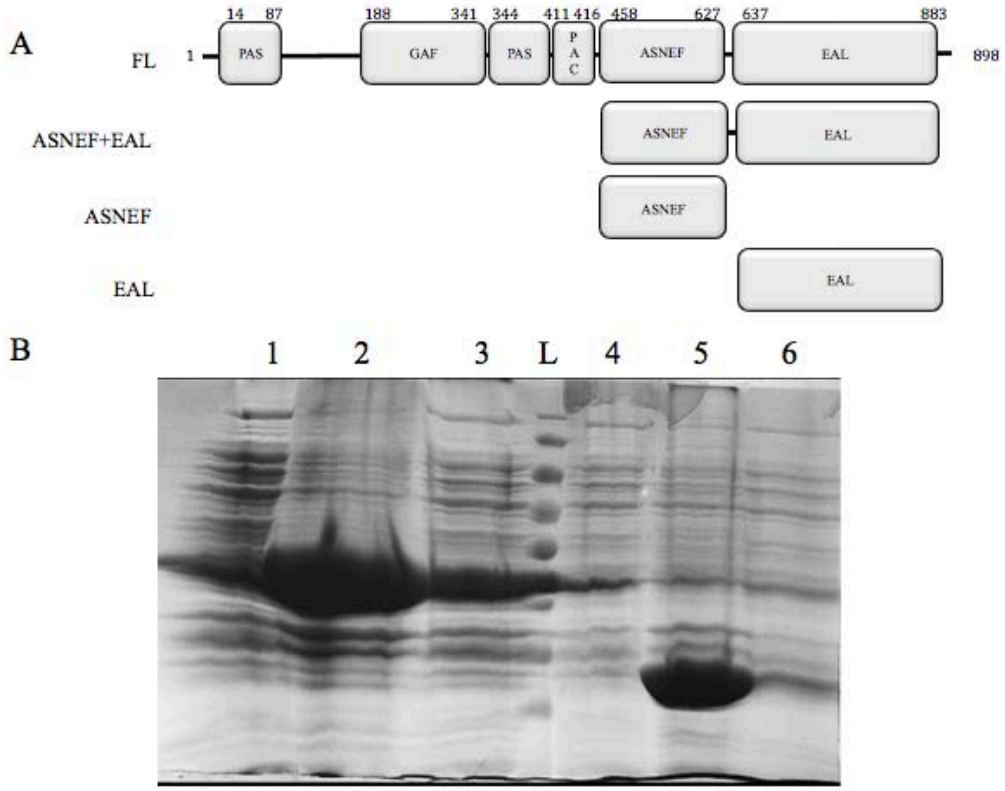

Fig. 3-3. Recombinant MorC is mainly present in the insoluble fraction of cellular proteins. (A) Several constructs expressing full-length protein and one or several domains were designed, created and cloned into BL21 for expression. (B) SDS-PAGE gel of ASNEF+EAL and EAL solubility check. Lane 1-3 shows ASNEF+ EAL protein fractions. Lane 1: whole cell; lane 2: insoluble fraction; lane 3: soluble fraction; L is the protein ladder. Lane 4-6 shoes EAL protein fractions. Lane 4: whole cell; lane 5: insoluble fraction; lane 6: soluble fraction.

3.13. Flagellin quantitation by Western analysis

3.13.1 Flagellin preparation

P. putida cell cultures were grown at 30ºC and collected at various OD_{600} that correspond with the early, mid and late log phase. Cells were harvested by centrifugation at 2000rpm for 90min, washed with 0.9% NaCl, and solubilized in 20mL water. After which, the flagella was sheared-off by vigorous vortexing for 5mins. Cells were then centrifuged at 10000 g for 1h followed by the collection of supernatants containing the flagellin.

3.13.2 Immunoblotting

After SDS-PAGE, proteins from the gels were transferred into ECL nitrocellulose membrane (Pall Corporation) at 100V for 90min in a buffer (20% methanol, Tris and glycine) at 4ºC. Subsequently, the membranes were washed twice with water and then blocked with 5% BSA with 0.05% Tween-20. All incubations were performed at room temperature for 2h or overnight at 4ºC. Mouse monoclonal antibody against the α subunit of *E.coli* RNA polymerase was purchased from Neoclone Biotechnology, WI, USA while the flagellin antibodies was raised in rabbits by 1st BASE Antibodies (1st BASE, Singapore).

All secondary antibodies were anti-rabbit/mouse IgG that had been conjugated with alkaline phosphatase (Sigma). Detection was performed with Immobilon ™ Western chemiluminescent AP substrate (Millipore).

Though preliminary trials resulted in poor blots, it is sufficiently clear that the RNA polymerase antibody was able to bind with relative specificity and gave good signals on the Western blots that were more intense with increased volumes of samples (Fig.

3-3). The flagellin antibody was non-specific however, resulting in multiple bands being detected in each lane. As such, the antibody is not suitable for flagellin quantification.

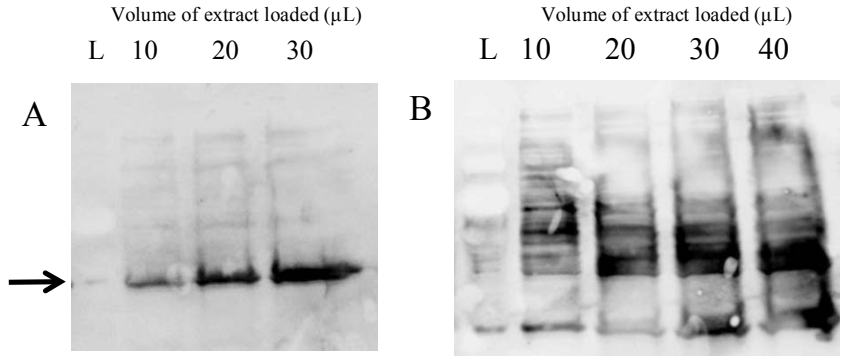

Fig. 3-4. Preliminary trials of Western blot analysis of flagellin levels. (A) Increasing volumes of cell extract was utilized for RNA polymerase probing to determine the specificity and sensitivity of the antibody. (B) Flagellin level was tested in different volumes of flagellin extract to verify the specificity and sensitivity of the antibody. Arrows depict the expected molecular weight of the protein being probed.

Chapter 4. Comparisons of MorA function between *P. putida* and *P. fluorescens*

High degree of genome plasiticity in *Pseudomonas* species can lead to presence or absence of proteins or differences in their isoforms that in turn leads to significant differences in cellular functions in the different species and their strains. In order to understand how MorA mediates c-di-GMP signaling in *P. putida* and *P. fluorescens*, I studied the motility and biofilm formation behavior of *morA* knockout strains in these 2 species. In order to understand how MorA mediates c-di-GMP signaling in *P. putida* and *P. fluorescens*, I studied the motility and biofilm formation behavior of *morA* knockout strains in these 2 species. In this Chapter, I present data to show that gentamycin cassette insertion lead to confounding effects in *morA* mutants in *P. putida* such that a 2-fold increase in motility was observed instead of the 2.8-fold previously reported with both the transposon mutant and directed insertional mutant. While hypermotility was reported in both *P. putida* and *P.aeruginosa,* no difference in swimming motility or biofilm formation was observed when *morA* is knocked out in *P. fluorescens* Pf0-1.

4.1. BACKGROUND

Previously in our laboratory, a genetic approach was used to identify negative regulators of swimming motility (Choi, 2005). It was thought that the knockout of such a gene would lead to enhanced motility. Therefore, mTn5-*gfp* was introduced into PNL-MK25 wild type and 3200 transposon insertion mutants were screened using 0.4% w/v soft agar. As a result, three enhanced motility mutants were identified. Two of the mutants exhibited 2.8-fold increase in motility and subsequent DNA sequencing results show that the transposon inserted into the same gene, which was named *morA*. The third mutant exhibited over 2-fold increase and was designated as *morB*.

While characterization of *morA* was previously carried out in our lab, the experiments were done with either the transposon mutants or the insertional mutant whereby a gentamycin cassette was inserted into *morA* (Fu, 2006, Li, 2006 and Lye, 2006). Though these mutants are suitable for fast screening and characterization of the gene function, it is an impediment for the study of the signaling members. This is because there are just a handful of selection markers that are commonly used in *Pseudomonas* species for molecular studies. These same few selection markers are also utilized in many plasmids and transposons for complementation and overexpression studies and other assays (Bloemberg *et al*, 1997; Choi and Schweizer, 2006). This being the case, it becomes difficult to study the relationship of different genes using the genetic approach.

Furthermore, the effect of inserting a large fragment into the genome is well documented to result in polar and anti polar effects. These effects are especially pronouced in operons or genes that shares the same transcription unit. While mTn5-*gfp* is well-designed, it is possible that data previously collected are influenced in a manner that is hard to predict. So, to ensure that the data obtained from the transposon mutants were not confounded by other factors but is reflective of gene function and also to allow for multiple gene knockout and complementation studies, markerless knockout mutant generation was carried out.

After obtaining Δ*morA* mutant strain, various phenotypic assays were conducted and then results were compared with the transposon mutants for verification.

4.2. RESULTS AND DISCUSSION

4.2.1. Generation of markerless knockout mutant strains

To generate markerless knockout mutant strains, an established protocol was adapted for our use (Choi and Schweizer, 2005). Firstly, PCR was used to generate 3 fragments namely: 5' gene fragment, 3' gene fragment and *frt* flanked gentamycin fragment with overlaps to facilitate fusion PCR (Fig. 4-1). A second PCR was then used to create the markerless recombination fragment flanked with restriction sites. While Choi and Schweizer mentioned that the prescribed PCR conditions to be critical for the generation of clean fragments, we were unable to obtain the recombination-proficient DNA fragment using those conditions. Extensive

optimization with the cycle conditions and polymerase mixture was performed in order to obtain our fragments of interest.

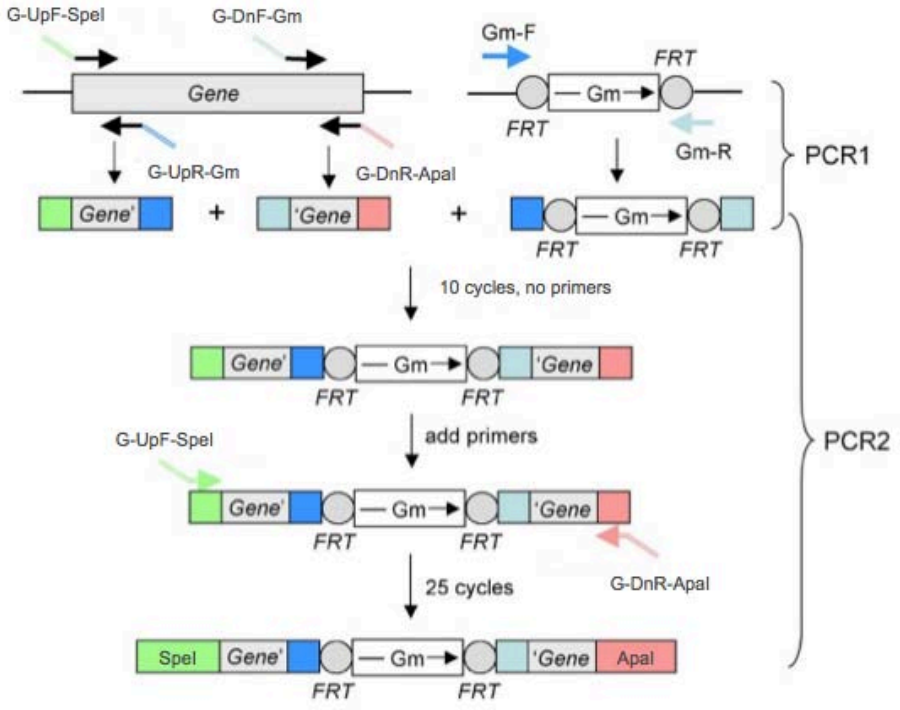

Fig. 4-1. Schematic illustration of mutant fragment generation by overlap extension PCR. During the first round of PCR (PCR1), the 5' and 3' gene fragment as well as the gentamycin (Gm) resistance cassette were amplified using four specific primers (G-UpF-SpeI, G-UpR-Gm, G-DnF-Gm and G-DnR-ApaI) as well as the Gm-specific primers (GmF and Gm-R). A total of three fragments with partial overlaps are generated and depicted in the figures as blue boxes. The RE sites are indicated by green and red boxes. These PCR fragments are then purified and assembled via overlap extension during PCR (PCR2) using the G-UpF-SpeI and G-DnR-ApaI primers, resulting in a recombination proficient mutant PCR fragment that can be directly introduced into the pEX18ApGW vector. (Modified from Choi and Schweizer, 2005)

This mutant gene fragment was then directly introduced into pEX18ApGW sucicide vector through conventional RE and ligation molecular biology technique instead of using the Gateway system. While the use of Gateway system was advantageous in that it avoided the problem of not being able to locate suitable RE sites in the gene of interest, conventional molecular biology method is faster as only one cloning step was required instead of first transferring the fragment into the pDnor221 vector and then into the pEX18ApGW vector. In our case, all our gene of interest was able to use the RE sites ApaI and SpeI which are also located on pEX18ApGW. As such, it was as efficient as using the Gateway system. Furthermore, by using existing reagents in the lab, we were able to save costs as there is no need to purchase additional reagents.

The putative mutant clone was generated by transferring the suicide plasmid pEX18ApGW-Gene::Gm into *P. putida*. During this time, single and double cross-over events can both occur. To resolve this, sucrose selection in the presence of gentamycin was performed. After the generation of double cross-over clones, the Gm primers was utilized on the genomic DNA to confirm that the gene have indeed been replaced by mutant gene fragment.

The gentamycin cassette is subsequently removed by the introduction of pFLP3 that allowed for the production of flippase recombination enzyme (FLP). FLP recognized specific FRT sequences for recombination to occur. This then resulted in the excision of the Gm resistance gene cassette, leaving behind a 123bp long FRT scar. Finally, a markerless but not scarless knockout strain is generated. Sequencing performed on the strain shows that the FRT scar is in-frame and do not contain any stop codon (Fig. 4-

3). This method is therefore very suitable to study operons or gene organized in polycistronic units (Choi and Schweizer, 2005).

PCR was carried out using gene specific primers (Table 3-2) and genomic DNA (gDNA) from these putative markerless clones to verify that the FRT recombination had taken place. A smaller PCR product size indicated the successful removal of a large portion of the various target genes. Fig. 4-2 show that the PCR product of the genes that did not undergo homologous recombination was on average, 2kb larger when compared to the genes that were disrupted.

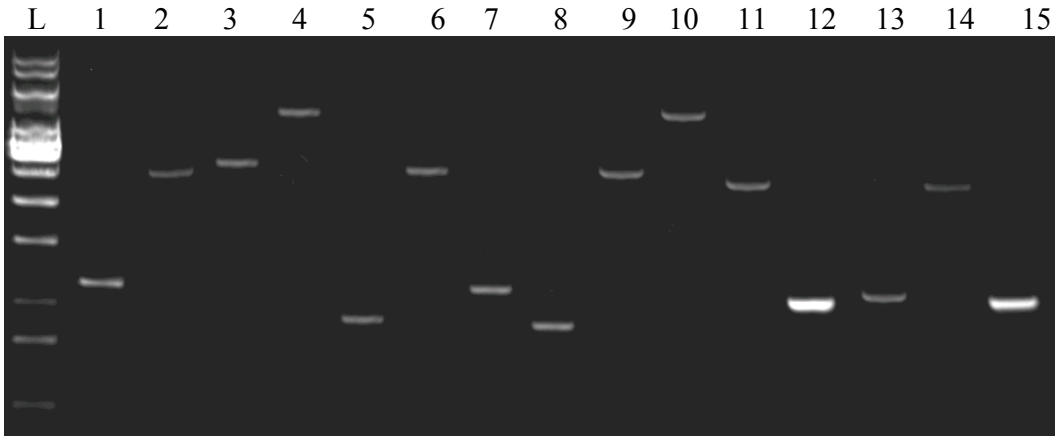

Fig. 4-2. Confirmation of markerless knockout mutant genotypes by PCR. PCR based confirmation of deletion of various genes using genomic DNA as template; M, 1 kb ladder (Fermentas); 1,2,3, *morA*, *morC* and *cyaA* genotype respectively tested using Δ*morA* gDNA as template; 4,5,6, *morA*, *morC* and *cyaA* genotype respectively tested using Δ*morC* gDNA as template; 7,8,9, *morA*, *morC* and *cyaA* genotype respectively tested using Δ*morA*Δ*morC* gDNA as template; 10,11,12, *morA*, *morC* and *cyaA* genotype respectively tested using Δ*cyaA* gDNA as template; 13,14,15, *morA*, *morC* and *cyaA* genotype respectively tested using Δ*morA*Δ*cyaA* gDNA as template.

In addition, all clones were verified via DNA sequencing for the removal of gene sequences as well as for the detection of the FRT scar that was left after the pFLP3 excision of the gentamycin resistant cassette. The electropherogram of Δ*morA* clone in Fig. 4-3 shows the 123bp FRT scar after FLP removed the gentamycin resistance gene. The electropherogram also shows that 3822bp of the 3849bp long morA had been successfully displaced from the chromosome.

It was noted that the suicide vector pEX18ApGW was designed for use with *P. aeruginosa.* The *bla* gene located on the suicide vector was intended to function as a negative selection with the use of carbenicillin in the medium to eliminate single cross-over recombinants as *P. aeruginosa* is carbenicillin sensitive. This is however, not applicable to *P. putida*, as it is carbenicillin resistant. As such, it presented more challenges to screen for the desired transformants. This being the case, it would be beneficient to replace the *bla* gene with another selection marker such as *tet* gene for the selection of tetracycline resistance instead.

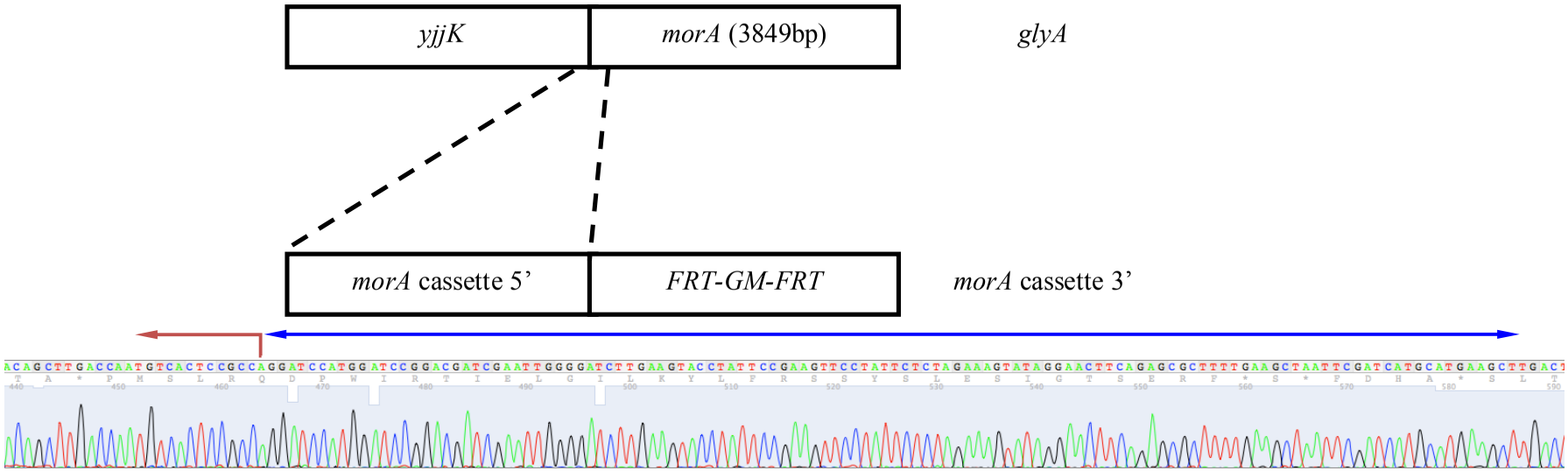

Fig. 4-3. *morA* markerless knockout strain DNA sequence analysis. *morA* markerless knockout cassette consists of three parts: 5' gene fragement, FRT-GM-FRT fragment and 3' gene fragment. Parts of *yjjK* and *glyA* was included in the 5' and 3' fragment respectively. After double homologus recombination, *morA* gene was removed from nucleotide position 22 to 3843 with a 123bp FRT scar inserted. *morA* nucleotide position 21 is shown at position 464 of the electropherogram (red arrow), FRT scar is shown at position 465 to 587 (blue arrow) and *morA* nucleotide position 3843 is shown on the electropherogram as position 587 (green arrow) respectively.

4.2.2. Verification of the markerless knockout Δ*morA* strain

4.2.2.1. Disruption of *morA* does not affect growth of the *ΔmorA* cells

As the Δ*morA* strain is critical to the downstream studies, phenotypic assays were first carried out to characterize the strain before proceeding with other strain generation and studies. The growth rates of WT, aloC3H transposon mutant (*morA*::mTn*5*-*gfp*). *ΔmorA* mutant and *ΔmorA:pGB1-morAFL* complementation strains were examined in LB medium for a period of 12h and were found to be comparable in all the four strains (Fig. 4-4). The transition from lag phase to the log phase was at 0.6 OD_{600} and was marked as early-log phase. The mid-log phase was at 1.6 OD_{600}. The transition from log phase to stationary phase was at 2.3 OD_{600} and was marked as log-to-stationary transition phase. All three strains also reached a similar maximum OD_{600} of ~ 2.3. Hence, disruption of *morA* did not affect the growth rate of the mutant strain.

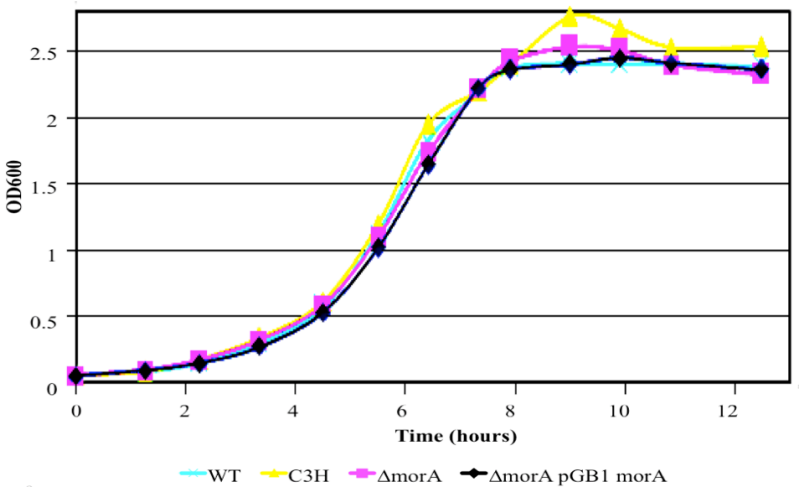

Fig. 4-4. Growth curve of various *P. putida* strains. Growth curves of *P. putida* WT and various mutants in LB medium showed no differences in the growth. Absorbance at 600nm (OD_{600}) of bacterial cultures growth in LB medium at 30ºC were measured at intervals of half to one hour.

4.2.2.2. Complementation confirms the effect of *morA* mutation

While the transposon mutant C3H and the targeted insertional mutant MorDCK03 exhibited 2.8-fold increase in motility, the *ΔmorA* strain showed about 2-fold increase in swimming motility through 0.4% (w/v) soft agar compared to WT (Fig. 4-5). This suggests that the gentamycin resistant cassette insertion have indeed caused some effects that have led to a more pronounced hypermotility phenotype to be observed in the motility assay. Studies were then carried out to ascertain whether the cloned *morA* gene was able to restore the phenotype in Δ*morA* and if additional copies of *morA* affects motility. Complementation of the *ΔmorA* strain with the cloned *morA* gene expressed from its native promoter was provided *in trans* on a stable low copy number plasmid (pGB1:*morA* FL). The vector pGB1 has been reported to be present in low copy number in *Pseudomonas* cells (Bloemberg *et al.*, 1997).

Restoration of the wild-type motility phenotype in the *ΔmorA* strain was observed with the complementation and at the same time, motility was reduced to lower than that of the WT (Fig. 4-5). The presence of the pGB1:*morA* FL plasmid in WT led to almost 40% decrease in motility phenotype when compared to WT. These results suggest a strict control of *morA* dosage within the cells; a slight perturbation in gene copy number resulted in measurable differences in motility.

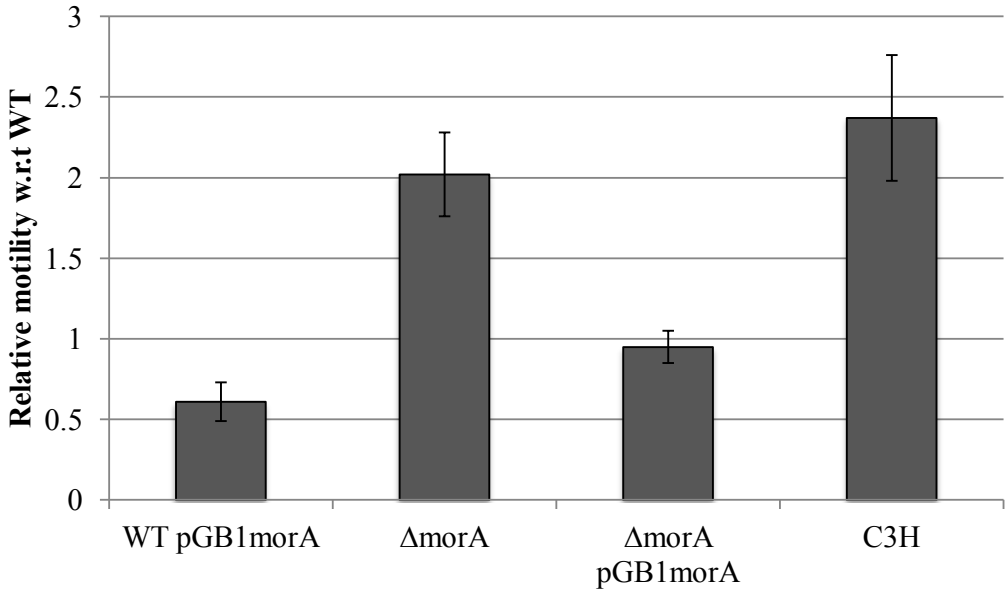

Fig. 4-5. Complementation of *morA* was able to store swimming motility phenotype. Swimming motility of WT, WT*pGB1morA*, *ΔmorA* mutant, *ΔmorApGB1morA* and C3H in LB semisolid agar (0.4% w/v) was examined. WT: *P. putida* parental strain PNL-MK25, WT*pGB1morA*: *morA* overexpression strain , *ΔmorA* mutant: markerless knockout mutant, *ΔMorApGB1morA*: *morA* complementation strain, C3H: transposon mutant. Results are based on three independent experiments with five replicates each.

Previous studies have indicated that biofilm formation requires appropriate flagellar biogenesis (Pratt and Kolter, 1998; Sauer *et al.*, 2002). Therefore, investigations were carried out to ascertain whether constitutive production of flagella in Δ*morA* had an effect on biofilm formation. Biofilm formation by WT and Δ*morA* mutant strain was examined on polystyrene surfaces by incubating bacterial cultures in polystyrene tubes for various time intervals. Biofilms were visualized by crystal violet staining. The amount of biofilm formed was then quantitated by solubilizing it in 1% SDS.

At 3 hours, biofilms formed by the mutants were significantly less than those produced by WT (Fig. 4-6). At 10 hours, the biofilms formed byΔ *morA* were visible, but were still less than those formed by WT (Fig. 4-6). The Δ*morA* mutant complemented with cloned *morA* completely restored the biofilm formation phenotype (Fig. 4-6). These results suggested that the precocious production of flagella inΔ *morA* mutants was correlated with a reduction in biofilm formation.

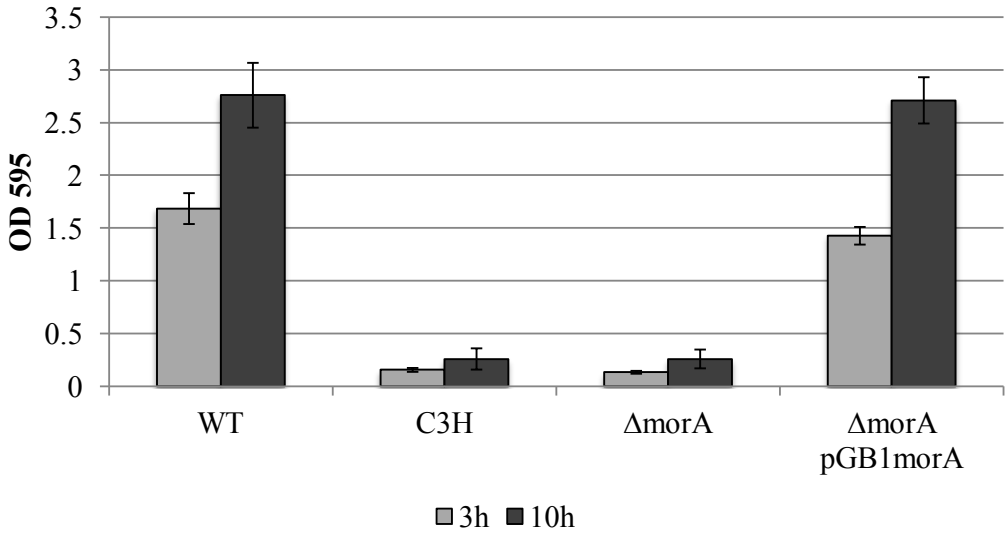

Fig. 4-6. *morA* affects biofilm formation in *P. putida* PNL-MK25. The plasmid pGB1*morA* were introduced into *ΔmorA* strain for complementation, leading to an increase in biofilm formation to levels higher than WT. Biofilms formed at 3 h and 10 h after inoculation in polystyrene tubes were stained with 0.1% crystal violet.

4.2.3. Characterization of MorA function in Pf0-1

4.2.3.1. Δ*morA*$_{Pf}$ shows no difference in motility when perturbed

PNL-MK 25 was selected as the study organism due to the many reason discussed in the Literature Review Section 2.1.2. Thus far, the PNL-MK 25 genome have not been annotated and so it is challenging to identify the genes disrupted in large-scale transposon mutagenesis. In order to verify our data from the random transposon mutant screen, gene walking has to be performed each time a gene sequence is required. The gene sequence required can be several Kb in length and may also be resistant to PCR-based gene walking techniques due to the high GC content found in many of the *Pseduomonas* genomes. Hence considerable time is required to obtain and verify these sequences. In the long term planning of experiments, this is a rate-limiting step should multiple genes are to be studied at the same time.

While *P. aeruginosa* PAO1 strain is annotated and was already utilized in our laboratory for various MorA related studies, it is not an ideal strain for large-scale experimentation as it is a biosafety level 2 organism that required more safety equipment as well as specially engineered and designed workspace. More importantly, it was previously shown that Δ*morA*$_{Pa}$ requires lower than 0.4% w/v agar motility plate to detect a difference of 11%, which makes the handling of the agar plate difficult (Wong, 2011). Thus motility plate assay as a screening method do not work well with PAO1. This difference in motility is more discernable when the cells were observed with video microscopy to compute cell speed. Δ*morA*$_{Pa}$ was found to be 25%, 21% and 12% faster than WT at the early-, mid- and late-log phases

respectively (Wong, 2011). This method however is manpower intensive and thus not suitable for large-scale studies.

As an alternative, we considered the use of *P. fluorescens* Pf0-1. The advantages of using Pf0-1 are many. Its genome had been annotated and it is well studied. Furthermore, it is a biosafety level 1 organism and thus do not require special set-up. Most importantly, the gene sequences obtained from gene walking from PNL-MK 25 aligned well with *Pseudomonas fluorescens* Pf0-1 and like PNL-MK 25; it is a soil organism that presents multitrichous polar flagella (Silby *et al.,* 2009). Together, these properties suggest that it is more likely that Δ$MorA_{Pf}$ would present the hypermotility phenotype on motility plate assay, making it optimal for large-scale screening. Hence, Δ*morA* in Pf0-1 was created and characterized to evaluate the possibilities of using it to replace PNL-MK25 as a model for further studies.

Intriguingly, Fig. 4-7 shows that the knockout of *morA* and overexpression of *morA* in Pf0-1 strain showed relative motility of 0.9 and 1 respectively. This shows that in Pf0-1, the perturbation of MorA did not lead to significant changes in the swimming motility. This is very different from the hypermotility phenotype that had been previously observed in both *P. putida* PNL-MK25 and *P.aeruginosa* PAO1. Pf0-1 is, therefore, an interesting subject to study in order to determine why its phenotype is so different when its genome is found to be very similar to that of PNL-MK25.

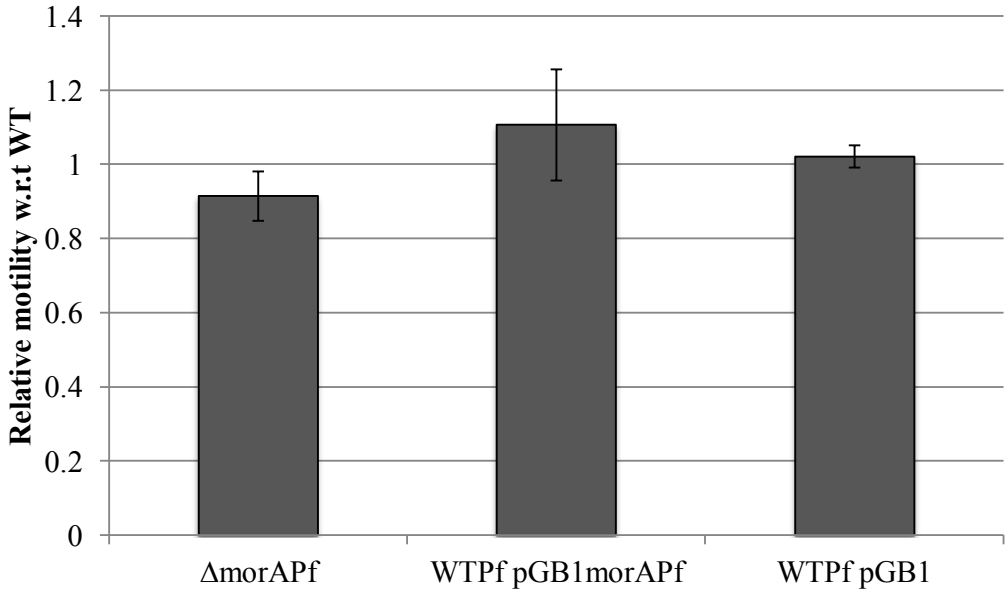

Fig. 4-7. Δ*morA*$_{Pf}$ does not affect swimming motility phenotype on plate motility assay. Swimming motility of Pf0-1 WT, *ΔMorA*$_{Pf}$ mutant, WT$_{Pf}$*pGB1MorA*$_{Pf}$ and WT$_{Pf}$*pGB1* in LB semisolid agar (0.4% w/v) was examined. Results are based on three independent experiments with five replicates each.

4.2.3.2. Δ*morA*$_{Pf}$ does not affect biofilm formation

As soil microbes are often nutrient limited, it was thought that bacterial adhesion to the soil is a strategy for the enhancement of ability to access nutrients that are in short supply or available only intermittently. Furthermore, it is also advantageous in preventing vertical displacement and maintaining aerobes in the top soil (DeFlaun *et al.*, 1990).

This being the case, we next examined biofilm formation. Fig. 4-8 also show a similar trend in that Δ*morA*$_{Pf}$ and WT$_{Pf}$ pGB1morA$_{Pf}$ exhibited similar amount of biofilm formation when compared to WT$_{Pf}$ at both early and late time point. It was also observed that the amount of biofilm formed by *P. fluorescens* strains are much less when compared to *P. putida*.

As there were no substantial differences that can be seen with both motility plate assay and biofilm formation tube assay, the Pf0-1 model was deemed to be unsuitable for our purposes of high-throughput screening of mutants. However, the use of the biofilm formation tube assay and plate motility assay might not be sufficiently sensitive to observe the differences presented by Δ*morA*$_{Pf}$. Thus this is not an exhaustive characterization of Δ*morA*$_{Pf}$ and more sensitive assays such as video microscopy or confocal microscopy of biofilm might be able to elucidate *morA* gene function in Pf0-1.

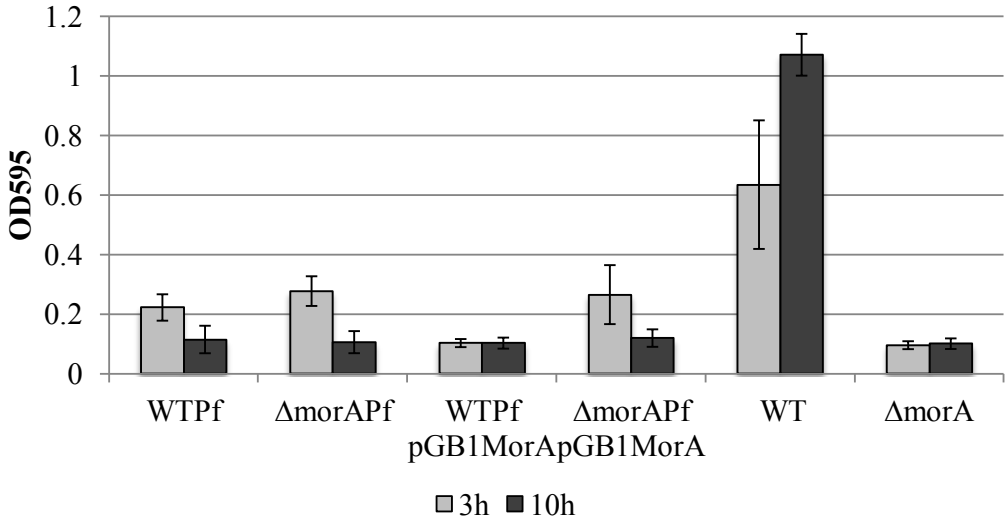

Fig. 4-8. Δ*morA*$_{Pf}$ does not affect biofilm formation. Biofilms formed at 3 h and 10 h after inoculation in polystyrene tubes were stained with 0.1% crystal violet. Results are based on three independent experiments with five replicates each.

4.2.4. SOLiD sequencing of *P. putida*

Since Pf0-1 mutant was not able to provide a good model for our purpose, it was thought that the annotation of PNL-MK25 would be ideal for solving the problems we currently face and also for easing future work. As such, SOLiD™ sequencing (Applied Biosystems) was performed to obtain a workable genome draft.

Preliminary data is presented in Table 4-1 while more details are provided in Appendix II. SOLiD™ sequencing is a massively parallel; ligation mediated sequencing method that generates tens of millions of 25-50nt reads in a single run. In this system, each base is read twice due to 2 base encoding, thus the error rate is lower than other sequencing methods. However, as the read length is very short, it is more difficult to obtain large contigs without repeats of the sequencing process. On top of that, *de novo* assemblies have a significantly higher raw device error rate than the 99.94% reported for SNP calling. As such, more work is required to obtain a fully annotated genome.

Table 4-1. SOLiD sequencing preliminary data.

No. of contigs	17041
Total length	7879539
Average length	462.0
Max length	2998
Min length	301
N50 length	438
N90 length	317

4.3. CONCLUSION AND FUTURE WORK

While pEX18ApGW had been used to satisfactory outcome in this project, positive selection could not be carried out as numerous strains of *Pseudomonas* such as Pf0-1 and PNL-MK25 used in this study, is resistant to the marker. To improve upon the matter requires that the vector be redesigned for use in *P. putida*. This can be achieved by the simple replacement of *bla* with *tet* gene for positive selection. Phenotypic characterization of Δ*morA* showed that Δ*morA* presented lower motility when compared to C3H and MorDCK03 *morA* knockout strains showing that insertion of gene fragment had lead to confounder effects

Though Pf0-1 is closely related to PNL-MK25, many differences are demostrated in their physiology. In particular, no differences were observed in swimming motility or biofilm formation in Δ$morA_{Pf}$. Therefore, *morA* is a negative motility regulator in *P. putida* PNL-MK25 but not in *P. fluorescens* Pf0-1.Since Δ$morA_{Pf}$ did not lead to changes in motility, a global gene expression studies should be performed in conjunction with the annotation of PNL-MK25. These data can be used to complement our current random mutant data set to elucidate important members of the MorA signaling pathway.

While SoLiD sequencing had not yielded a complete annotated PNL-MK25 genome data, it is already evident that the genome is more similar to Pf0-1 than *P. putida* KT2440. This being the case, it would be worthwhile to revisit the classification of the strain. Currently, more bioinformatics analysis as well as P454 sequencing is planned to complete the genome annotation.

Chapter 5. Two independent mechanisms that affect hypermotility.

Genetic revertants can be used to uncover members of pathways controlled by specific groups of genes. Two such revertants namely, *cyaA* and *opuAC* that reduced the hypermotility of *morA* mutants are partially characterized in the study report in this Chapter. I present data to show that *cyaA* function in an antagonistic manner with *morA* while *opuAC* acts independently of *morA* to control motility. Incidentally, the disruption of *opuAC* leads to 45% increase of pyoverdine secretion to the medium.

5.1. BACKGROUND

The loss of MorA has been previously shown to increase *fliC* expression in *P. putida* that, in turn, increases flagellin level. As such, MorA was proposed to be a key component of an alternative regulatory system that normally limits the expression of flagellar biosynthesis pathway to the late phases of growth (Choy, 2005).

In order to investigate the members of the MorA signaling pathway, random mutagenesis was carried out on MorDCK03 strain using mTn5-*gfp* (Suarez *et al.*, 1997). As *morA* loss leads to hypermotility, we screened for hypermotility reversion to wild type levels to uncover intermediates in MorA signaling pathway. We hypothesized that any disruption in the flagellar pathway would cause serious defects in the motility of the cell via the malformation or malfunction of the flagella causing non-motile cells. Thus non-motile mutants were excluded from the study during the primary and secondary selection process.

An estimated 3500 transconjugants were screened via plate motility assay for decrease of colony diameter that would indicate a reversion in the motility phenotype. Through the primary screening, 408 transconjugants were selected for video microscopy assay for motility of individual cells. Of which, a total of 76 mutants were found to show reversion of hypermotility phenotype while retaining the ability to swim. Several genes were identified in these transconjugants via single primer PCR (Ng, 2006). Among these motility reversion mutants, *cyaA,* ABC-type glycine betaine transport system (*opuAC*) and a putative diguanylate cyclase/phosphodiesterase

(GGDEF & EAL domains) with PAS/PAC and GAF sensor(s) that we designated *morC* were selected for further studies.

As MorA contains both DGC and PDE domain, MorC, being a putative GGDEF-EAL bidomain protein, offers an intriguing view in the complexity of c-di-GMP regulation by offering clues as to how c-di-GMP is being regulated at multiple levels to regulate the various pathways in the cell. MorC will be discussed in greater details in Chapter 6.

cyaA encodes an adenylate cyclase, that in turn, suggests linkages between two different second messenger pathways in the swimming motility regulation. It was previously reported in *V. cholerae* that cAMP-cAMP receptor protein (CRP) regulatory complex could work independent of VpsR to regulate biofilm matrix proteins (Fong and Yildiz, 2008). VpsR is a member of the NtrC subclass of response regulators of the two-component signal transduction systems that possesses an N-terminal domain that can be phosphorylated by a cognate sensor histidine kinase. This is achieved by cAMP-CRP regulating the expression of a set of genes encoding DGCs and PDEs. Mutational and phenotypic analysis further identified a DGC, CdgA to be responsible for biofilm formation increase in Δ*crp* mutant. ABC-type glycine betaine transport system was disrupted in two motility reversion mutants, suggesting that it is important in the MorA regulation of motility pathway.

To verify that the random transposon screening was successful, phenotypic assays were previously carried out to characterize the identified mutants. However, in order verify the motility reversion mutants and to also facilitate genetic studies; markerless

knockout of these mutants were generated in this study and their phenotypes were then characterized.

5.2. RESULTS AND DISCUSSION

5.2.1 CyaA acts in an antagonistic manner to MorA to control motility

In order to validate the data obtained from the random mutagenesis screening, *cyaA* single and Δ*morA*Δ*cyaA* double markerless knockout mutants were generated. Subsequently, plate motility assay and biofilm formation assay was conducted. The data obtained was then compared to the parameters used for the screening of motility reversion mutants for any reduction in motility when compared to Δ*morA* strain.

The results presented in Fig. 5-1 shows that there is indeed a clear reduction of motility from 2-fold to 0.5-fold in Δ*morA*Δ*cyaA* showing that CyaA is required for the hypermotility phenotype observed in Δ *morA*. This requirement is independent of *cyaA* copy number as the hypermotility phenotype is observed in both Δ*morA*pGB1cyaA and Δ*morA* when *cyaA* is present in multiple copies and as a single copy, respectively. The products of both genes act negatively in the control of motility as can be seen in the hypomotility phenotype presented in both overexpression strains (Fig. 4-5; Fig. 5-1B).

Table 5-1 summarizes the findings and shows that there is a clear trend in the relationship between MorA and CyaA. MorA exerts dominant effect over CyaA in the

control of motility. This is derived from the observation that the absence of MorA leads to hypermotility while the presence of MorA in both absence and presence of CyaA leads to an intermediate motility. In addition, *cyaA* did not show any observable changes in motility.

Overexpression of either *morA* or *cyaA* when both genes are present, leads to hypomotility (Table 5-1). This is the same phenotype observed when both genes are knocked out thus it is likely that *morA* and *cyaA* interact in an antagonistic manner and that at least one gene is required for swimming motility. It is also observed that *morA* determines the direction in which *cyaA* controls motility as the presence of both *morA* and *cyaA* leads to reduction in motility while the absence of *morA* with *cyaA* leads to increase in motility.

A

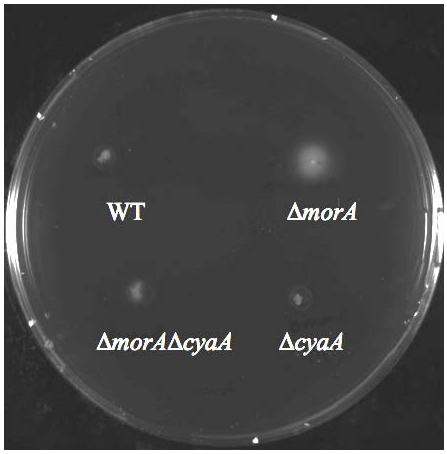

B

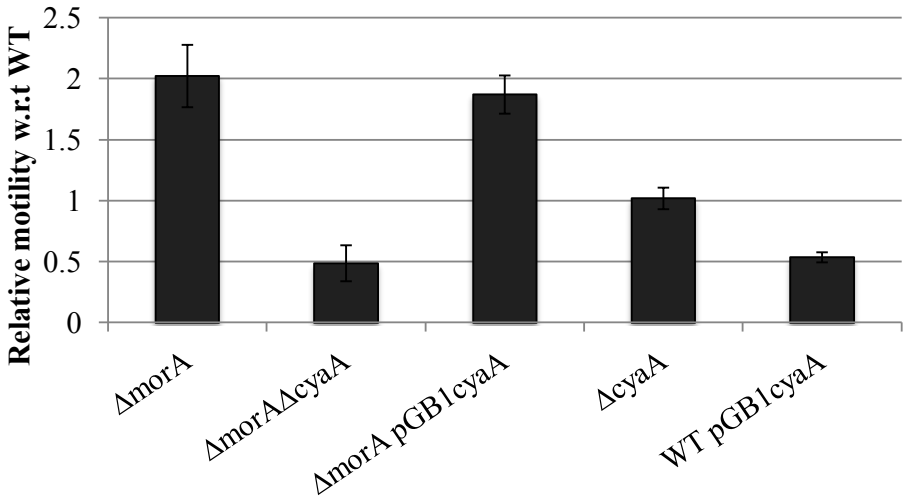

Fig. 5-1. CyaA acts in an antagonistic manner to MorA to control motility. (A) The swimming motility of various strains in semisolid LB agar (0.4%[wt/vol] agar) was examined after incubation at 30ºC for 24h. (B) The bar chart shows the relative motility of the mutants as compared to the WT. Relative motility is derived by dividing the colony diameter of the mutants by the colony diameter of WT. Δ*morA* acting as a control showed about 2-fold increase in swimming motility through 0.4% (w/v) soft agar compared to WT. The results were based on three independent experiments, each with five replicates; error bars indicate standard deviations and are represented as vertical bars.

Table 5-1. Effects of combinations of *morA* and *cyaA* genes on motility.

Strains	*cyaA*	*morA*	Relative motility to WT
WT pGB1cyaA	++	+	**0.5**
WT pGB1morA	+	++	**0.5**
Δ*morA*Δ*cyaA*	**-**	**-**	**0.5**
WT	+	+	**1**
Δ*cyaA*	**-**	+	**1**
Δ*morA* pGB1cyaA	++	**-**	**2**
Δ*morA*	+	**-**	**2**

(-) denotes the absence of gene expression; (+) denotes wildtype expression of gene; (++) denotes overexpression of gene. Swimming motility is calculated relative to WT. Relative motility is derived by dividing the colony diameter of the mutants by the colony diameter of WT.

5.2.2. CyaA does not affect biofilm formation

Fig. 5-2 shows that in all strains, the effects on biofilm formation were seen at the early time point of 3 hours and persisted to the later time point of 10 hours. Similar to the motility reversion mutant, *cyaA* knockout in Δ*morA* background increased biofilm formation when compared to Δ*morA*. The complementation of Δ*morA*Δ*cyaA* with pGB1cyaA was able to complement for loss of *cyaA* such that the biofilm formation was reduced back to the level of Δ*morA*.

The assay results show that *cyaA* alone does not affect biofilm formation. This was determined from the lack of significant difference when comparingΔ *cyaA* and WT pGB1cyaA with WT. The changes in biofilm formation observed in Δ*morA*Δ*cyaA* and Δ*morA* pGB1cyaA can also be attributed to the absence of *morA* rather than due to *cyaA*. This can be seen in the reduced biofilm formation when comparing between Δ*cyaA* and Δ*morA*Δ*cyaA* as well as in WT pGB1cyaA and Δ*morA* pGB1cyaA respectively.

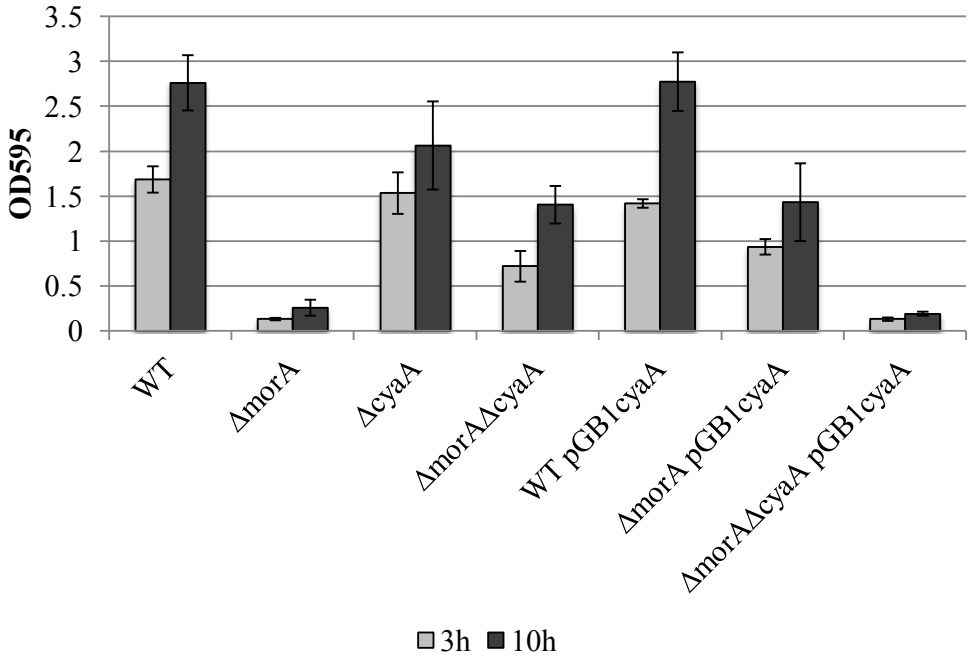

Fig. 5-2. CyaA does not affect biofilm formation in *P. putida.* The plasmid pGB1cyaA was introduced into various mutant strains for complementation and overexpression. Biofilms formed at 3h and 10h after inoculation in polystyrene tubes were stained with 0.1% crystal violet. The results are based on three independent experiments, each with five replicates; error bars indicate standard deviations and are represented as vertical bars.

5.2.3. OpuAC functions independent of MorA in control of motility

ABC-type glycine betaine transport system was identified in two random transposon mutants, Q12 and H6. In both mutants, the transposon was inserted into the substrate-binding region of the transport system (OpuAC). Unlike most genes, *opuAC*, containing 2 captial letters was the designated gene name given in NCBI. *opuAC* is the third gene in an operon encoding 4 genes for the ABC-type glycine betaine transport system. This being the case, it is possible that unforeseen effect can affected our characterization when the motility reversion mutant was used for characterization. Δ*opuAC* was thus generated using the markerless knockout protocol discussed previously (Choi and Schweizer, 2005). As the protocol was designed to not affect the neighbouring genes, the results obtained reflect the effect due to the loss of the substrate-binding region only.

Unexpectedly, the disruption of *opuAC* in Δ*morA* background did not lead to lower motility than that observed in Δ*morA* (Fig. 5-3). Instead, Δ*morA*Δ*opuAC* double knockout strain showed the same motility phenotype as *morA*, that is, a 2-fold increase in motility. It should be noted that motility is lowered when compared to Δ*opuAC* single knockout mutant, suggesting that the hypermotility phenotype is modulated by the loss of *morA*. Since Δ*opuAC* specifically disrupted the third gene in the operon, it is likely that the motility reversion mutants reflected phenotypic changes due to either the disruption of the the fourth gene in the operon that encodes for the inner membrane protein or the disruption of both genes. Δ*opuAC* showed an even more pronounced hypermotility phenotype of 3-fold increase when compared to WT. Hence *opuAC* is a negative regulator of motility. Overexpression of *morA* in

Δ*opuAC* and Δ*morA*Δ*opuAC* caused the motility ofΔ *opuAC* to decrease by 40% and Δ*morA*Δ*opuAC* to be reduced by 20%. This data demonstrates that MorA is able to perturb motility without OpuAC. When comparing Δ*opuAC* pGB1morA and WT pGB1morA as well as Δ*opuAC* pGB1morA and Δ*morA* Δ*opuAC* pGB1morA, it is evident that disruption of *opuAC* in the presence of *morA* still leads to hypermotility. Together, these results suggest that *opuAC* functions independent of MorA in controlling motility.

A

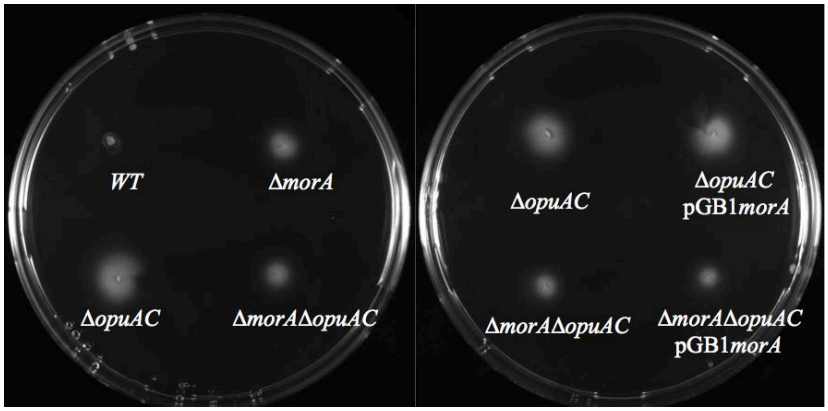

B

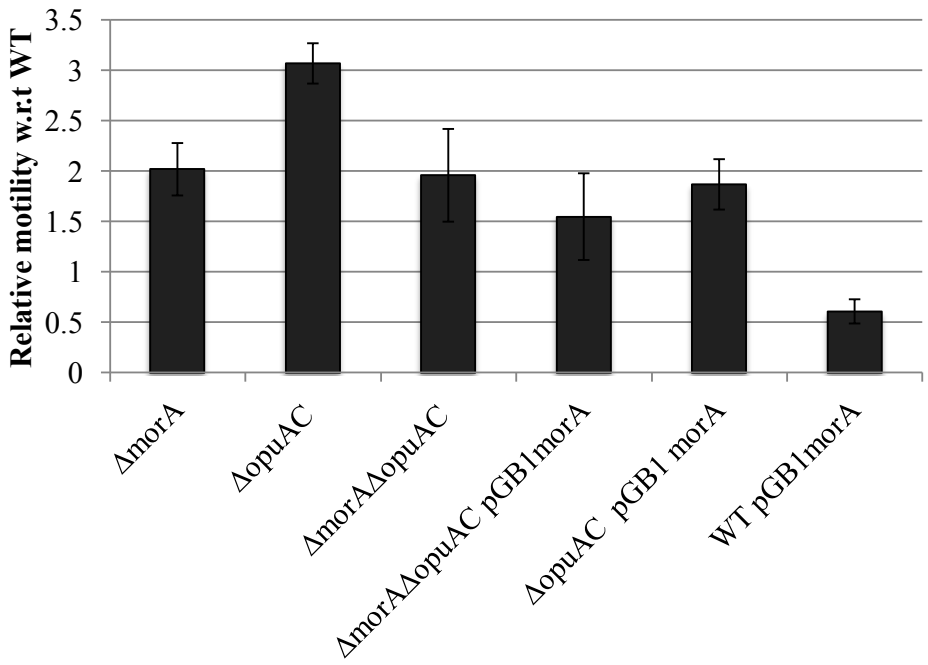

Fig. 5-3. *opuAC* acts independently of *morA* in *P. putida*. (A) The swimming motility of various strains in semisolid LB agar (0.4%[wt/vol] agar) was examined after incubation at 30ºC for 30h. (B) The bar chart shows the relative motility of the mutants as compared to the WT. Relative motility is derived by dividing the colony diameter of the mutants by the colony diameter of WT. Δ*morA* acting as a control showed about 2-fold increase in swimming motility through 0.4% (w/v) soft agar compared to WT. The results are based on three independent experiments, each with five replicates; error bars indicate standard deviations and are represented as vertical bars. Asterisk * indicate that the values compared are significantly different. Significance was calculated using Tukey's pairwise comparison of means, p=0.05.

5.2.4. Δ*opuAC* strains have reduced biofilm formation

Biofilm formation assay was carried out to further characterize the strain and clarify the relationship between *morA* and *opuAC*. Δ*morA*Δ*opuAC* had 7-fold increase in biofilm formation after 10hours incubation when compared to Δ*morA*. Δ*opuAC* mutant, on the other hand, presented low level of biofilm formation such that the amount is similar to that observed in Δ*morA* (Fig. 5-4). This suggests that loss of *opuAC* leads to reduced biofilm formation.

Overexpression of *morA* in Δ*opuAC* led to increase in biofilm formation to similar level as WT, showing that *morA* is able to perturb biofilm formation without OpuAC. Likewise, Δ*opuAC* pGB1morA and Δ*morA*Δ*opuAC* pGB1morA had increased biofilm formation when compared to their background strain. Hence, it is likely that MorA does not affect biofilm formation via OpuAC. The motility plate assay data combined with biofilm formation data allow us to conclude that OpuAC functions independent of MorA.

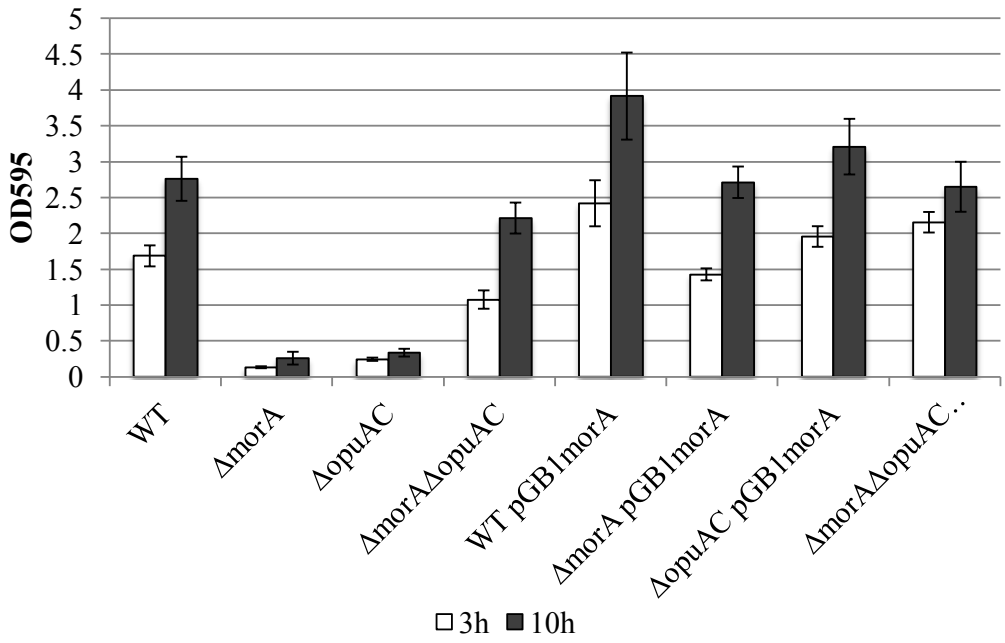

Fig. 5-4. Δ*opuAC* strain has reduced biofilm formation. Biofilms formed at 3h and 10h after inoculation in polystyrene tubes were stained with 0.1% crystal violet. The results are based on three independent experiments, each with five replicates; error bars indicate standard deviations and are represented as vertical bars.

5.2.5. Δ*opuAC* leads to increased production of pyoverdine

Interestingly, the M9 medium in which theΔ *opuAC* strain was grown was particularly fluorescent when compared to WT (Fig. 5-5A). As no difference was observed when growth curve was previously performed with LB medium, a growth curve using M9 medium was performed and shown in Fig. 5-5. The curve show that OD_{600} readings were comparable till the mid-log phase after which the two strains begin to differ in which Δ*opuAC* showed higher OD_{600} readings. After 24 hours of incubation, the difference was substantial: Δ*opuAC* showed OD_{600} reading of 2.29 while WT showed a reading of 1.56, respectively. As such, the use of OD_{600} readings as a comparison of growth between WT and Δ*opuAC* is not accurate. To accurately compare growth, other methods such as direct microscopic counts or viable cell counts (colony counts) would have to be utilized in future work.

It is known that fluorescent pseudomonads produce a line of siderophores with high complexing constants, of which, one of the most important representatives are the pyoverdines (Neilands, 1995). The pyoverdines are comprised of a dihydroxyquinoline moiety that imparts fluorescence (chromophore), a peptide chain comprising 6–12 partially modified amino acids bound to the carboxyl group, and a small dicarboxylic acid connected amidically to the NH2-group of the chromophore. Frequently several pyoverdines co-occur differing only in the nature of the dicarboxylic acid side chain. The pyoverdines may also be accompanied by related compounds, which are considered as their biosynthetic precursors or later modifications (Budzikiewicz, 2007).

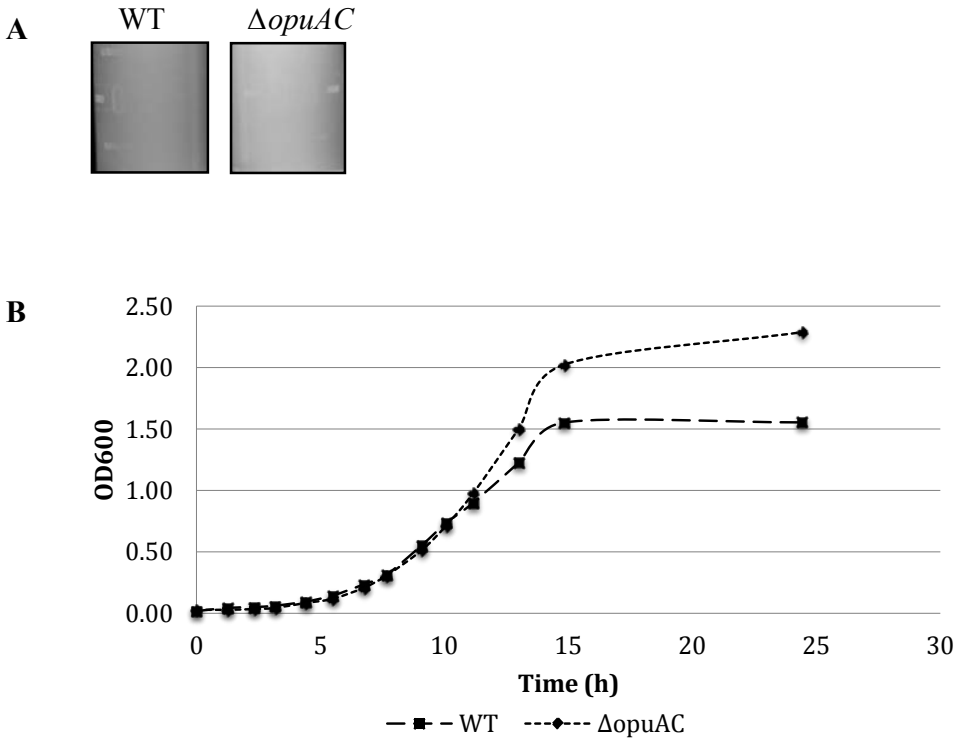

Fig. 5-5. Δ*opuAC* and WT shows differences in the stationary phase of growth curve. (A) M9 culture medium innoculated with Δ*opuAC* strain can be observed to be of lighter shade (more fluorescent) when compared to WT cells under UV lamp. (B) Growth curve of WT and Δ*opuAC* strain in M9 medium demonstrated effect of increased pyoverdine production on absorbance readings from mid-log phase onwards. Absorbance at 600nm (OD600) of bacterial cultures growth in M9 medium at 30ºC were measured at intervals of half to one hour.

These compounds possess the same peptide chain as the pyoverdine but differ in the nature of the chromophore (Budzikiewicz, 2004).

One of the most important functions that pyoverdine serves, due to its high-affinity towards iron (III), is the chelation and transport of iron (reviewed by Matzanke, 2011). Though iron is widely found nature, the majority of this iron is present in the form of insoluble material that severely limits its bioavailability. To measure differences in pyoverdine levels between WT and Δ*opuAC*, a scan was performed to obtain the relative fluorescence reading from 300nm to 600nm. Fig. 5-6 shows that the M9 medium displayed basal level of fluorescence after 430nm while in both WT and Δ*opuAC*, there were similar readings recorded between 300nm to 574nm. After which, the two strains showed differences in the amount of fluorescence readings. The largest difference was captured at between 584 to 598nm, with 588nm showing an increase of 45%.

This preliminary data suggests that the loss of *opuAC* had led to increased pyoverdine synthesis and export, while it is not clear at the moment why this has occurred; it is an important finding due to the many important roles pyoverdine plays in iron transport, virulence and plant-microbe interaction (Neilands, 1995).

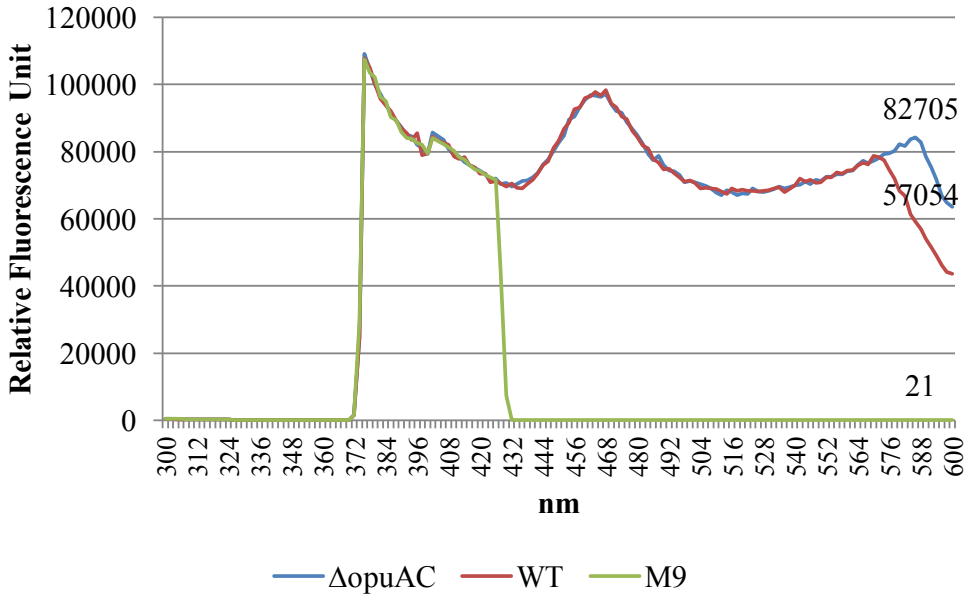

Fig. 5-6. Pyoverdine production was increased by 45% in Δ*opuAC*. Fluorescence scan of culture media shows that pyoverdine production was elevated in Δ*opuAC*. 24h old bacterial culture was centrifuged to remove bacterial cells and then culture medium was subjected to fluorescence scanning (300nm-600nm) to obtain relative fluorescence unit readings. Relative fluorescence unit reading at 588nm presented the largest difference between WT and Δ*opuAC*; values at 588nm are shown as data labels on the chart.

5.3. CONCLUSION AND FUTURE WORK

In this Chapter, CyaA and OpuAC was found to utilize different strategies to control motility. The data derived from motility plate assay suggests that CyaA interact with MorA in an antagonistic manner to control motility but do not affect biofilm formation. In this antagonistic relationship, it is also apparent that MorA exerted dominant effect on motility over CyaA.

OpuAC, on the other hand, is a negative motility regulator that functions independently of MorA to regulate motility and biofilm formation. In addition, Δ*opuAC* presented 45% more pyoverdine production when compared to WT, suggesting that there may be a linkage between osmoregulation with iron transport. Also, *P. fluorescens* and *P. putida* has very diversified pyoverdines (Meyer *et al.,* 1997). Thus, the identification and characterization of pyoverdine(s) in *P. putida* PNL-MK25 need to be first carried out before other experiments. Since Fig. 5-6 showed that differential readings were registered from 560nm to 600nm, TLC or HPLC analysis with a standard control should be used to determine the specific pyoverdine contributing to the fluorescence reading. Since M9 do not contain an iron source, the cells are grown in iron-starved condition that would have promoted increased pyoverdine production. Thus, the same experiment should be repeated in M9 medium with the addition of varying concentration of iron to see if Δ*opuAC* presents more pyoverdine than WT under such condition to understand the conditions that led to increased pyoverdine production.

Fig. 5-7 summarizes the interactions of MorA, CyaA and OpuAC to control various phenotypes that include motility, biofilm formation, chemotaxis and pyoverinde production. This report hints at the interaction between cAMP and c-di-GMP second messenger signaling system in *P. putida.* As Δ*cyaA* presented WT level of motility, complementation was not performed though overexpression of *cyaA* was studied. On the other hand, overexpression and complementation of *opuAC* was not performed. Thus, to complete the genetic studies, these strains need to be generated for phenotypic analysis.

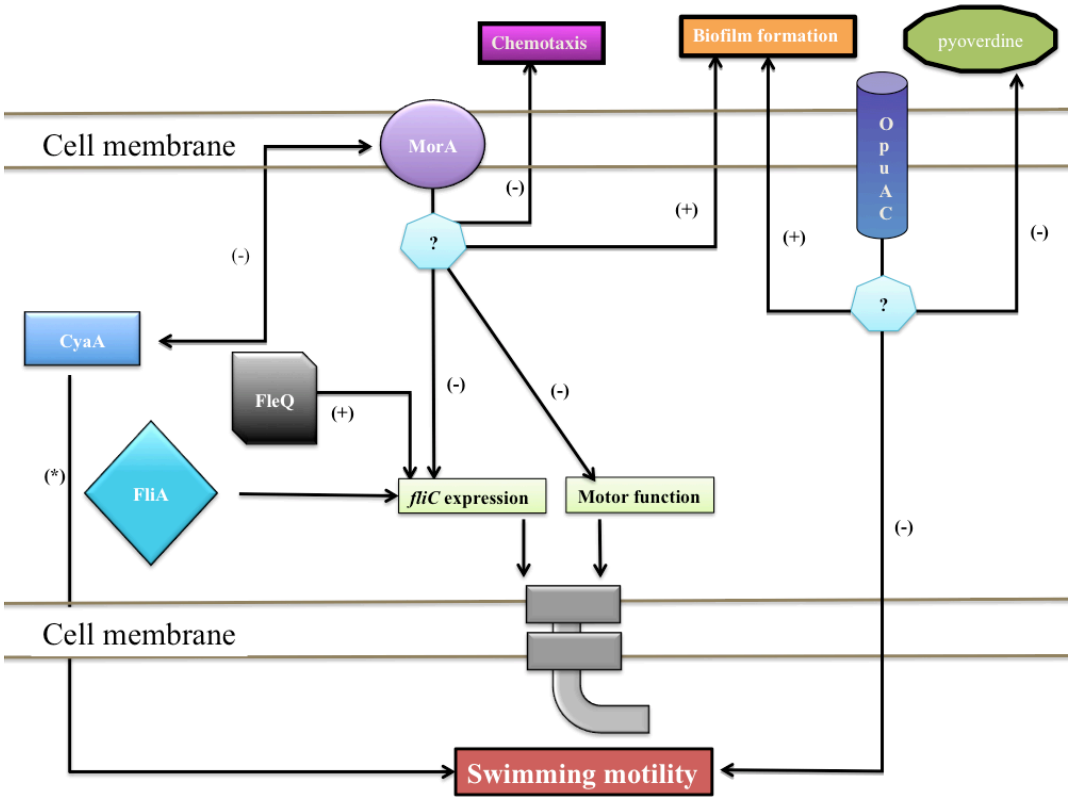

Fig. 5-7. Different strategies employed by CyaA and OpuAC to control motility. Though CyaA interacts in an antagonistic manner with MorA, MorA exerts dominant effects over motility and can determine cyaA control over the direction of motility. OpuAC, on the other hand, acts independently of MorA to control both motility and biofilm formation. (+) and (-) denotes positive and negative regulation, respectively, while (?) denotes unknown intermediates.

Chapter 6. MorC is a positive regulator of motility that affects cell speed

Genetic approaches can be used to combine mutations in a single strain in order to place these genes in single or different pathways. In this Chapter, results are presented that show that MorC is a positive regulator of motility that functions downstream of MorA. While MorA affects motility, biofilm formation and chemotaxis, MorC is revealed to have no effects on biofilm formation or chemotaxis. Gene expression and cellular localization studies demonstrate that MorC is selectively expressed in the early and late log phase. Motility assay with truncated MorC construct and site directed mutants indicated that the activities of MorC are dependent on its PDE domain as well as MorA interacting with MorC through long-range conformational changes. Video microscopy in conjunction with TEM structural studies provided additional evidence to suggest that MorC affects motility via changes in cell speed where the residues in its EAL motif were observed to serve specific function at early and late-log growth phase.

6.1. BACKGROUND

As discussed in Section 5.1, 76 motility reversion mutants were able to reverse the hypermotility phenotype of *morA* mutant while not resulting in non-motility. In order to identify the genes disrupted by the transposon, single primer PCR was used to obtain the sequences flanking the transposon insertion sites (Ng, 2006). From the BLAST analysis, a motility reversion mutant, O13, exhibiting two-fold decrease in motility and increased biofilm formation, was identified as a putative diguanylate cyclase/phosphodiesterase (GGDEF & EAL domains) with PAS/PAC and GAF sensor(s). As the loss of gene function leads to reduced motility, we named this gene the motility regulator, *morC*. In this Chapter, we set out to characterize MorC effects on motility and described alongside its relationship with MorA.

6.2. RESULTS AND DISCUSSION

6.2.1. MorC is highly conserved in *Pseudomonas* species

DNA sequencing results show that the miniTn5-*gfp* transposon was inserted between nucleotide position 2252 and 2253 (Fig. 6-1A). Subsequently, gene walking was performed to obtain full length DNA sequence (Appendix III). The results reveal that the *morC* gene is 2697bp long and predicted to encode for a polypeptide of 898 amino acids with a predicted molecular weight of 100KDa. *morC* is flanked by genes encoding for an alkaline phosphatase D-like phosphodiesterase and a methionine sulfoxide reductase that helps to repair oxidative damage by reducing methionine sulfoxide to methionine (Fig. 6-1A). In order to create the markerless knockout construct, *morC* gene sequence 5' fragment and 3' fragment was amplified from nt position 369 to 735 and 2454 to 2697, respectively. As such, nt position 736 to 2453 was removed in Δ*morC* and replaced with the FRT scar.

Searches of DNA sequence databank using BLAST showed that *morC* homologs are present in many *Pseudomonas* species and they shared high degree of sequence similarity values ranging from 40% to 96%. Members of the MorC family: (i) are present as single copy in *Pseudomonas* genomes, (ii) are likely localized in the cytoplasm, (iii) possess a central sensory domain of PAS-PAC motifs, (iv) contain the GAF cyclic nucleotide-binding domain and (v) have C-terminal ASNEF and EAL domains. Homologs of MorC are also found in other bacterial families though these typically contain the GGDEF motif rather than ASNEF motif. This suggests that the ASNEF motif serves a specific function in the *Pseudomonas* genus. A phylogram was drawn to examine the phylogenetic relationships between MorC and its homologues

(Appendix IV). The phylogram revealed that *morC* is most closely related to Pfl01_0460 of *P. fluorescens* Pf0-1. This observation was also consistent with other sequences previously obtained in our laboratory from this strain that matched closely with those from *P. fluorescens* Pf0-1 genome and not *P. putida* KT2440.

Homology studies show that PA5017 is the MorC homolog in *P. aeruginosa*. Previous studies conducted to characterize its function found that the absence of PA5017 in both PA68 and PAK strain negatively affected swimming motility and chemotaxis while increasing biofilm formation (Kulasakara *et al.,* 2006; Li *et al.,* 2007). Reverse-phase HPLC was performed on Δ*PA5017* nucleotide extract and protein extract in which the assay did not show any DGC or PDE enzymatic activity. However, the results were not conclusive as it was thought that assay has limited sensitivity at 12pmol/mg cell wet weight. Since it is an *in vitro* assay, it was also possible that activating signals were lacking in the mixture.

A

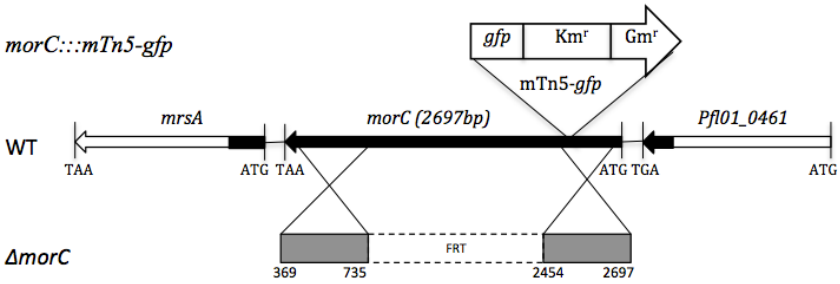

B

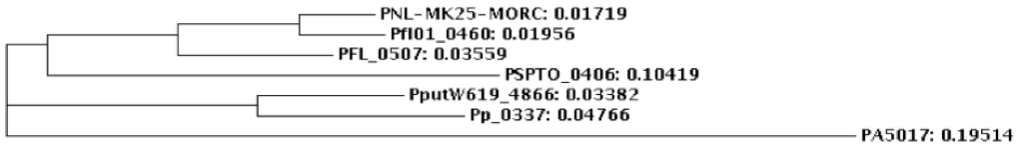

C

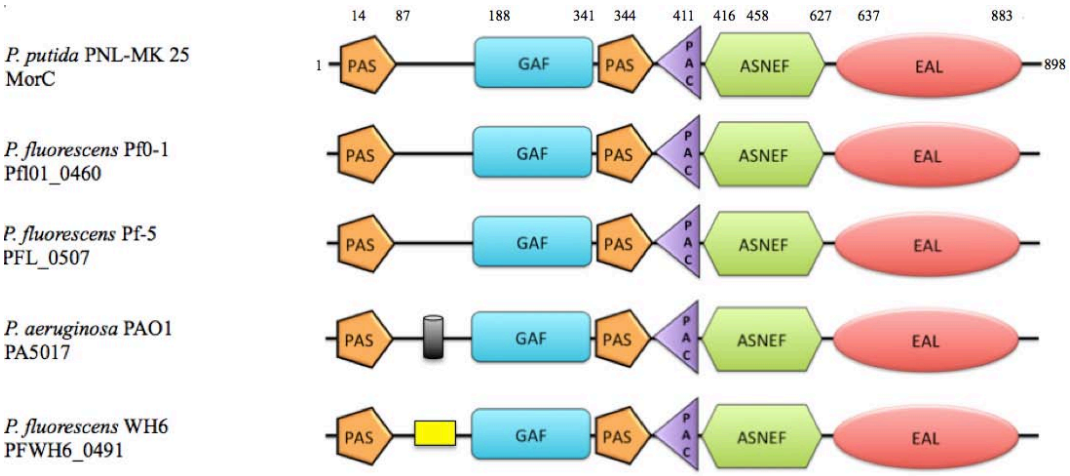

Fig. 6-1. Conservation of *morC* gene in *Pseudomonas* species. (A) Organization of *P. putida* PNL-MK25 morC locus. The solid arrows show the direction of the genes. Transposon mutant strain carries the mTn5-gfp insertion at nucleotide position 2252 of *morC*. *morC* is flanked by genes encoding for methionine sulfoxide reductase A (*mrsA*) and a conserved hypothetical protein predicted to be a phophodiesterase/ alkaline phosphatase D-like. Δ*morC* is a markerless knockout mutant generated with homologous recombination. (B) Phylogram tree of MorC and its homologues was generated by Clustalw (http://www.ebi.ac.uk/clustalw). (C) MorC domain architecture is highly conserved. Grey cylinders are segments of low compositional complexity. The domains were predicted using the Simple Modular Architecture Research Tool (http://smart.embl-heidelberg.de).

6.2.2. MorC is a positive regulator of motility that functions downstream from MorA

Disrupting *morC* in the Δ*morA* background led to the reduction of motility from 2-fold to 0.5-fold, suggesting that MorC is essential for the transduction of signals in MorA signaling pathway (Fig. 6-2). To investigate the effects of *morC* on motility, *morC* markerless single knockout strain was generated. This strain presented a reduction of motility to 0.5-fold, indicating that MorC is a positive regulator of motility. It should also be pointed out that both Δ*morC* and Δ*morA*Δ*morC* showed 0.5-fold motility. While overexpression of *morA* leads to decrease in motility, the introduction of pGB1morA into Δ*morA*Δ*morC* did not lead to significant reduction in motility. These two results jointly suggest that MorC functions downstream from MorA. Though the introduction of mTN7T-morC in Δ*morA*Δ*morC* did not led to full complementation, it led to an increase in motility to WT level.

Complementation of the Δ*morC* strain with the *morC* gene driven by native promoter (mTn7T-morC) resulted in restoration of motility to WT level while the overexpression of *morC* in WT via transposon insertion lead to 50% increase in motility. Our laboratory has previously shown that there was a strict dosage control over *morA* such that slight perturbation of gene copy number by using a low copy number vector (pGB1) for complementation still led to measurable differences in phenotypes. MorC, however, showed 50% increase in motility regardless of whether overexpression was achieved with a low copy number vector, pGB3 or transposon integration into the chromosome. This indicates that phenotypic changes have remained at a constant level regardless of gene copy number. It was also noted that

the overexpression and knockout of *morC* leads to 0.5-fold change in motility. Therefore, an alternate possibility could be that the regulatory proteins present in the cell is limited and in turn, restricts the phenotypic changes.

A

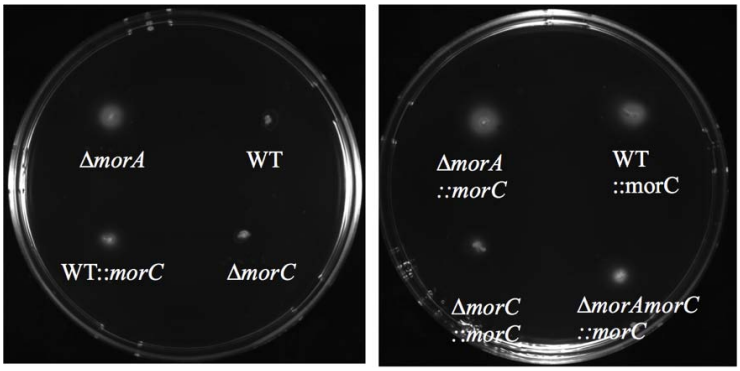

B

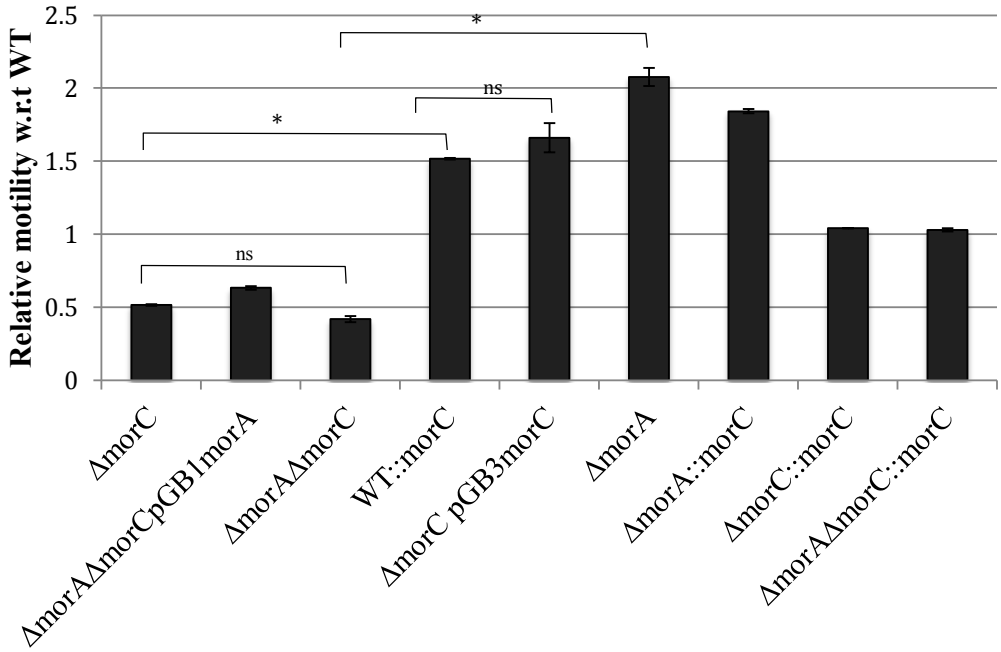

Fig. 6-2. Δ*morC* mutant exhibits reduced swimming motility. The swimming motility of various strains in semisolid agar (0.4%[wt/vol] agar) was examined. The results are based on three independent experiments, each with five replicates. Asterisk * indicate that the values compared were significantly different while ns indicate no significant differences. Significance was calculated using Tukey's pairwise comparison of means, p=0.05.

6.2.3. Mutation in *morC* does not affect biofilm formation in *P. putida*

Previous studies shows that biofilm formation requires appropriate flagellar biogenesis (Pratt and Kolter, 1998; Sauer *et al*, 2002). Also, Choy *et al* (2004) demonstrated that Δ*morA* mutant led to a significant reduction in biofilm formation while increasing motility. As MorC is implicated in MorA signaling pathway, we then investigated if MorC also affect biofilm formation. It should be noted that biofilm formation assay was not used as a parameter during the transposon mutant screening. As such, similar results to those observed in Δ*morA* were not expected.

Biofilm formation was examined on polystyrene surfaces by incubating bacterial cultures on polystyrene tubes for 3 and 10 hours. The biofilms were then visualized by crystal violet staining; solubilized in 1% SDS and then quantitated by OD_{595} readings. Biofilm formed by Δ*morC* and WT showed no significant differences while the knockout of *morC* in Δ*morA* background leads to increased biofilm formation when compared to Δ*morA*. Δ*morA*Δ*morC* pGB1morA on the other hand showed an increase in biofilm when compared to Δ*morA*Δ*morC* to level comparable to Δ*morC*. Together, the data suggests that MorC alone do not cause biofilm formation changes. Indeed, biofilm formation was affected in the presence or absence of MorA. Hence, we propose that MorA regulates biofilm formation by a pathway not involving MorC.

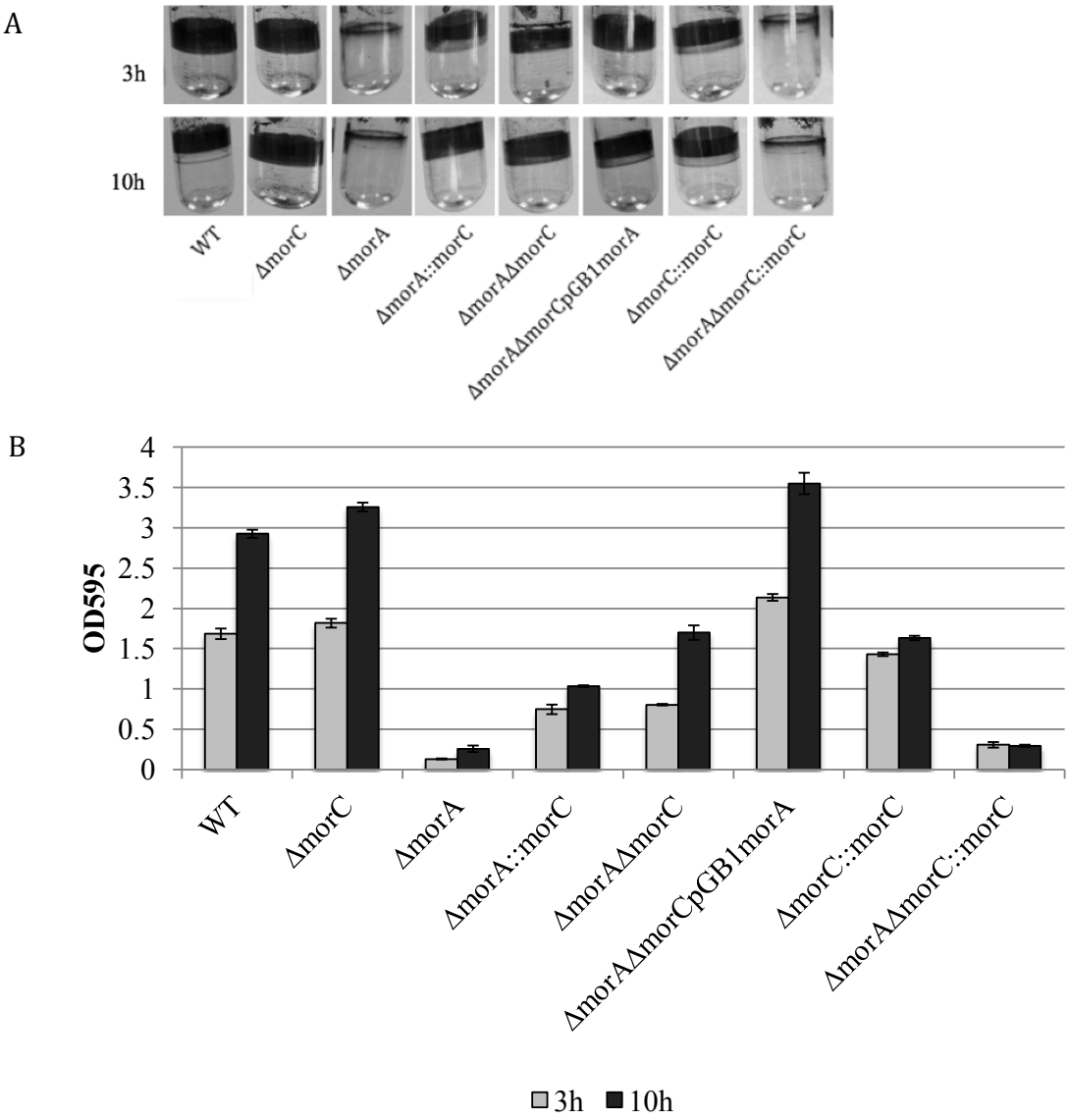

Fig. 6-3. MorC does not affect biofilm formation. (A) Various strains were grown in LB broth in polystyrene tubes at 30^0C with 250rpm shaking for 3 and 10hours. The biofilms were stained with 0.1% crystal violet and then solubilized in 1% SDS for quantitation. (B) The results are from three independent experiments with three technical replicates. The error bars indicate standard deviation.

6.2.4. Mutation in *morC* does not affect chemotaxis

Chemotaxis is the process by which bacteria moves towards attractants or away from repellants. This process is tightly coupled to bacterial motility. Since, PA5017 was reported to affect chemotaxis (Li *et al.,* 2007), we examined the chemotactic response of the various MorC mutants using an adapted chemotaxis assay (Shi *et al.,* 1998). A universal chemoattractant, aspartate, was used in the experiments. In all cases, the mutants formed a concentric ring around the agar plug containing aspartate after a 6h incubation period, indicating movement of these cells towards the plug. Thus showing that chemotaxis was able to occur. Fig. 6-4 clearly shows that the concentric rings are similar in size in all the plates. Hence, MorC do not affect chemotactic response toward aspartate when compared to WT.

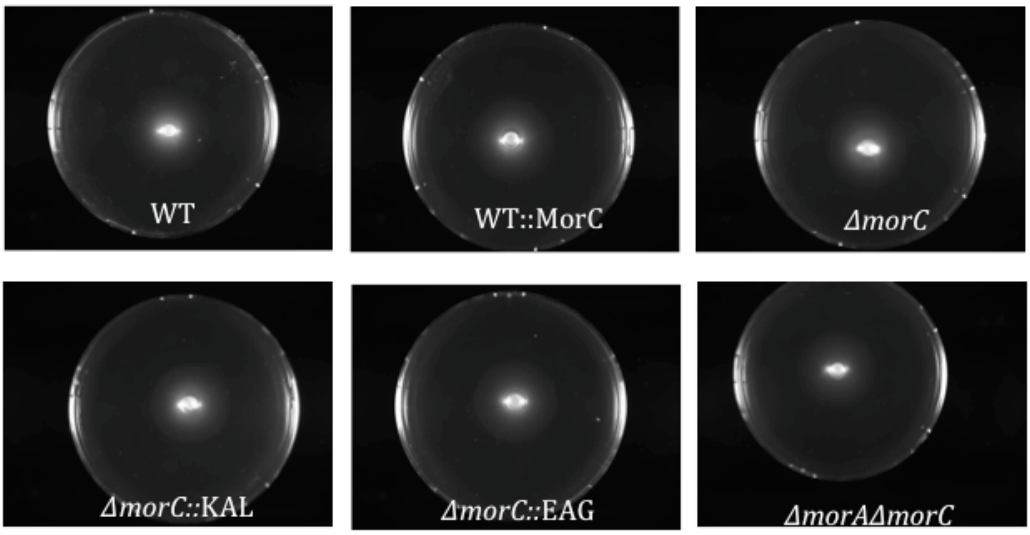

Fig. 6-4. Chemotactic response of various *morC* mutants towards 100mM aspartate. Overnight cultures were washed and resuspended in half-strength M9 medium and adjusted to OD_{600}=1.0. The cultures were mixed with 0.4% (w/v) agar (1:24 ratio) and poured onto a petri plate with an agarose core containing 100mM of aspartate followed by incubation at 30ºC.

6.2.5. Sequence analysis of MorC suggests that it is a functional PDE

Sequence analysis of MorC was carried out to ascertain the likely function of the protein (Fig. 6-5). It was found that the ASNEF motif was conserved in place of the GGDEF motif (Fig. 6-5A). Similar cases had previously been reported in inactive DGCs such as CC3396 and FimX that contains altered GEDEF and GDSIF motif sequences respectively (Christen *et al.,* 2005; Kazmierczak *et al.,* 2006). The allosteric c-di-GMP binding RXXD I-site that is known to be located five residues upstream of the GGDEF motif is not present in MorC as well (Christen *et al.,* 2006; De *et al.,* 2008). As such, it is thought that the DGC function is likely to be absent in MorC.

Likewise, the EAL domain is considered intact if it contains the canonical EAL motif and the conserved DDFGTGYS motif (Schmidt *et al.,* 2005). This motif was later designated to be part of the β6-loop required for substrate binding and catalysis (Rao *et al.,* 2009). Key residues implicated for Mg^{2+} and c-di-GMP interactions have also been previously identified in a biochemical study (Rao *et al.,* 2008). It can be seen in Fig. 6-5B that MorC contains the EAL motif, β6-loop as well as the key residues required for Mg^{2+} and c-di-GMP interactions. Hence, it is likely that MorC contains a functional PDE domain. Interestingly, other than the canonical EAL motif located at residues 673 to 675, another EAL motif was found in MorC to be located at residues 754 to 756. When MorC PDE domain modeling was conducted, it was observed that $_{754}$EAL$_{756}$ is located away from the active site (Fig. 6-5C).

A

B

C

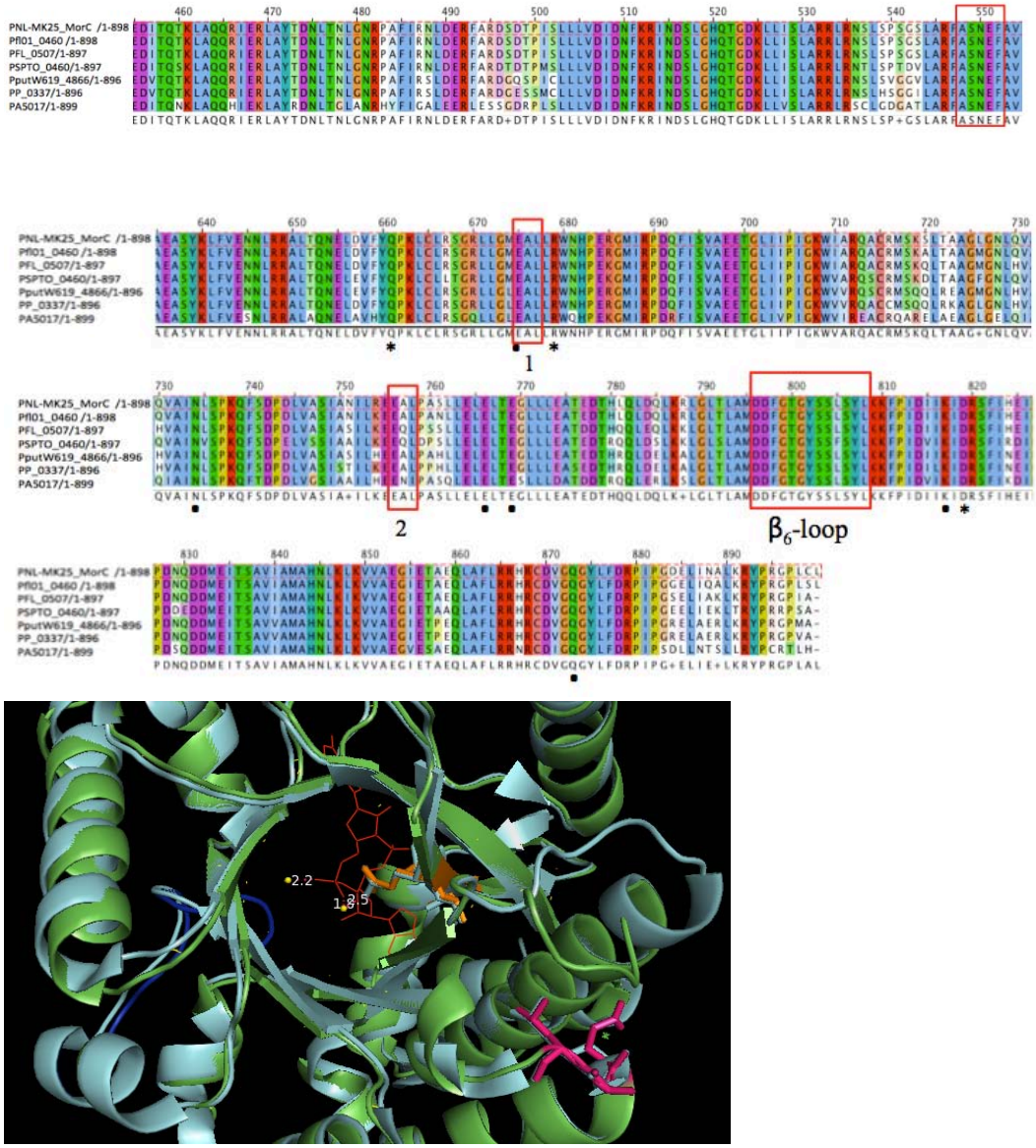

Fig. 6-5. The sequence of MorC suggests that it may encode for an inactive DGC domain with a functional PDE domain. (A) MorC does not contain either the GG[D/E]EF motif or the RXXD (I) site. (B) MorC encodes the catalytic EAL motif at residue 673 to 675 (box1) as well as the conserved β6-loop and key residues required for Mg^{2+} (.) and c-di-GMP (*) interaction. Interestingly, an additional EAL motif was located at residues 754 to 756 (box 2). Annotation adapted from Seshasayaee *et al* and Rao *et al.* (C) Model of MorC EAL domain (pale teal) superimposed on tdEAL (green, PDB ID: 3n3t). The oranges sticks represent the side-chains of $_{673}$EAL$_{675}$ interacting with Mg^{2+}. The model indicates that the E673 site interacts with Mg^{+} that in turns interact with the phosphate groups of c-di-GMP. The pink sticks represent the side chains of $_{754}$EAL$_{756}$ while the blue sticks represents the β6-loop.

6.2.6. MorC function is dependent on its PDE domain

To investigate if the PDE domain is essential to the function of MorC, we generated a truncated MorC construct (ΔEAL) in which the PDE domain was removed. Indeed, the complementation of Δ*morC* with ΔEAL was not able to restore motility back to WT level but remained at 0.5-fold (Fig. 6-6). To further examine if the function is associated with the EAL motif, site-directed mutations in the conserved residues were created; namely E673K and L675G. Mutations in these residues have been shown to affect protein activity (Kirillina *et al.,* 2004). The role of the negative charge exerted by the glutamic acid residue was studied by mutating it to lysine that is positively charged while keeping the mass of both residues comparable. To study the role played by the leucine residue that is hydrophobic in nature, it was mutated to glycine that is also hydrophobic in nature while being smaller in mass. Indeed, the introduction of both E673K and L675G variants into the Δ*morC* strain showed relative motility of 0.4-fold verifying that they were unable to complement for the loss of MorC. This was also observed when E673K and L675G were introduced into *morA*Δ*morC* background. Therefore, the EAL motif is critical for its function.

When the $_{754}$EAL$_{756}$ motif was mutated and introduced into Δ*morC*, the E754K site mutant presented motility of 0.68-fold while L756G site mutant led to increased motility at 1.32-fold. Thus the L756G mutation led to a hyperactive protein, leading to a phenotype similar to *morC* overexpression. Since $_{754}$EAL$_{756}$ is located away from the active site, it is likely that there are long-range effects involved in the regulation of MorC protein function. It was also previously reported in FimX that the binding of

c-di-GMP onto the non-catalytic EAL domain can trigger long range conformational changes in the N-terminal REC domain and the adjacent linker that in turn lead to changes in protein localization and type IV pilus biogenesis (Qi *et al.,* 2011).

Interestingly, the introduction of E754K and L756G into Δ*morA*Δ*morC* background does not lead to the same hypermotility phenotype observed when the constructs were introduced into Δ*morC*. Thus the loss of *morA* has led to the loss of the hypermotility phenotype. Since $_{754}$EAL$_{756}$ is located outside the active site, this data suggests that MorA and MorC may interact directly or indirectly via long-range conformation changes. In all, it suggests that while MorC function is dependent on the PDE domain, it is not certain at this point if its function is solely due to enzymatic activities. To determine MorC enzymatic activities, several recombinant MorC constructs fused with C-terminal 6His tag in pET vector were made. However, recombinant protein expression trial showed that these proteins were not soluble (Fig. 3-2). As such, the MorC PDE enzymatic activity could not be determined at this point.

A

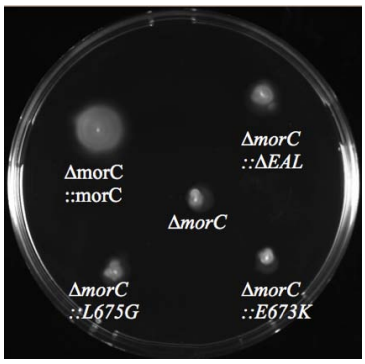

B

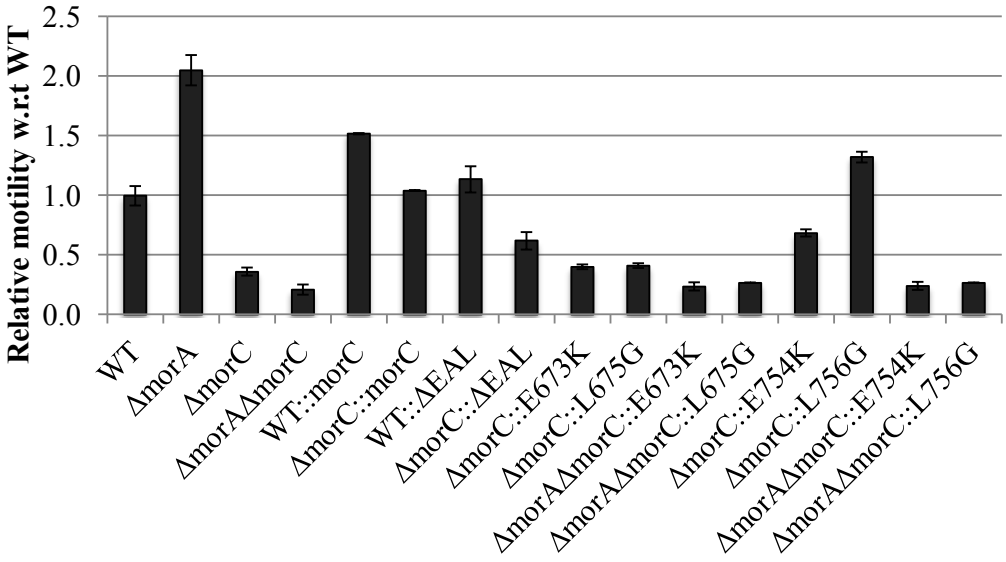

Fig. 6-6. MorC function is dependent on its PDE domain. The loss of EAL domain alone is sufficient to abrogate morC complementation. Site directed mutations at both E and L residues of the canonical motif led to loss of complementation while mutations in $_{754}$EAL$_{756}$ led to hypermotility. Interestingly, this was lost when MorA is absent. The swimming motility of various strains in semisolid agar (0.4%[wt/vol] agar) was examined. The results are based on three independent experiments, each with five replicates.

6.2.7. *morC* is expressed in a growth-stage dependent manner

In order to better understand how MorC is regulated, RT-PCR was performed on WT cells to study *morC* expression. Cell pellets were collected from the WT culture at OD readings corresponding to early-, mid- and late-log phases. The RNA extracted was then normalized before cDNA synthesis.

Fig. 6-7A shows that *morC* was expressed in the early and late-log phase but not in the mid-log phase while *morA* and *cyaA* were constitutively expressed. The abundant *morA* expression at all growth phases suggests that its expression is unregulated. While *cyaA* expression profile show that it was also constitutively expressed, its expression level was gradually increased as the growth phase progressed. Therefore, it is likely that its expression is being regulated. It was also evident from the expression profile that *morC w*as expressed at a low level when compared to *morA* and *cyaA*.

We next studied the expression profile of m*orC* in WT cells using qRT-PCR. The fluorescence detection cycle threshold values for the control 16S ribosomal RNA were similar in all three growth phases, indicating that similar amount of cDNA was used for the experiments.

Fig. 6-7B shows that *morC* had similar expression profile observed in RT-PCR, its mRNA expression was more pronounced in the early and late log phases with lowered expression in the mid-log phase. *morC* shows expression of 11, 5 and 15-fold more expression in the three growth phases when compared to 16S rRNA, corroborating

that the expression of MorC is more pronounced in a growth-phase dependent manner.

A

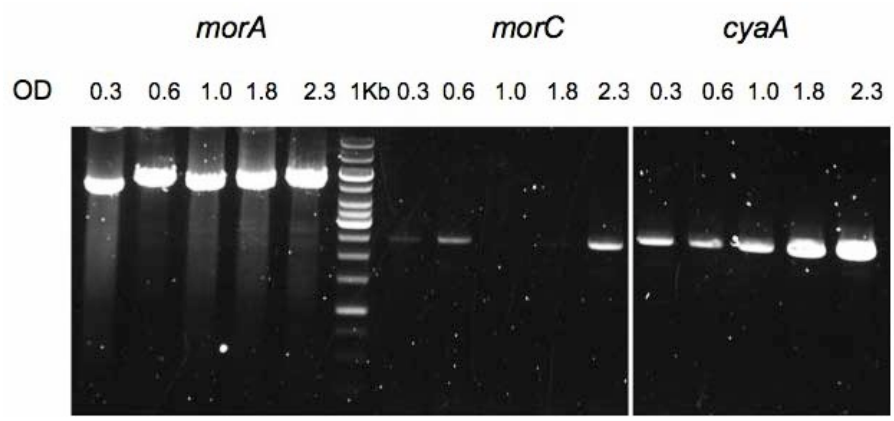

B

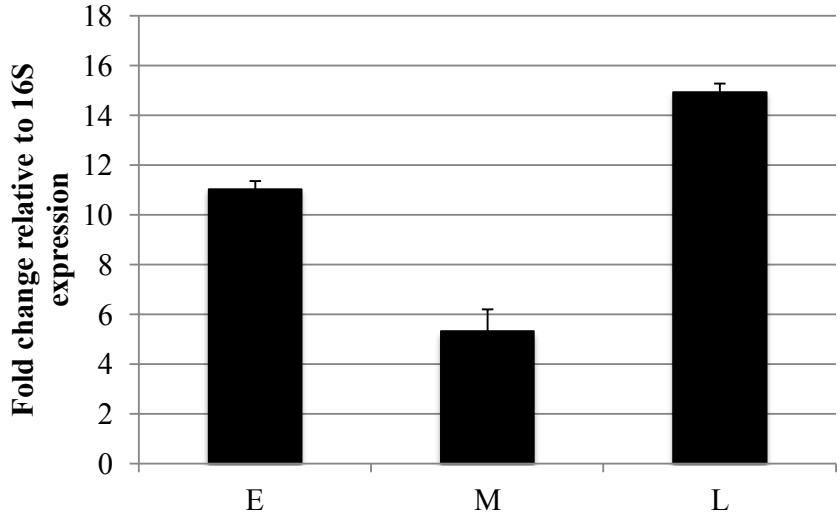

Fig. 6-7. *morC* expression is growth stage dependent. The various cells were harvested at early-log phase (E), mid-log phase (M) and log-to-stationary phase (L). Fold change of gene expression in WT was normalized with 16s RNA expression. The results shown are from three independent experiments. The error bars indicate standard deviations from three technical replicates

6.2.8. MorC is expressed in a growth-stage dependent manner

As MorA is a membrane bound regulator, *gfp* tag was used investigate its cellular localization. Fig. 6-8A shows that MorA is constitutively expressed in all three growth phases. Furthermore, MorA is localized to the two cell poles in all three phases (personal communications, Fu SJ). MorC, on the other hand, has shown no transmembrane domain in protein domain prediction. Thus, it is likely that MorC is a cytosolic protein. The gene expression results suggest that MorC functions at early and late log phase while not affecting mid-log phase. In order to find out if MorC has a specific cellular location or colocalizes with MorA, MorC was tagged with GFP and observed at various growth phases.

Confocal microscopy showed that MorC was expressed throughout the entire cell cytoplasm with no specific cellular location unlike MorA (Fig. 6-8B). It was also observed that GFP expression was only seen in the early and late log phases, suggesting that *morC* gene expression is reflective of MorC protein expression in that GFP was not observed in the mid-log phase. Thus *morC* is not regulated by its protein localization but instead it is regulated through the timing of its gene expression. Moreover, the loss of fluorescence in the mid-log phase suggests that there was no accumulation of MorC and that it was actively removed. Also, MorC shows the same distribution in the cell in the presence or absence of MorA implying that colocalization is neither necessary for their interaction nor for MorC to function. Therefore, it is likely that MorA and MorC interact indirectly.

A

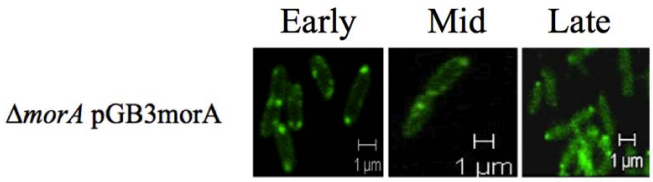

B

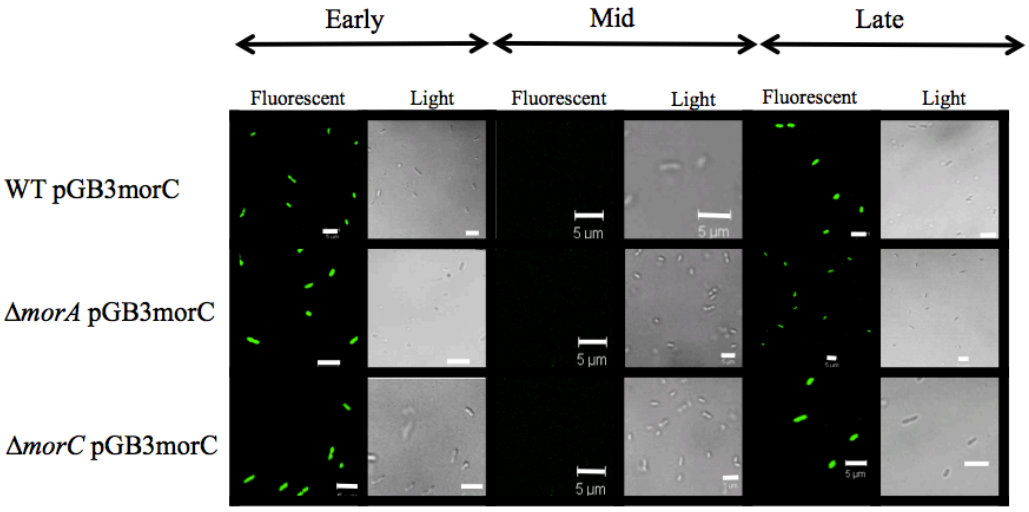

Fig. 6-8. MorC-GFP is observed throughout the cells in growth-stage dependent manner. (A) MorA is constitutively expressed and localized to the cell poles. MorA tagged with GFP was observed under confocal microscopy at various growth phases. (B) Construct expressing *gfp* tagged *morC* was introduced into WT, Δ*morA* and Δ*morC*. It can be seen that MorC was expressed only in the early and late-log phase but not in the mid-log phase. (Scale bar: 5µm)

6.2.9. MorC is a new regulator of *fliC* expression

MorA was previously reported to affect *fliC* expression without affecting flagellar master regulators, *fleQ* and *fliA*. As such, hyperflagallation, increased cell speed and increased flagellated cell number seen in *morA* mutant was attributed to the precocious expression of *fliC*. Δ*morA* in Fig. 6-9 shows that *fliC* expression was increased significantly in the early-growth phase and throughout the three growth phases. This is similar to the data previously obtained with MorDCK03 (Choy, 2005). Since MorC is implicated in MorA control of swimming motility, we next studied *fliC* expression in Δ*morC,* WT::morC and Δ*morA*Δ*morC* in order to determine if MorC controls motility via changes in flagellin levels. Fig. 6-9 shows *fliC* expression was downregulated in Δ*morC* at early, mid and late-log phase at 0.25, 0.29 and 0.15 fold, respectively, while the overexpression of *morC* leads to 12.93-fold and 5.81-fold increase in *fliC* expression at early and late-log phase respectively.

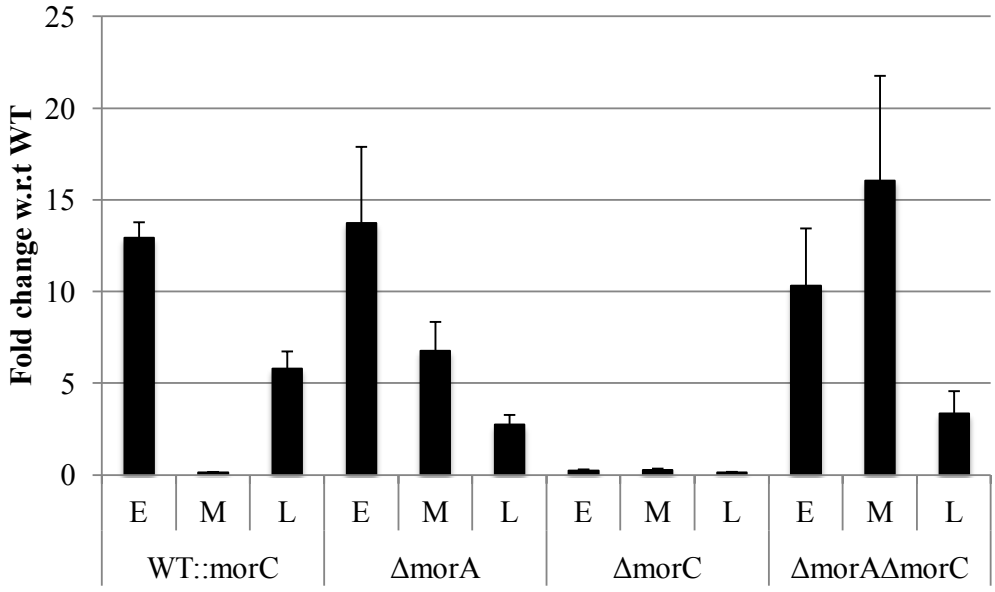

Fig. 6-9. MorC is a new regulator of *fliC* expression. The samples were harvested at early-log phase (E), mid-log phase (M) and log-to-stationary phase (L) to study *fliC* expression changes. C_t value of 23S RNA was used to normalize the C_t value of *fliC* gene expression. Fold change of *fliC* expression in *P. putida* mutant over that of wild type was then plotted. The results shown are from three independent experiments. The error bars indicate standard deviations from three technical replicates.

6.2.10. MorC do not affect motility via flagellar number

While the *fliC* expression results implied that flagellin level is responsible for motility changes, it is also known that there are multiple levels of control on flagellation. For example, HP0518 in *H. pylori* is involved in the post transcription modification, namely the deglycosylation of flagellin. The mutant strain derived flagellin contains 3-fold more pseudaminic acid and led to a hypermotile phenotype (Asakura *et al.,* 2010). As such, we attempted to find out if *fliC* expression have indeed led to a change in the amount of flagellin present via Western blot performed with antibodies raised with samples collect in our laboratory (Wong, 2011). However, Western blot data presented in Fig. 3-3B showed that the antibodies were not functional and could not provide clear signals.

Since Δ*morA* mutant was reported to show 98% flagellated cells at all three growth phases (Choy et al, 2004), we next examine if MorC affect motility pathway via the flagellation of bacterial cells. As changes in bacterial movement can be due to changes in flagellar number, structure or the rotation frequency of the flagellar apparatus, TEM ultrastructural studies were performed on various strains. The TEM studies show that the length of flagella, polar localization of flagella and the cell size were similar between the mutant and WT cells. Together with similar growth rates of the various strains, it is likely that the cell division rate is the same as well.

Although Δ*morC* cells were less motile than WT cells and showed no difference in *fliC* expression, it has 4-fold more flagellated cells than WT cells in the early-log phase and 2-fold more flagellated cells in the mid-log phase. While Δ*morA* and

ΔmorC showed increased flagellated cells, Δ*morA*Δ*morC* showed reduced flagellated cells in all three growth phases. Despite WT::morC, MorC::morC and the site directed mutants E673K and L675G showing diverse motility phenotypes, they showed an overall comparable flagellar number. Therefore, MorC control over motility is unrelated to the flagellation but rather, rests on the control of motor- related function.

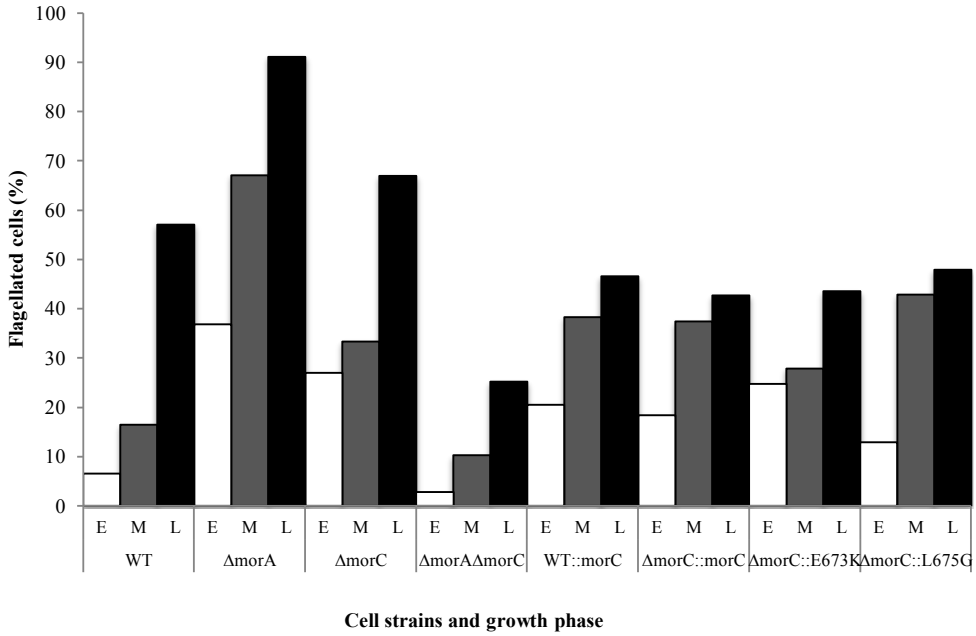

Fig. 6-10. MorC does not enhance swimming motility via flagellation related processes. The various cells were harvested at early-log phase (E), mid-log phase (M) and log-to-stationary phase (L). Proportion of flagellated cells expressed as a percentage of the total number of cells counted using TEM. Counts were based on an average of 100 cells.

6.2.11. MorC controls motility via cell speed

As the flagellated cell numbers were not consistent with the trend observed in motility plate assay, it was likely that MorC does not control motility via flagellation-related processes. Thus, we next examine if MorC controls motility by affecting motor function. This was accomplished by observing swimming cells by video microscopy to obtain single cell speeds at the early, mid and late-log phases. Since *P. putida* cells were previously found to move in short distances with overlapping trajectories, it is difficult to determine the turn angles (Wong, 2011).

As such, video microscopy was used to investigate if MorC affects motility by controlling cell speed. Fig. 6-11 shows that Δ*morC* and WT have comparable cell speed of 2.8 and 2.5μm/s at early-log and 3.6 and 3.4 μm/s respectively for mid-log phase, differing significantly in the late-log phase. Δ*morC* showed a cell speed of 2.5μm/s at late log phase translating to a 60% decrease in speed when compared to WT. MorC overexpression, on the other hand, led to a 128% increase in cell speed at early-log phase to 6.4μm/s while remaining comparable to WT at late-log phase.

Interestingly, E673K and L675G, while showing comparable motility fold change in the plate assay (Fig. 6-6B), did not show the same speed profile at the various growth phases. L675G showed increased cell speed as compared to Δ*morC* to 4μm/s in the early-log phase and reduced cell speed in mid and late-log. E673K, on the other hand, showed a slight decrease in cell speed in the early and mid-log phase and increased cell speed to 5μm/s in the late-log phase. This suggests that that E residue in the EAL

motif regulates the cell speed in the early-log phase while the L residue in the EAL motif serves the same function in the late-log phase.

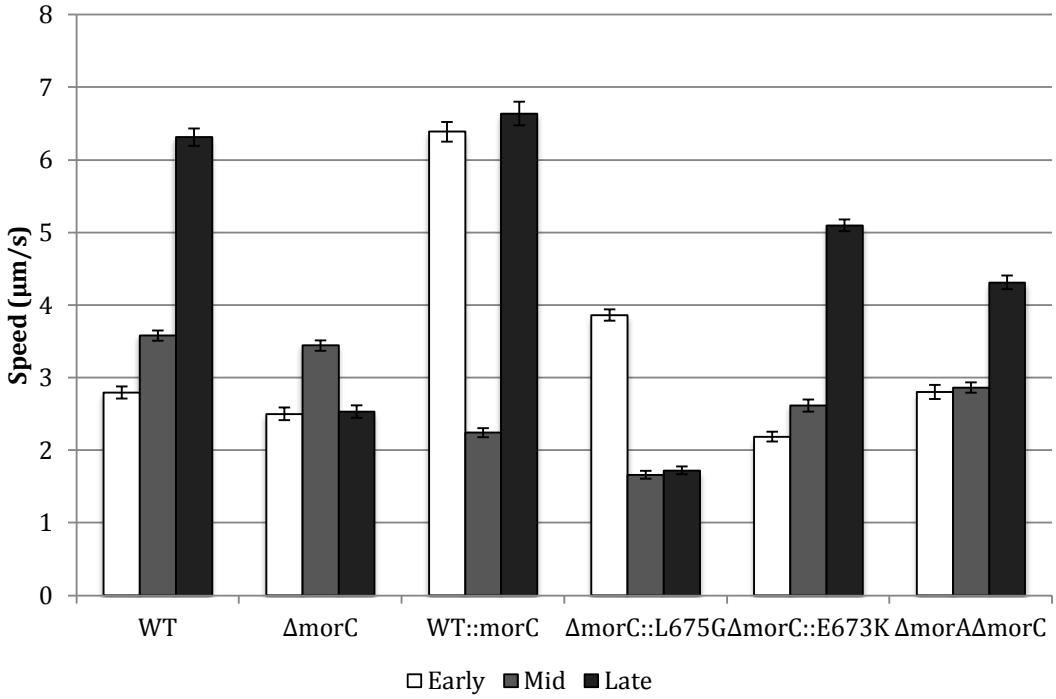

Fig. 6-11. Cell speed analysis shows that MorC affects the cell speed in a growth-stage dependent manner. Video microscopy showed that Δ*morC* cells were 60% less motile in the late-log phase when compared to WT while *morC* overexpression led to a 128% increase in motility in the early-log phase. Values are means of 300 bacterial cell speeds tracked from 2 videos each from 3 clones for each strain.

6.3. CONCLUSION AND FUTURE WORK

MorC is a well-conserved protein that contains PAS/PAC, GAF, ASNEF and EAL domains. Interestingly, the ASNEF motif is conserved only in the *Pseudomonas spp* while being present as the GGDEF motif in other bacterial genus in both Gram-positive and Gram-negative bacteria. As such, mutating the motif to GGDEF may shed light on the function served by the ASNEF motif in MorC.

MorC is a positive regulator of motility that functions downstream of MorA. Unlike MorA, single copy and multi-copies overexpression of *morC* leads to 0.5 fold increase in swimming motility when compared to WT. Thus, MorC is not affected by gene dosage. MorC is highly specific in its activity; it controls motility while not affecting biofilm formation or chemotaxis.

RT-PCR showed that both *morA* and *cyaA* is expressed throughout the growth phases while *morC* is not. There was steady and abundant *morA* expression throughout the growth phases while *cyaA* expression increased as the culture moves toward stationary phase. As such, it can be concluded that *morA* expression is likely to be unregulated while *cyaA* expression is regulated. Another point of note is that the amount of *morC* transcript is low when compared to *morA*, suggesting that MorC is not required in large amount to cause phenotypic differences. Subsequently, qRT-PCR showed that *morC* gene expression was elevated in the early and late-log phases but not in mid-log phase.

GFP fused MorC used in cellular localization also showed that MorC is expressed throughout the cell in a growth-phase dependent manner in the early and late log phases but not the mid-log phase. Together with gene expression studies, it can be concluded that MorC is likely to be active in the early and late-log phases.

fliC gene expression studies shows that *fliC* transcript level was increased in the early and late-log phases when *morC* is overexpressed. Similarly, disruption of *morC* leads to decreased *fliC* gene expression. Thus MorC is a newly identified *fliC* regulator. Flagellated cell numbers, however, did not correlate with gene expression.

Based on protein sequence analysis, MorC is likely a functional PDE that contains 2 EAL motifs. Motility plate assay show that truncated MorC missing the PDE domain was unable to complementΔ *morC*.. Furthermore, mutations in the canonical EAL motif lead to loss of complementation while mutations in the non-canonical EAL motif lead to hypermotility. This hypermotile phenotype is lost when *morA* is disrupted. Structural modeling shows that the non-canonical EAL motif is located away from the active site suggesting that its effect on function maybe due to changes in the protein structure. Since MorC function is likely related to its structure, resolving its structure will be helpful in furthering our understanding of its activities.

Single cell swimming speed analysis showed that cell speed was increased in the early-log phase when MorC was overexpressed whileΔ *morC* exhibited decreased cell speed in the late-log phase. Site-directed mutants at the canonical site showed that there is a residue-specific effect at the early and late-log phases.

Lastly, due to the difficulties in obtaining recombinant proteins for enzymatic studies, many questions remained unanswered. Therefore, more diverse types of tags and expression systems may be attempted to obtain full-length proteins and site-directed mutant proteins.

Fig.6-11 summarizes the strategies deployed to control motility as well as the relationship of between MorA, CyaA, OpuAC and MorC. Thus far, it is unclear if these players interact directly or indirectly. To elucidate the relationship between CyaA and MorC, overexpression of *cyaA* and *morC* should be carried out in Δ*morC* and Δ*cyaA* strains respectively.

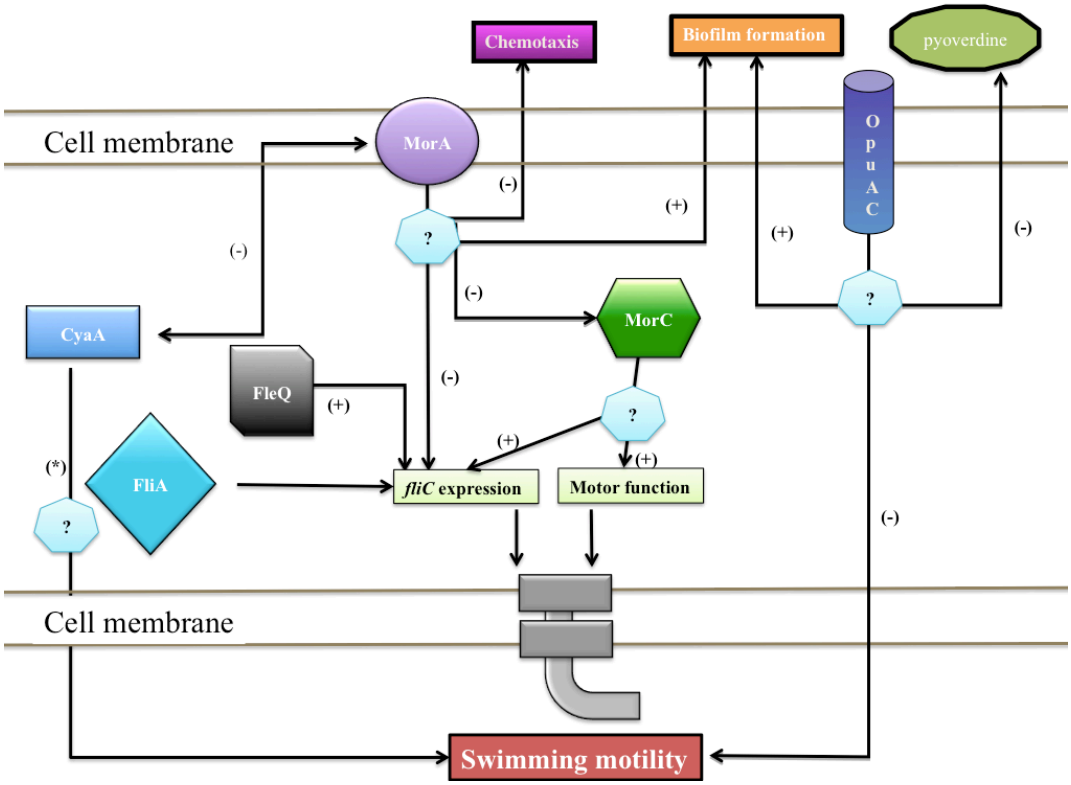

Fig. 6-12. Different strategies deployed to control motility via MorA signaling pathway. Though CyaA interacts in an antagonistic manner with MorA, MorA exerts dominant effects over motility and can determine CyaA control over the direction of motility. OpuAC, on the other hand, acts independently of MorA to control both motility and biofilm formation. In addition, MorC is found to act downstream of MorA as a positive regulator that controls motility through cell speed while not affecting biofilm formation or chemotaxis. (+) and (-) denotes positive and negative regulation respectively while (?) denotes unknown factors or players. (*) denotes that the direction of control is dependent on MorA.

BIBLIOGRAPHY

Adaikkalam V, Swarup S. Molecular characterization of an operon, *cueAR*, encoding a putative P1-type ATPase and a MerR-type regulatory protein involved in copper homeostasis in *Pseudomonas putida*. Microbiology 2002; 148: 2857-2867.

Aldridge P, Hughes KT. Regulation of flagellar assembly. Curr Opin Microbiol 2002; 5: 160-165.

Aldridge P, Paul R, Goymer P, Rainey P, Jenal U. Role of the GGDEF regulator PleD in polar development of *Caulobacter crescentus*. Mol Microbiol 2003; 47: 1695-1708.

Amsler CD, Cho M, Matsumura P. Multiple factors underlying the maximum motility of *Escherichia coli* as cultures enter post-exponential growth. J Bacteriol 1993; 175: 6238-6244.

An S, Wu J, Zhang LH. Modulation of *Pseudomonas aeruginosa* biofilm dispersal by a cyclic-Di-GMP phosphodiesterase with a putative hypoxia-sensing domain. Appl Environ Microbiol 2010; 76: 8160-8173.

Aravind L, Koonin EV. The HD domain defines a new superfamily of metal-dependent phosphohydrolases. Trends Biochem Sci 1998; 23: 469-472.

Aravind L, Lakshminarayan MI, Anantharaman V. Natural history of sensor domains in bacterial signaling systems. In: Stephen Spiro and Ray Dixon *Sensory Mechanisms in Bacteria: Molecular Aspects of Signal Recognition*. 2010. brussel: Caister Academic

Arnold K. The SWISS-MODEL workspace: a web-based environment for protein structure homology modelling. Bioinformatics 2006; 22: 195-201.

Asakura H, Churin Y, Bauer B, Boettcher JP, Bartfeld S, Hashii N, Kawasaki N, Mollenkopf HJ, Jungblut PR, Brinkmann V, Meyer TF. *Helicobacter pylori* HP0518 affects flagellin glycosylation to alter bacterial motility. Mol Microbiol 2010; 78: 1130–1144.

Ausmees N, Jonsson H, Höglund S, Ljunggren H, Lindberg M. Structural and putative regulatory genes involved in cellulose synthesis in *Rhizobium leguminosarum* bv. trifolii. Microbiology 1999; 145: 1253-1262.

Bardy SL, Ng SY, Jarrell KF. Prokaryotic motility structures. Microbiology 2003; 149: 295-304.

Bloemberg GV, O'Toole GA, Lugtenberg BJJ, Kolter R. Green fluorescent protein as a marker for *Pseudomonas* spp. Appl Env Microbiol 1997; 63: 4543-4551.

Boehm A, Kaiser M, Li H, Spangler C, Kasper CA, Ackermann M, Kaever V, Sourjik V, Roth V, Jenal U. Second messenger-mediated adjustment of bacterial swimming velocity. Cell 2010; 141: 107-116.

Boopathi E, Rao KS. A sideophore from *Pseudomonas putida* type A1: structural and biological characterization. Biochim Biophys Acta 1999; 1435: 30-40.

Bordeleau E, Fortier L-C, Malouin F, Burrus V. c-di-GMP turn-over in *Clostridium difficile* is controlled by a plethora of diguanylate cyclases and phosphodiesterases. PLoS Genet 2011; 7: e1002039.

Branda S, Vika, Friedman L, Kolter R. Biofilms: the matrix revisited. Trends Microbiol 2005; 13: 20-26.

Budzikiewicz H. Siderophores of the Pseudomonadaceae sensu stricto (fluorescent and non-fluorescent *Pseudomonas* spp.). Progr Chem Org Nat Prod 2004; 87: 81–237.

Budzikiewicz, H., Schäfer, M., Fernández, D. U., Matthijis, S. and Cornelis, P. Characterization of the chromophores of pyoverdins and related siderophores by electrospray tandem mass spectrometry. Biometals 2007; 20:135-144

Chin KH, Lee YC, Tu ZL, Chen CH, Tseng YH, Yang JM, Ryan RP, McCarthy Y, Dow JM, Wang AHJ, Chou SH. The cAMP receptor-like protein CLP is a novel c-di-GMP receptor linking cell-cell signaling to virulence gene expression in *Xanthomonas capestris.* J Mol Biol 2010; 396: 646-662.

Choi KH, Kumar A, Schweizer HP. A 10-min method for preparation of highly electrocompetent *Pseudomonas aeruginosa* cells: Application for DNA fragment transfer between chromosomes and plasmid transformation. J Microbiol Methods 2005; 54: 391-397.

Choi KH, Schweizer, HP. An improved method for rapid generation of unmarked *Pseudomonas aeruginosa* deletion mutants. BMC Microbiol 2005; 5: 30-40.

Choi KH, Schweizer HP. mini-Tn*7* insertion in bacteria with single *att*Tn*7* sites: example *Pseudomonas aeruginosa.* Nature Protocols 2006; 1: 153-161.

Choy WK. MorA, a novel membrane localized regulator in *Pseudomonas spp*. National University of Singapore, Ph.D dissertation 2005.

Choy WK, Zhou L, Syn CK, Zhang LH, Swarup S. MorA defines a new class of regulators affecting flagellar development and biofilm formation in diverse *Pseudomonas* species. J Bacteriol 2004; 186: 7221-7228.

Christen M, Christen B, Folcher M, Schauerte A, Jenal U. Identification and characterization of a cyclic di-GMP-specific phosphodiesterase and its allosteric control by GTP. J Biol Chem 2005; 2280: 30829-30837.

Christen B, Christen M, Paul R, Schmid F, Folcher M, Jenoe P, Meuwly M, Jenal U. Allosteric control of cyclic di-GMP signaling. J Biol Chem 2006; 281: 32015- 32024.

Collins CH, Lyne PM, Grange JM, Falkinham III JO. Collins and Lyne's Microbiological Methods. 2004. London: Hodder Arnold Publishers (8th edition).

Csonka LN, Hanson AD. Prokaryotic osmoregulation: genetics and physiology. Annu Rev Microbiol 1991; 45: 569-606.

D'Argenio DA, Miller SI. Cyclic di-GMP as a bacterial second messenger. Microbiology 2004; 150: 2497-502.

Dasgupta N, Wolfgang MC, Goodman AL, Arora SK, Jyot J, Lory S, Ramphal R. A four-tiered transcriptional regulatory circuit controls flagellar biogenesis in *Pseudomonas aeruginosa.* Mol Microbiol 2003; 50: 809-824.

DeFlaun MF, Tanzer AS, Joseph AL, Marshall B, Levy SB. Development of an adhesion assay and characterization of an adhesion-deficient mutant of *Pseudomonas fluorescens*. Appl Env Microb 1990; 56: 112-119.

De N, Pirruccello M, Krasteva PV, Bae N, Raghavan RV, Sondermann H. Phosphorylation-independent regulation of the diguanylate cyclase WspR. PLoS Biol 2008; 6: e67.

Ferreira RBR, Antunes LCM, Greenberg EP, McCarter LL. *Vibrio parahaemolyticus* ScrC modulates cyclic dimeric GMP regulation of gene expression relevant to growth on surfaces. J Bacteriol 2008; 190: 851-860.

Fong JC, Yildiz FH. Interplay Between cAMP-CRP and c-di-GMP Signaling in *Vibrio cholerae* Biofilm Formation. J Bacteriol 2008; 190: 6646-6659.

Frisk A, Jyot J, Arora SK, Ramphal R. Identification and functional characterization of *flgM*, a gene encoding the anti-sigma 28 factor in *Pseudomonas*. J Bacteriol 2002; 184: 1514–1521.

Fu SJ. Expression studies of GGDEF protein family members in *Pseudomonas*. National University of Singapore, Honours thesis 2006.

García B, Latasa C, Solano C, Portillo FGD, Gamazo C, Lasa I. Role of the GGDEF protein family in *Salmonella* cellulose biosynthesis and biofilm formation. Mol Microbiol 2004; 54: 264-277.

Galperin MY, Natale D A, Aravind L, Koonin EV. A specialized version of the HD hydrolase domain implicated in signal transduction. J Mol Microbial Biotechol 1999; 1: 303-305.

Galperin MY, Nikolskaya AN, Koonin EV. Novel domains of the prokaryotic two-component signal transduction systems. FEMS Microbiol Lett 2001; 203: 11-21.

Givskov M, Eberl L, Christiansen G, Benedik MJ, Molin S. Induction of phospholipase- and flagellar synthesis in *Serratia liquefaciens* is controlled by expression of the flagellar master operon f*lhD*. Mol Microbiol 1995; 15: 445-454.

Gupta K, Kumar P, Chatterji D, Ahmed N. Identification, activity and disulfide

connectivity of C-di-GMP regulating proteins in *Mycobacterium tuberculosis.* PloS one 2010; 5: e15072.

Härtig C, Loffhagen N, Harms H. Formation of *trans* fatty acids is not involved in growth-linked membrane adapation of *Pseudomonas putida.* Appl Environ Microbiol 2005; 71: 1915-1922.

Harwood CS, Fosnaugh K, Dispensa M. Flagellation of *Pseudomonas putida* and analysis of its motile behavior. J Bacteriol 1989; 171: 4063-4066.

Hengge R. Principles of c-di-GMP signaling in bacteria. Nat Rev Microbiol 2009; 7: 263-273.

Holland LM, O'Donnell ST, Ryjenkov DA, Gomelsky L, Slater SR, Fey PD, Gomelsky M, O'Gara JP. A staphylococcal GGDEF domain protein regulates biofilm formation independently of cyclic dimeric GMP. J Bacteriol 2008; 190: 5178-5189.

Huang B, Whitchurch CB, Mattick JS. FimX, a multidomain protein connecting environmental signals to twitching motility in *Pseudomonas aeruginosa.* J Bacteriol 2003; 185: 7068-7076.

Jarrell, KF, McBride MJ. The surprisingly diverse ways that prokaryotes move. Nat Rev Microbiol 2008; 6: 466-476.

Jayaraman A, Wood TK. Bacterial quorum sensing: signals, circuits, and implications for biofilms and disease. Annu Rev Biomed Eng 2008; 10: 145-167.

Jenal U. Cyclic di-guanosine-monophosphate comes of age: a novel secondary messenger involved in modulating cell surface structures in bacteria. Curr Opin Microbiol 2004; 7: 185-191.

Jonas K, Edwards AN, Simm R, Romeo T, Römling U, Melefors O. The RNA binding protein CsrA controls cyclic di-GMP metabolism by directly regulating the expression of GGDEF proteins. Mol Microbiol 2008; 70: 236-257.

Karatan E, Watnick P. Signals, regulatory networks, and materials that build and break bacterial biofilms. Microbiol Mol Biol Rev 2009; 73: 310-347.

Kazmierczak BI, Lebron MB, Murray TS. Analysis of FimX, a phosphodiesterase that governs twitching motility in *Pseudomonas aeruginosa.* Mol Microbiol 2006; 60: 1026-1043.

Kempf B, Bremer E. Uptake and synthesis of compatible solutes as microbial stress responses to high-osmolality environments. Arch Microbiol 1998; 170: 319-330.

Kiefer F, Arnold K, Kunzli M, Bordoli L, Schwede T. The SWISS-MODEL Repository and associated resources. Nucleic Acids Res 2009; 37(Database): D387-D392.

Kirillina O, Fetherston JD, Bobrov AG, Abney J, Perry RD. HmsP, a putative phosphodiesterase, and HmsT, a putative diguanylate cyclase, control Hms-dependent biofilm formation in *Yersinia pestis.* Mol Microbiol 2004; 54: 75-88.

Kuchma SL, Brothers KM, Merritt JH, Liberati NT, Ausubel FM, O'Toole GA. BifA, a cyclic-di-GMP phosphodiesterase, inversely regulates biofilm formation and swarming motility by *Pseudomonas aeruginosa* PA14. J Bacteriol 2007; 189: 8165-8178.

Kulasakara H, Lee V, Brencic A, Liberati N, Urbach J, Miyata S, Lee DG, Neely AN, Hyodo M, Hayakawa Y, Ausubel FM, Lory S. Analysis of *Pseudomonas aeruginosa* diguanylate cyclases and phosphodiesterases reveals a role for bis-(3'-5')-cyclic-GMP in virulence. P Natl Acad Sci USA 2006; 103: 2839-2844.

Landini P, Zehnder AJB. The global regulatory *hns* gene negatively affects adhesion to solid surfaces by anaerobically grown *Escherichia coli* by modulating expression of flagellar genes and lipopolysaccharide production. J Bacteriol 2002; 184:1522-1529.

Letunic I, Doerks T, Bork P. SMART 6: recent updates and new developments. Nucleic Acids Res 2009; 37(Database): D229-D232.

Li F. The role of a novel second messenger, c-di-GMP in *Pseudomonas putida* via enzymatic study of MorA. National University of Singapore, MSc thesis 2006.

Li Y, Xia H, Bai F, Xu H, Yang L, Yao H, Zhang L, Zhang X, Bai Y, Saris PEJ, Tolker-Nielsen T, Qiao M. Identification of a new gene *PA5017* involved in flagella-mediated motility, chemotaxis and biofilm formation in *Pseudomonas aeruginosa*. FEMS Microbiol Lett 2007; 272: 188–195.

Lopez JE, Henkels MD. Utilization of Heterologous Siderophores Enhances Levels of Iron Available to *Pseudomonas putida* in the Rhizosphere. Appl Environ Microb 1999; 65: 5357-5363.

Lye HM. Structural and functional characterization of *Pseudomonas* MorA. National University of Singapore, Honours thesis 2006.

Macnab RM. Genetics and biogenesis of bacterial flagella. Annu Rev Genet 1992; 26: 129-156.

Macnab RM. How bacteria assemble flagella. Annu Rev Microbiol 2003; 57: 77-100.

Macnab RM. Type III flagellar protein export and flagellar assembly. Biochim Biophys Acta 2004; 1694: 207-217.

Manson MD, Armitage JP, Hoch JA, Macnab RM. Bacterial locomotion and signal transduction. J Bacteriol 1998; 180: 1009-1022.

Matzanke, B. F. Iron Transport: Siderophores. Encyclopedia of Inorganic and Bioinorganic Chemistry 2011.

Merkel TJ, Barros C, Stibitz S. Characterization of the *bvgR* locus of *Bordetella pertussis*. J Bacteriol 1998; 180: 1682-1690.

Meyer, J., Stinzil, A., Coulanges, V., Shivaji, S., V, J. A., Taraz, K. and Budzikiewic, H. Siderotyping of fluorescent Pseudomonads: characterization of pyoverdines of *Pseudomonas fluorescens* and *Pseudomonas putida* strains from Antarctica. Microbiology 1998; 144: 3119-3126.

Mills E, Pultz IS, Kulasekara HD, Miller SI. The bacterial second messenger c-di-GMP: mechanisms of signaling. Cell microbiol 2011; 13: 1122-1129.

Muller R. Bacterial Degradation of Xenobiotics. Microbial Control of Pollution 1992; 48: 52.

Mytelka DS, Chamberlin MJ. *Escherichia coli* fliAZY operon. J Bacteriol 1996; 178: 24-34.

Neilands JB. Methods of siderophores. Structure and Bonding 1984; 58: 1–24.

Nelson KE, Weinel C, Paulsen IT, Dodson RJ, Hilbert H, Martins dos Santos VA, Fouts DE, Gill SR, Pop M, Holmes M, Brinkac L, Beanan M, DeBoy RT, Daugherty S, Kolonay J, Madupu R, Nelson W, White O, Peterson J, Khouri H, Hance I, Chris Lee P, Holtzapple E, Scanlan D, Tran K, Moazzez A, Utterback T, Rizzo M, Lee K, Kosack D, Moestl D, Wedler H, Lauber J, Stjepandic D, Hoheisel J, Straetz M, Heim S, Kiewitz C, Eisen JA, Timmis KN, Dusterhoft A, Tummler B, Fraser CM. Complete genome sequence and comparative analysis of the metabolically versatile *Pseudomonas putida* KT2440. Environ Microbiol 2002; 4: 799-808.

Ng WL. Signaling pathway involved in the action of MorA: a genetic approach. National University of Singapore, Honours thesis 2006.

O'Connor K, Duetz W, Wind B, Dobson ADW. The Effect of Nutrient Limitation of Styrene Metabolism in *Pseudomonas putida* CA-3. Appl Environ Microbiol 1996; 62: 3594-3599.

O'Toole GA, Kolter R. Flagellar and twitching motility are necessary for *Pseudomonas aeruginosa* biofilm development. Mol Microbiol 1998; 30: 295–304.

Palleroni NJ. The Road to the Taxonomy of *Pseudomonas*. In: Pierre Cornelis *Pseudomonas: Genomics and Molecular Biology* 2008. brussel: Caister Academic Press. p1-19.

Parkinson JS, Ames P, Studdert CA. Collarborative signaling by bacterial chemoreceptors. Curr Opin Microbiol 2005; 8: 116-121.

Paul K, Brunstetter D, Titen S, Blair D. F. A molecular mechanism of direction switching in the flagellar motor of *Escherichia coli.* P Natl Acad Sci USA 2011; 108: 17171-17176.

Paul R, Weiser S, Amiot NC, Chan C, Schirmer T, Giese B, Jenal U. Cell cycle-dependent dynamic localization of a bacterial response regulator with a novel di-guanylate cyclase output domain. Genes Dev 2004; 18: 715-727.

Pei, J., Grishin, N.V. GGDEF domain is homologous to adenylyl cyclase. Proteins 2001; 42: 210–216.

Perry RD, Bobrov AG, Kirillina O, Jones HA, Pedersen L, Abney J, Fetherston JD. Temperature regulation of the hemin dtorage (Hms+) Phenotype of *Yersinia pestis* is posttranscriptional. J Bacteriol 2004; 186: 1638-1647.

Poolman B, Glaasker E. Regulation of compatible solute accumulation in bacteria. Mol Microbiol 1998; 29: 397-407.

Pratt LA, Kolter R. Genetic analysis of *Escherichia coli* biofilm formation: roles of flagella, motility, chemotaxis and type I pili. Mol Microbiol 1998; 30: 285-93.

Prouty MG, Correa NE, Klose KE. The novel sigma54- and sigma28-dependent flagellar gene transcription hierarchy of *Vibrio cholerae*. Mol Microbiol 2001; 39: 1595-1609.

Prüß BM, Markovic D, Matsumura P. The *Escherichia coli* flagellar transcriptional activator *flhD* regulates cell division through induction of the acid response gene *cadA*. J Bacteriol 1997; 179: 3818-3821.

Prüß BM, Matsumura P. Cell cycle regulation of flagellar genes. J Bacteriol 1997; 179: 5602-5604.

Qi Y, Chuah MLC, Dong X, Xie K, Luo Z, Tang K, Liang ZX. Binding of cyclic diguanylate in the non-catalytic EAL domain of FimX induces a long-range conformational change. J Biol Chem 2011; 286: 2910-2917.

Rao F, Pasunooti S, Ng Y, Zhuo W, Lim L, Liu AW, Liang ZX. Enzymatic synthesis of c-di-GMP using a thermophilic diguanylate cyclase. Anal Biochem 2009; 389: 138-142.

Rao F, Qi Y, Chong HS, Kotaka M, Li B, Li J, Lescar J, Tang K, Liang ZX. The functional role of a conserved loop in EAL domain-based cyclic di-GMP-specific phosphodiesterase. J Bacteriol 2009; 191: 4722-4731.

Rao F, Yang Y, Qi Y, Liang ZX. Catalytic mechanism of cyclic di-GMP-specific phosphodiesterase: a study of the EAL domain-containing RocR from *Pseudomonas aeruginosa*. J Bacteriol 2008; 190: 3622-3631.

Richarme G, Caldas TD. Chaperone properties of the bacterial periplasmic substrate-binding proteins. J Biol Chem 1997; 272: 15607-15612.

Robleto EA, Lopez-Hernandez IM, Silby W, Levy SB. Genetic analysis of the AdnA regulon in *Pseudomonas fluorescens*: nonessential role of flagella in adhesion to sand and biofilm formation. J Bacteriol 2003; 185: 453-460.

Rojas A, Duque E, Mosqueda G, Golden G, Hurtado A, Ramos JL, Segura A. Three efflux pumps are required to provide efficient tolerance to toluene in *Pseudomonas putida* DOT-1E. J Bacteriol 2001; 183: 3967-3973.

Rojas A, Segura A, Guazzaroni ME, Teran W, Hurtado A, Gallegos MT, Ramos JL. *In vivo* and *in vitro* evidence that TtgV is the specific regulator of the TtgGHI multidrug and solvent efflux pump of *Pseudomonas putida.* J Bacteriol 2003; 185: 4755-4763.

Romling U, Amikam D. Cyclic di-GMP as a second messenger. Curr Opin Microbiol 2006; 9: 218-228.

Ross P, Weinhouse H, Aloni Y, Michaeli D, Weinberger-Ohana P, Mayer R, Braun S, de Vroom E, van der Marel G, van Boom J, Benziman M. Regulation of cellulose synthethase in *Acetobacter xylinum* by cyclic diguanylic acid. Nature 1987; 325: 279-281.

Ryan RP, Fouhy Y, Lucey JF, Crossman LC, Spiro S, He YW, Zhang LH, Heeb S, Cámara M, Williams P, Dow JM. Cell-cell signalling in *Xanthomonas campestris* involves an HD-GYP domain protein that functions in cyclic di-GMP turnover. P Natl Acad Sci USA 2006; 103: 6712-6717.

Samatey FA, Imada K, Nagashima S, Vonderviszt F, Kumasaka T, Yamamoto M, Namba K. Structure of the bacterial flagellar protofilament and implications for a switch for supercoiling. Nature 2001; 410: 331-337.

Sambrook, J., and Russell, D. Molecular Cloning 2001. Cold Spring Harbor Laboratory Press (3rd Edition).

Sauer K, Camper AK. Characterization of phenotypic changes in *Pseudomonas putida* in response to surface-associated growth. J Bacteriol 2001; 183: 6579-6589.

Sauer K, Camper AK, Ehrlich GD, Costerton JW, Davies DG. *Pseudomonas aeruginosa* displays multiple phenotypes during development as a biofilm. J Bacteriol 2002; 184: 1140-1154.

Schmidt AJ, Ryjenkov DA, Gomelsky M. The ubiquitous protein domain EAL is a cyclic diguanylate-specific phosphodiesterase: enzymatically active and inactive EAL domains. J Bacteriol 2005; 187: 4774-4781.

Schultz J, Milpetz F, Bork P, Ponting C. SMART, a simple modular architecture research tool: identification of signalling domains. P Natl Acad Sci USA 1998; 95: 5857-5864.

Seshasayee ASN, Fraser GM, Luscombe NM. Comparative genomics of cyclic-di-GMP signalling in bacteria: post-translational regulation and catalytic activity. Nucleic Acids Res 2010; 38: 5970-5981.

Shi W, Yang Z, Geng Y, Wolinsky LE, Lovett MA. Chemotaxis in *Borrelia burgdorferi.* J Bacteriol 1998; 180: 231-235.

Silby MW, Cerdeño-Tárraga AM, Vernikos GS, Giddens SR, Jackson RW, Preston GM, Zhang XX, Moon CD, Gehrig SM, Godfrey SAC, Knight CG, Malone JG, Robinson Z, Spiers AJ, Harris S, Challis GL, Yaxley AM, Harris D, Seeger K, Murphy L, Rutter S, Squares R, Quail MA, Saunders E, Mavromatis K, Brettin TS, Bentley SD, Hothersall J, Stephens E, Thomas CM, Parkhill J, Levy SB, Rainey PB, Thomson NR. Genomic and genetic analyses of diversity and plant interactions of *Pseudomonas fluorescens*. Genome Biology 2009; 10: R51.

Stoodley P, Sauer K, Davies DG, Costerton JW. Biofilms as complex differentiated communities. Annu Rev Microbiol 2002; 56: 187-209.

Suarez A, Guttler A, Stratz M, Staendner LH, Timmis KN, Guzman CA. Green fluorescent protein-based reporter systems for genetic analysis of bacteria including monocopy applications. Gene 1997; 196: 69-74.

Sudarsan N, Lee ER, Weinberg Z, Moy RH, Kim JN, Link KH, Breaker RR. Riboswitches in eubacteria sense the second messenger cyclic di-GMP. Science 2008; 321: 411-413.

Suslow TV. Bacteriophage-resistant plant growth-promoting rhizobacteria (1986). US Patent No. 4,584,274.

Syn CKC. Gene expression studies in a solvent-tolerant PGPR strain of *Pseudomonas* sp. National University of Singapore, Ph.D dissertation 2001.

Syn CKC, Magnuson JK, Kingsley MT, Swarup S. Characterization of *Pseudomonas putida* genes responsive to nutrient limitation. Microbiology 2004; 150: 1661-1669.

Syn CKC, Swarup S. A scalable protocol for the isolation of large-sized genomic DNA within an hour from several bacteria. Anal Biochem 2000; 278: 86-90.

Tal R, Wong H, Calhoon R, Gelfand D, Fear A, Volman G, Mayer R, Ross P, Amikam D, Weinhouse H. Three *cdg* operons control cellular turnover of cyclic di-GMP in *Acetobacter xylinum:* genetic organization and occurrence of conserved domains in isoenzymes. J Bacteriol 1998; 180: 4416-4425.

Tam R, Saier MHJ. Structural, functional and evolutionary relationships among extracellular solute-binding receptors of bacteria. Microbiol Rev 1993; 57: 320-346.

Tamayo R, Pratt JT, Camilli A. Roles of cyclic diguanylate in the regulation of bacterial pathogenesis. Annu Rev Microbiol 2007; 61: 131–148.

Tao F, He YW, Wu DH, Swarup S, Zhang LH. The cNMP domain of *Xanthomonas campestris* global regulator Clp defines a new class of c-di-GMP effectors. J Bacteriol 2010; 192: 1020-1029.

Tarutina M, Ryjenkov DA, Gomelsky M. An unorthodox bacteriophytochrome from *Rhodobacter sphaeroides* involved in turnover of the second messenger c-di-GMP. J Biol Chem 2006; 281: 34751-34758.

Ueda A, Wood TK. Connecting quorum sensing, c-di-GMP, pel polysaccharide, and biofilm formation in *Pseudomonas aeruginosa* through tyrosine phosphatase TpbA (PA3885). PLoS Pathog 2009; 5: e1000483.

Vandenbergh PA, Wright AM. Plasmid involvement in acyclic isoprenoid metabolism by *Pseudomonas putida*. Appl Environ Microbiol 1983; 45: 1953-1955.

Yamamoto S, Kasai H, Arnold DL, Jackson RW, Vivian A, Harayama S. Phylogeny of the genus *Pseudomonas*: intrageneric structure reconstructed from the nucleotide sequences of *gyrB* and *ropD* genes. Microbiology 2000; 146: 2385-2394.

Yan H, Chen W. 3′,5′-Cyclic diguanylic acid: a small nucleotide that makes big impacts. Chem Soc Rev 2010; 39: 2914–2924.

Weber H, Pesavento C, Possling A, Tischendorf G, Hengge R. Cyclic-di-GMP-mediated signalling within the sigma network of *Escherichia coli*. Mol Microbiol 2006; 62: 1014-1034.

Wolfe AJ, Visick KL. Get the message out: Cyclic-di-GMP regulates multiple levels of flagellum-based motility. J Bacteriol 2008; 190: 463-475.

Wong CC. Mechanisms for coordinate control of motility and biofilm formation by the sensor-regulator MorA in *Pseudomonas* spp. National University of Singapore, Ph.D dissertation 2011.

Appendix I

Alignment of PNL-MK25 MorC EAL domain to tdEAL (PDB ID: 3n3t) (41% similarity)

Sequence similarity of MorC to tdEAL, used for *in silico* modeling of domain structure

```
>lcl|29108 3N3T:A|PDBID|CHAIN|SEQUENCE
Length=294

 Score =  213 bits (541),  Expect = 5e-60, Method: Compositional matrix adjust.
 Identities = 109/264 (41%), Positives = 161/264 (61%), Gaps = 2/264 (1%)

Query  3    EALNAEASYKLFVENNLRRALTQNELDVFYQPKLCLRSGRLLGMEALLRWNHPERGMIRP  62
            E L  +   +L ++  LR+AL +NEL + YQP + L SGR++G EAL+RW  PERG++ P
Sbjct  15   ENLYFQGHERLTLDTRLRQALERNELVLHYQPIVELASGRIVGGEALVRWEDPERGLVMP  74

Query  63   DQFISVAEETGLIIPIGKWIARQACRMSKSLTAAGLG--NLQVAINLSPKQFSDPDLVAS  120
              FI  AE+TGLI+ +  W+    C   ++    G    +L +++N+S +QF    L  +
Sbjct  75   SAFIPAAEDTGLIVALSDWVLEACCTQLRAWQQQGRAADDLTLSVNISTRQFEGEHLTRA  134

Query  121  IANILREEALPASLLELELTEGLLLEATEDTHLQLDQLKRLGLTLAMDDFGTGYSSLSYL  180
            +   L    L    LELE+TE ++L  T++    LD L+  G+ LA+DDFGTGYSSLSYL
Sbjct  135  VDRALARSGLRPDCLELEITENVMLVMTDEVRTCLDALRARGVRLALDDFGTGYSSLSYL  194

Query  181  KKFPIDIIKIDRSFIHEIPDNQDDMEITSAVIAMAHNLKLKVVAEGIETAEQLAFLRRHR  240
             + P   +KID+SF+ +IP +  + +I + ++A+A  L ++VVAEGIETA+Q AFLR
Sbjct  195  SQLPFHGLKIDQSFVRKIPAHPSETQIVTTILALARGLGMEVVAEGIETAQQYAFLRDRG  254

Query  241  CDVGQGYLFDRPIPGDELINALKR  264
            C+ GQG L   P   D   + L R
Sbjct  255  CEFGQGNLMSTPQAADAFASLLDR  278
```

Appendix II

SoLiD sequencing data analysis summary

SoLiD sequencing of PNL-MK25 genome was carried out at the University of Oklahoma health sciences center. Data obtained from 50bp tags at 300x coverage was then analyzed with CLC Bio software.

CLC Bio analysis summary

1. Assembly report

1.1 Summary statistics

	Count	Average length	Total bases
Reads	41,577,094	49.15	2,043,717,829
Matched	571	17.44	9,960
Not matched	41,576,523	49.16	2,043,707,869
References	3	188,742	566,228

1.2 General algorithm parameters

Parameter	Value
Conflict Resolution	Vote (A, C, G, T)
Non specific matches	random
Masking of references	none

1.3 Reads parameters

Reads	Length	Type	Parameters
octet_20090828_fc1_PSEPU_WT169_F3	Short	Single	Default

1.4 Reference sequences

Reference	Length	# Matches	# Forward Matches	# Reversed Matches
AE016854	67,473	49	20	29
AE016855	73,661	71	38	33
AM235768	425,094	451	238	213

# Paired-end Matches	Min coverage	Max coverage
0	0	1
0	0	3
0	0	29

1.5 Distribution of read length

Length	Count	Percentage	Cummulative Percentage
1	62,970	0.2%	0.2%
2	15,822	0.0%	0.2%
3	3,591	0.0%	0.2%
4	27,798	0.1%	0.3%
5	114,282	0.3%	0.5%
6	1,139	0.0%	0.5%
7	81,330	0.2%	0.7%
8	770	0.0%	0.7%
9	19,321	0.0%	0.8%
10	207	0.0%	0.8%
11	116	0.0%	0.8%
12	5,478	0.0%	0.8%
13	2,818	0.0%	0.8%
14	1,825	0.0%	0.8%
15	7,561	0.0%	0.8%
17	16,018	0.0%	0.9%
18	5,169	0.0%	0.9%
19	2,019	0.0%	0.9%
20	1,883	0.0%	0.9%
21	612,218	1.5%	2.4%
22	10,983	0.0%	2.4%
23	4,559	0.0%	2.4%
25	7,669	0.0%	2.4%
26	4,355	0.0%	2.4%
27	272	0.0%	2.4%
28	27	0.0%	2.4%
29	1,142	0.0%	2.4%
30	395	0.0%	2.4%
31	25	0.0%	2.4%
32	922	0.0%	2.4%
33	505	0.0%	2.4%

Length	Count	Percentage	Cummulative Percentage
34	356	0.0%	2.4%
35	349	0.0%	2.4%
36	2,579	0.0%	2.4%
37	5,745	0.0%	2.5%
38	390	0.0%	2.5%
39	364	0.0%	2.5%
40	4,936	0.0%	2.5%
41	6,266	0.0%	2.5%
42	1,466	0.0%	2.5%
43	7,133	0.0%	2.5%
44	2,597	0.0%	2.5%
47	742	0.0%	2.5%
48	27	0.0%	2.5%
50	40,530,955	97.5%	100.0%

1.6 Distribution of matched read length

Length	Count	Percentage	Cummulative Percentage
15	431	75.5%	75.5%
17	73	12.8%	88.3%
18	3	0.5%	88.8%
19	1	0.2%	89.0%
21	26	4.6%	93.5%
22	5	0.9%	94.4%
23	1	0.2%	94.6%
26	2	0.4%	94.9%
50	29	5.1%	100.0%

1.7 Distribution of non-matched read length

Length	Count	Percentage	Cummulative Percentage
1	62,970	0.2%	0.2%
2	15,822	0.0%	0.2%

Length	Count	Percentage	Cummulative Percentage
3	3,591	0.0%	0.2%
4	27,798	0.1%	0.3%
5	114,282	0.3%	0.5%
6	1,139	0.0%	0.5%
7	81,330	0.2%	0.7%
8	770	0.0%	0.7%
9	19,321	0.0%	0.8%
10	207	0.0%	0.8%
11	116	0.0%	0.8%
12	5,478	0.0%	0.8%
13	2,818	0.0%	0.8%
14	1,825	0.0%	0.8%
15	7,130	0.0%	0.8%
17	15,945	0.0%	0.9%
18	5,166	0.0%	0.9%
19	2,018	0.0%	0.9%
20	1,883	0.0%	0.9%
21	612,192	1.5%	2.4%
22	10,978	0.0%	2.4%
23	4,558	0.0%	2.4%
25	7,669	0.0%	2.4%
26	4,353	0.0%	2.4%
27	272	0.0%	2.4%
28	27	0.0%	2.4%
29	1,142	0.0%	2.4%
30	395	0.0%	2.4%
31	25	0.0%	2.4%
32	922	0.0%	2.4%
33	505	0.0%	2.4%
34	356	0.0%	2.4%
35	349	0.0%	2.4%
36	2,579	0.0%	2.4%
37	5,745	0.0%	2.5%

Length	Count	Percentage	Cummulative Percentage
38	390	0.0%	2.5%
39	364	0.0%	2.5%
40	4,936	0.0%	2.5%
41	6,266	0.0%	2.5%
42	1,466	0.0%	2.5%
43	7,133	0.0%	2.5%
44	2,597	0.0%	2.5%
47	742	0.0%	2.5%
48	27	0.0%	2.5%
50	40,530,926	97.5%	100.0%

Appendix III

MorC gene and protein sequences. The *morC* gene is 2697 bp in length and predicted to encode a polypeptide of 898 amino acid. The PAS domains are highlighted in grey, PAC domain in black, GAF domain in green, ASNEF domain in blue, EAL domain in yellow and the notable motifs in teal. The domains are predicted using Simple Modular Architecture Research Tool (http://smart.embl-heidelberg.de).

```
  1  AUGAAGAGCCAGCCCGAUGCCGCCAGCCGUAUGGCGGCCGAGGUAGUGACGCAGUUGCCU
  1   M  K  S  Q  P  D  A  A  S  R  M  A  A  E  V  V  T  Q  L  P

 61  GUGCCCUCGCGGCUCGGCAUGCUGCGUUUCGAGCGCUUGAAUGAAGCCAGUUGGGCAAUG
 21   V  P  S  R  L  G  M  L  R  F  E  R  L  N  E  A  S  W  A  M

121  CUGUUCCUCGAUCCCAACUGCGAACGCCAGUUCGGCCAGCCGGCCGUCGAGCUCUGCGCG
 41   L  F  L  D  P  N  C  E  R  Q  F  G  Q  P  A  V  E  L  C  A

                          PAS motif 1
181  CUGGUCGGCUCGCCUUACGCCAGCCUGAUGGAGCCCGAGGCGCGCUAUCAACUGCACGAU
 61   L  V  G  S  P  Y  A  S  L  M  E  P  E  A  R  Y  Q  L  H  D

241  GCGAUCCAGCAGCAACUGAGCAAAAGCGCACAUUACGUGGUGCGCUACACCCUGCACACC
 81   A  I  Q  Q  Q  L  S  K  S  A  H  Y  V  V  R  Y  T  L  H  T

301  GCCGCCGGCGCGUUGAACAUCCUCGAGCUGGGCGAAGCCUACAAACAGCACAACCGGCAC
101   A  A  G  A  L  N  I  L  E  L  G  E  A  Y  K  Q  H  N  R  H

361  UUGCUGCGCGGCUACCUGCUGGCAGUCGACGAGGUGUUCGACGAAACCCAGGCGCUGCCU
121   L  L  R  G  Y  L  L  A  V  D  E  V  F  D  E  T  Q  A  L  P

421  UCGGUCGACCUGGAAACCCAGAACUCGCGCCUGCAAAUCGCCCUUGAGCUGAACCAGCGU
141   S  V  D  L  E  T  Q  N  S  R  L  Q  I  A  L  E  L  N  Q  R

481  GCCCAGCAGGAACAACUGCAGCAUCUGGAGCGCGUGCGUGCCCAGCAGGAUCUGAUUCUG
161   A  Q  Q  E  Q  L  Q  H  L  E  R  V  R  A  Q  Q  D  L  I  L

541  CUGCUCGCACGCCAGCGCUACAGCACGCACAACUCGCUGCAGGAAGCCGCCGAACUGAUC
181   L  L  A  R  Q  R  Y  S  T  H  N  S  L  Q  E  A  A  E  L  I

601  ACCCGCUGCGCCUGCGAUAUCUACGAGAUCGACUGCGCUAGCCUGUGGAACCUCGAAGGC
201   T  R  C  A  C  D  I  Y  E  I  D  C  A  S  L  W  N  L  E  G

661  CAGCGCUUGCUGCCGAUCUCCGCUUACCAUCGCGCGACCCAGGAAUACAUCCUGCCGGAG
221   Q  R  L  L  P  I  S  A  Y  H  R  A  T  Q  E  Y  I  L  P  E

721  CCGAUCGAUAUCAGCGGCUUCCCUGACUACAUGGAAGCCCUGCACAGCAGCCGCGCCAUC
241   P  I  D  I  S  G  F  P  D  Y  M  E  A  L  H  S  S  R  A  I

                          GAF domain
781  GAUGCCCACAACGCCAUGCACGAUCCGCGUACCCGCGAGAUGGCCGAGGCGAUGCGUCCG
261   D  A  H  N  A  M  H  D  P  R  T  R  E  M  A  E  A  M  R  P

841  CGUGAUGUCAACGCCAUGCUCGAUGCCAGCAUUCGCGUCGACGGCCAGGUUGUCGGCGUG
281   R  D  V  N  A  M  L  D  A  S  I  R  V  D  G  Q  V  V  G  V
```

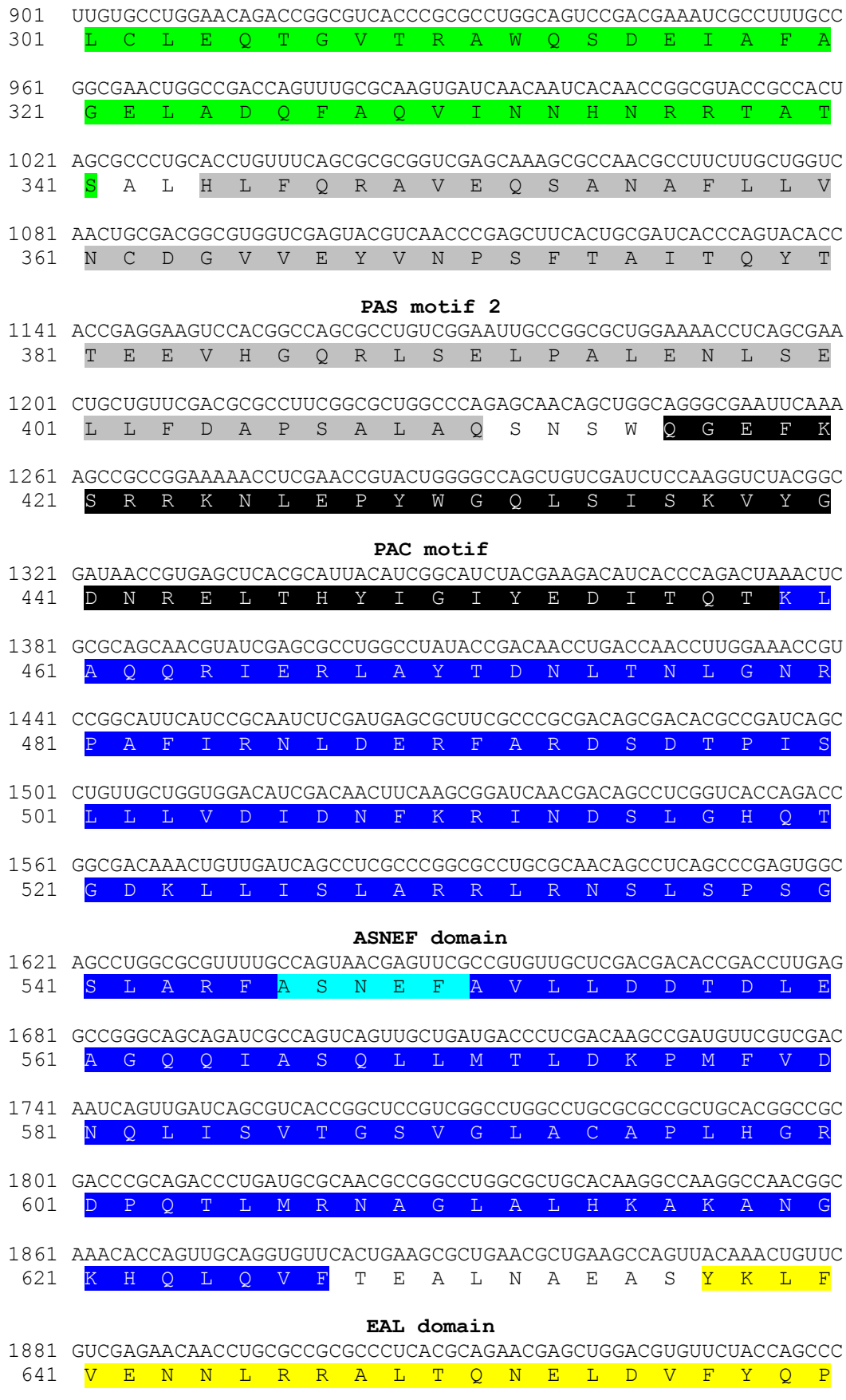
901 UUGUGCCUGGAACAGACCGGCGUCACCCGCGCCUGGCAGUCCGACGAAAUCGCCUUUGCC
301 L C L E Q T G V T R A W Q S D E I A F A
961 GGCGAACUGGCCGACCAGUUUGCGCAAGUGAUCAACAAUCACAACCGGCGUACCGCCACU
321 G E L A D Q F A Q V I N N H N R R T A T
1021 AGCGCCCUGCACCUGUUUCAGCGCGCGGUCGAGCAAAGCGCCAACGCCUUCUUGCUGGUC
341 S A L H L F Q R A V E Q S A N A F L L V
1081 AACUGCGACGGCGUGGUCGAGUACGUCAACCCGAGCUUCACUGCGAUCACCCAGUACACC
361 N C D G V V E Y V N P S F T A I T Q Y T
PAS motif 2
1141 ACCGAGGAAGUCCACGGCCAGCGCCUGUCGGAAUUGCCGGCGCUGGAAAACCUCAGCGAA
381 T E E V H G Q R L S E L P A L E N L S E
1201 CUGCUGUUCGACGCGCCUUCGGCGCUGGCCCAGAGCAACAGCUGGCAGGGCGAAUUCAAA
401 L L F D A P S A L A Q S N S W Q G E F K
1261 AGCCGCCGGAAAAACCUCGAACCGUACUGGGGCCAGCUGUCGAUCUCCAAGGUCUACGGC
421 S R R K N L E P Y W G Q L S I S K V Y G
PAC motif
1321 GAUAACCGUGAGCUCACGCAUUACAUCGGCAUCUACGAAGACAUCACCCAGACUAAACUC
441 D N R E L T H Y I G I Y E D I T Q T K L
1381 GCGCAGCAACGUAUCGAGCGCCUGGCCUAUACCGACAACCUGACCAACCUUGGAAACCGU
461 A Q Q R I E R L A Y T D N L T N L G N R
1441 CCGGCAUUCAUCCGCAAUCUCGAUGAGCGCUUCGCCCGCGACAGCGACACGCCGAUCAGC
481 P A F I R N L D E R F A R D S D T P I S
1501 CUGUUGCUGGUGGACAUCGACAACUUCAAGCGGAUCAACGACAGCCUCGGUCACCAGACC
501 L L L V D I D N F K R I N D S L G H Q T
1561 GGCGACAAACUGUUGAUCAGCCUCGCCCGGCGCCUGCGCAACAGCCUCAGCCCGAGUGGC
521 G D K L L I S L A R R L R N S L S P S G
ASNEF domain
1621 AGCCUGGCGCGUUUUGCCAGUAACGAGUUCGCCGUGUUGCUCGACGACACCGACCUUGAG
541 S L A R F A S N E F A V L L D D T D L E
1681 GCCGGGCAGCAGAUCGCCAGUCAGUUGCUGAUGACCCUCGACAAGCCGAUGUUCGUCGAC
561 A G Q Q I A S Q L L M T L D K P M F V D
1741 AAUCAGUUGAUCAGCGUCACCGGCUCCGUCGGCCUGGCCUGCGCGCCGCUGCACGGCCGC
581 N Q L I S V T G S V G L A C A P L H G R
1801 GACCCGCAGACCCUGAUGCGCAACGCCGGCCUGGCGCUGCACAAGGCCAAGGCCAACGGC
601 D P Q T L M R N A G L A L H K A K A N G
1861 AAACACCAGUUGCAGGUGUUCACUGAAGCGCUGAACGCUGAAGCCAGUUACAAACUGUUC
621 K H Q L Q V F T E A L N A E A S Y K L F
EAL domain
1881 GUCGAGAACAACCUGCGCCGCGCCCUCACGCAGAACGAGCUGGACGUGUUCUACCAGCCC
641 V E N N L R R A L T Q N E L D V F Y Q P

Canonical EAL motif

```
1981 AAGCUGUGCCUGCGCAGCGGUCGCCUGCUGGGCAUGGAAGCGCUGUUGCGCUGGAACCAC
 661  K  L  C  L  R  S  G  R  L  L  G  M  E  A  L  L  R  W  N  H

2041 CCGGAGCGCGGCAUGAUCCGCCCGGACCAGUUCAUCAGCGUCGCCGAGGAAACCGGCCUG
 681  P  E  R  G  M  I  R  P  D  Q  F  I  S  V  A  E  E  T  G  L

2101 AUCAUUCCGAUCGGCAAGUGGAUUGCUCGUCAGGCCUGCCGCAUGAGCAAAUCCCUGACC
 701  I  I  P  I  G  K  W  I  A  R  Q  A  C  R  M  S  K  S  L  T

2161 GCUGCCGGCCUAGGCAAUCUGCAGGUGGCAAUCAAUCUGUCACCGAAACAGUUCUCCGAU
 721  A  A  G  L  G  N  L  Q  V  A  I  N  L  S  P  K  Q  F  S  D
```

Non-canonical EAL motif

```
2221 CCGGAUCUGGUCGCCUCGAUCGCCAACAUCCUCAGGGAAGAAGCGCUGCCGGCCAGUCUG
 741  P  D  L  V  A  S  I  A  N  I  L  R  E  E  A  L  P  A  S  L

2281 CUCGAACUGGAGCUGACCGAAGGCUUGUUGCUGGAAGCCACCGAAGACACGCAUUUGCAG
 761  L  E  L  E  L  T  E  G  L  L  L  E  A  T  E  D  T  H  L  Q
```

β_6-loop

```
2341 CUCGACCAGCUCAAACGCUUGGGCCUGACCCUGGCCAUGGAUGACUUCGGCACCGGGUAC
 781  L  D  Q  L  K  R  L  G  L  T  L  A  M  D  D  F  G  T  G  Y

2401 UCGUCGCUGAGCUAUCUGAAGAAAUUUCCGAUCGACAUCAUCAAGAUUGAUCGCAGCUUC
 801  S  S  L  S  Y  L  K  K  F  P  I  D  I  I  K  I  D  R  S  F

2461 AUCCAUGAAAUCCCGGACAACCAGGACGACAUGGAAAUCACCUCCGCGGUGAUCGCCAUG
 821  I  H  E  I  P  D  N  Q  D  D  M  E  I  T  S  A  V  I  A  M

2521 GCCCACAACCUGAAACUCAAGGUCGUCGCCGAAGGCAUCGAAACCGCCGAGCAACUGGCG
 841  A  H  N  L  K  L  K  V  V  A  E  G  I  E  T  A  E  Q  L  A

2581 UUCCUGCGCCGGCAUCGUUGCGACGUCGGCCAGGGUUACCUGUUCGACCGACCGAUUCCG
 861  F  L  R  R  H  R  C  D  V  G  Q  G  Y  L  F  D  R  P  I  P

2641 GGUGAUGAGCUGAUCAAUGCGCUCAAGCGCUAUCCGCGCGGCCCGCUCUGCCUCUAA
 881  G  D  E  L  I  N  A  L  K  R  Y  P  R  G  P  L  C  L  *
```

Appendix IV

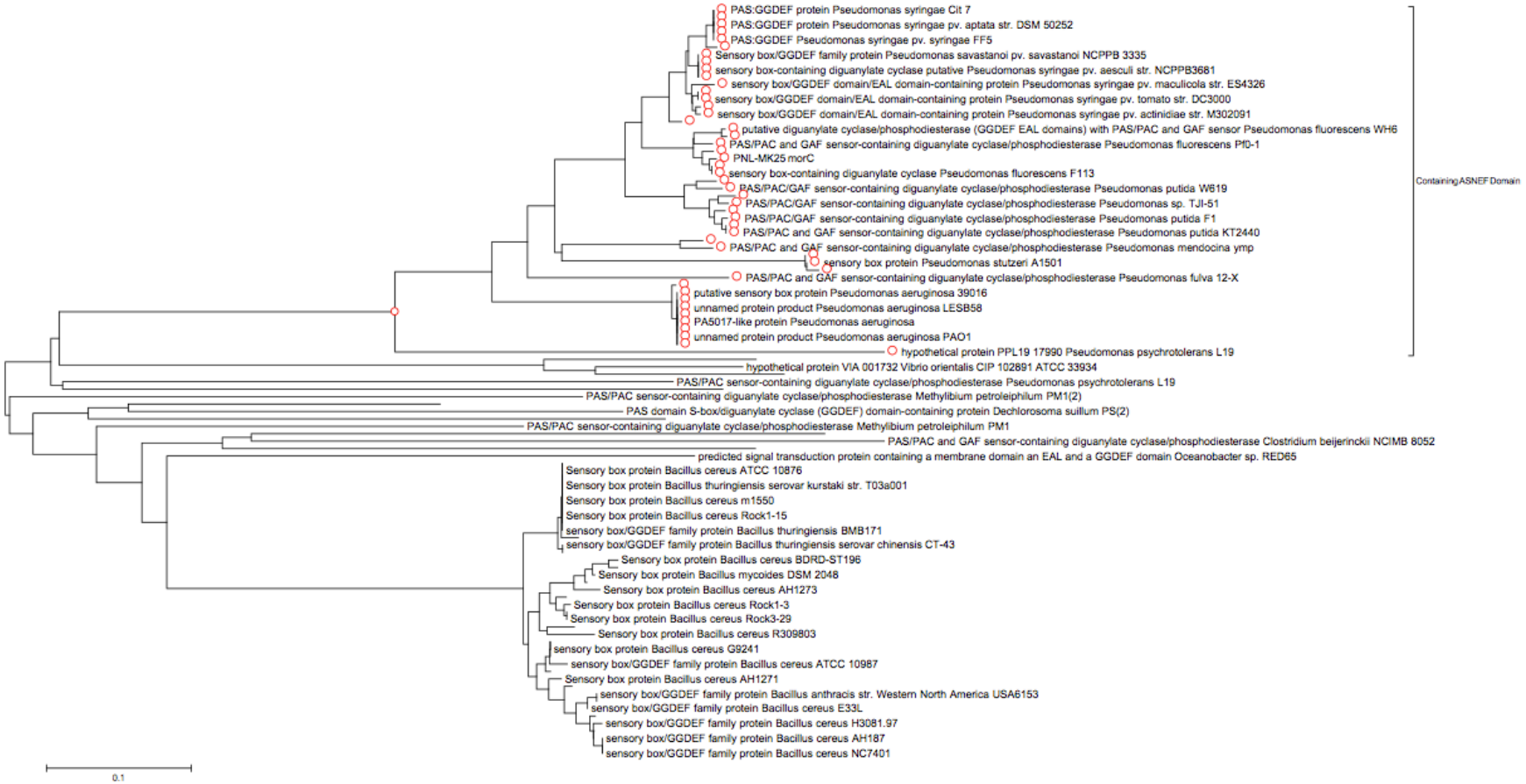

Phylogram tree of MorC homologs shows that MorC is well-conserved in many bacterial genomes. ASNEF motif is conserved in the *Pseuduomonas spp* while being presented as GGDEF in the other bacterial species. Bacterial species containing ASNEF motif are highlighted with a red circle and were found to cluster together at the top of the tree.

Appendix V

Taxonomy report of MorC conservation.

Taxonomy Report

```
Bacteria ..........................................................  242 hits  141 orgs [root; cellular organisms]
. Proteobacteria ..................................................  100 hits   65 orgs
. . Gammaproteobacteria ...........................................   99 hits   64 orgs
. . . Pseudomonas .................................................   92 hits   61 orgs [Pseudomonadales; Pseudomonadaceae]
. . . . Pseudomonas brassicacearum subsp. brassicacearum NFM421 ....    2 hits    1 orgs [Pseudomonas brassicacearum; Pseudomonas brassicacearum subsp
. . . . Pseudomonas fluorescens ...................................    8 hits    4 orgs [Pseudomonas fluorescens group]
. . . . . Pseudomonas fluorescens Pf-5 ............................    2 hits    1 orgs
. . . . . Pseudomonas fluorescens Pf0-1 ...........................    2 hits    1 orgs
. . . . . Pseudomonas fluorescens WH6 .............................    2 hits    1 orgs
. . . . . Pseudomonas fluorescens SBW25 ...........................    2 hits    1 orgs
. . . . Pseudomonas syringae group ................................   34 hits   27 orgs
. . . . . Pseudomonas syringae ....................................    9 hits    8 orgs [Pseudomonas syringae group genomosp. 1]
. . . . . Pseudomonas syringae pv. syringae .......................    4 hits    3 orgs
. . . . . Pseudomonas syringae pv. syringae FF5 ...................    1 hits    1 orgs
. . . . . Pseudomonas syringae pv. syringae 642 ...................    1 hits    1 orgs
. . . . . Pseudomonas syringae pv. syringae B728a .................    2 hits    1 orgs
. . . . . Pseudomonas syringae pv. pisi str. 1704B ................    1 hits    1 orgs [Pseudomonas syringae pv. pisi]
. . . . . Pseudomonas syringae pv. aptata str. DSM 50252 ..........    1 hits    1 orgs [Pseudomonas syringae pv. aptata]
. . . . . Pseudomonas syringae Cit 7 ..............................    1 hits    1 orgs
. . . . . Pseudomonas syringae pv. aceris str. M302273PT ..........    1 hits    1 orgs [Pseudomonas syringae pv. aceris]
. . . . . Pseudomonas syringae pv. actinidiae str. M302091 ........    1 hits    1 orgs [Pseudomonas syringae group pathovars incertae sedis; Pseudom
. . . . . Pseudomonas syringae pv. oryzae str. 1_6 ................    2 hits    1 orgs [Pseudomonas coronafaciens; Pseudomonas syringae pv. oryzae]
. . . . . Pseudomonas syringae group genomosp. 2 ..................   15 hits   12 orgs
. . . . . Pseudomonas amygdali ....................................    9 hits    8 orgs
. . . . . Pseudomonas syringae pv. lachrymans .....................    2 hits    2 orgs
. . . . . . Pseudomonas syringae pv. lachrymans str. M302278PT .....    1 hits    1 orgs
. . . . . . Pseudomonas syringae pv. lachrymans str. M301315 ......    1 hits    1 orgs
. . . . . Pseudomonas syringae pv. morsprunorum str. M302280PT .....    1 hits    1 orgs [Pseudomonas syringae pv. morsprunorum]
. . . . . Pseudomonas syringae pv. aesculi ........................    3 hits    3 orgs
. . . . . . Pseudomonas syringae pv. aesculi str. 2250 ............    1 hits    1 orgs
. . . . . . Pseudomonas syringae pv. aesculi str. NCPPB3681 ......    1 hits    1 orgs
. . . . . . Pseudomonas syringae pv. aesculi str. 0893_23 ........    1 hits    1 orgs
. . . . . Pseudomonas syringae pv. tabaci ATCC 11528 ..............    2 hits    1 orgs [Pseudomonas syringae pv. tabaci]
. . . . . Pseudomonas syringae pv. mori str. 301020 ..............    1 hits    1 orgs [Pseudomonas syringae pv. mori]
. . . . . Pseudomonas savastanoi ..................................    6 hits    4 orgs
. . . . . Pseudomonas savastanoi pv. savastanoi NCPPB 3335 .......    2 hits    1 orgs [Pseudomonas savastanoi pv. savastanoi]
. . . . . Pseudomonas syringae pv. phaseolicola 1448A ............    2 hits    1 orgs [Pseudomonas syringae pv. phaseolicola]
. . . . . Pseudomonas syringae pv. glycinea .......................    2 hits    2 orgs
. . . . . . Pseudomonas syringae pv. glycinea str. B076 ..........    1 hits    1 orgs
. . . . . . Pseudomonas syringae pv. glycinea str. race 4 ........    1 hits    1 orgs
. . . . . Pseudomonas syringae group genomosp. 3 ..................    8 hits    6 orgs
. . . . . Pseudomonas syringae pv. tomato .........................    7 hits    5 orgs
. . . . . Pseudomonas syringae pv. tomato str. DC3000 ............    2 hits    1 orgs
. . . . . Pseudomonas syringae pv. tomato T1 ......................    2 hits    1 orgs
. . . . . Pseudomonas syringae pv. tomato Max13 ...................    1 hits    1 orgs
. . . . . Pseudomonas syringae pv. tomato K40 .....................    1 hits    1 orgs
. . . . . Pseudomonas syringae pv. tomato NCPPB 1108 ..............    1 hits    1 orgs
. . . . . Pseudomonas syringae pv. maculicola str. ES4326 ........    1 hits    1 orgs [Pseudomonas syringae pv. maculicola]
. . . . Pseudomonas entomophila L48 ...............................    2 hits    1 orgs [Pseudomonas entomophila]
. . . . Pseudomonas putida group ..................................   13 hits    7 orgs
. . . . . Pseudomonas putida ......................................   11 hits    6 orgs
. . . . . Pseudomonas putida W619 .................................    2 hits    1 orgs
. . . . . Pseudomonas putida BIRD-1 ...............................    1 hits    1 orgs
. . . . . Pseudomonas putida KT2440 ...............................    2 hits    1 orgs
. . . . . Pseudomonas putida S16 ..................................    2 hits    1 orgs
. . . . . Pseudomonas putida GB-1 .................................    2 hits    1 orgs
. . . . . Pseudomonas putida F1 ...................................    2 hits    1 orgs
. . . . . Pseudomonas fulva 12-X ..................................    2 hits    1 orgs [Pseudomonas fulva]
. . . . Pseudomonas sp. TJI-51 ....................................    2 hits    1 orgs
. . . . Pseudomonas aeruginosa group ..............................   26 hits   17 orgs
. . . . . Pseudomonas mendocina ...................................    4 hits    2 orgs
. . . . . Pseudomonas mendocina ymp ...............................    2 hits    1 orgs
. . . . . Pseudomonas mendocina NK-01 .............................    2 hits    1 orgs
. . . . . Pseudomonas aeruginosa ..................................   22 hits   15 orgs
. . . . . Pseudomonas aeruginosa UCBPP-PA14 .......................    2 hits    1 orgs
. . . . . Pseudomonas aeruginosa PAb1 ............................    1 hits    1 orgs
. . . . . Pseudomonas aeruginosa 152504 ..........................    1 hits    1 orgs
. . . . . Pseudomonas aeruginosa PACS2 ...........................    1 hits    1 orgs
. . . . . Pseudomonas aeruginosa LESB58 ..........................    2 hits    1 orgs
. . . . . Pseudomonas aeruginosa 138244 ..........................    1 hits    1 orgs
. . . . . Pseudomonas aeruginosa M18 .............................    1 hits    1 orgs
. . . . . Pseudomonas aeruginosa PAO1 ............................    2 hits    1 orgs
. . . . . Pseudomonas aeruginosa C3719 ...........................    2 hits    1 orgs
. . . . . Pseudomonas aeruginosa 2192 ............................    2 hits    1 orgs
. . . . . Pseudomonas aeruginosa 39016 ...........................    2 hits    1 orgs
. . . . . Pseudomonas aeruginosa NCGM2.S1 ........................    1 hits    1 orgs
. . . . . Pseudomonas aeruginosa PA7 ............................    2 hits    1 orgs
. . . . . Pseudomonas aeruginosa NCMG1179 ........................    1 hits    1 orgs
. . . . Pseudomonas stutzeri ......................................    5 hits    3 orgs [Pseudomonas stutzeri group; Pseudomonas stutzeri subgroup]
. . . . . Pseudomonas stutzeri DSM 4166 ..........................    1 hits    1 orgs
. . . . . Pseudomonas stutzeri A1501 .............................    2 hits    1 orgs
. . . . . Pseudomonas stutzeri ATCC 17588 = LMG 11199 ............    2 hits    1 orgs
. . . Vibrio ......................................................    5 hits    2 orgs [Vibrionales; Vibrionaceae]
. . . . Vibrio orientalis CIP 102891 = ATCC 33934 .................    3 hits    1 orgs [Vibrio orientalis]
. . . . Vibrio caribbenthicus ATCC BAA-2122 .......................    2 hits    1 orgs [Vibrio caribbenthicus]
. . . Bermanella marisrubri .......................................    2 hits    1 orgs [Oceanospirillales; Oceanospirillaceae; Bermanella]
. . Dechlorosoma suillum PS .......................................    1 hits    1 orgs [Betaproteobacteria; Rhodocyclales; Rhodocyclaceae; Azospira;
. Bacillales ......................................................  142 hits   76 orgs [Firmicutes; Bacilli]
. . Bacillus cereus group .........................................  140 hits   75 orgs [Bacillaceae; Bacillus]
. . . Bacillus cereus ..............................................   78 hits   40 orgs
. . . . Bacillus cereus Rock4-18 ...................................    2 hits    1 orgs
. . . . Bacillus cereus Rock3-29 ...................................    2 hits    1 orgs
. . . . Bacillus cereus Rock3-28 ...................................    2 hits    1 orgs
. . . . Bacillus cereus ATCC 10987 .................................    2 hits    1 orgs
. . . . Bacillus cereus Rock1-3 ....................................    2 hits    1 orgs
. . . . Bacillus cereus AH603 ......................................    2 hits    1 orgs
. . . . Bacillus cereus BDRD-ST196 .................................    2 hits    1 orgs
. . . . Bacillus cereus G9241 ......................................    2 hits    1 orgs
. . . . Bacillus cereus MM3 ........................................    2 hits    1 orgs
. . . . Bacillus cereus AH1273 .....................................    2 hits    1 orgs
. . . . Bacillus cereus AH1272 .....................................    2 hits    1 orgs
```